

FATIGUE PERFORMANCE OF GLASS/EPOXY NANOCOMPOSITES FOR
WIND TURBINE BLADES

THESIS

Presented to the Graduate Council of
Texas State University-San Marcos
in Partial Fulfillment
of the Requirements

for the Degree

Master of SCIENCE

by

Adekunle Temitope Akinola

San Marcos, Texas
May, 2010

COPYRIGHT

by

Adekunle Temitope Akinola

2010

ACKNOWLEDGMENTS

I thank the almighty God for bringing me this far, and making my academic goal a reality. I would like to express my deepest thanks and sincere gratitude to my advisor, Dr. Jitendra Tate for helping to build my technical, writing and research skills. I am really grateful for his help and assistance. I also appreciate my committee members, Dr. Ajit D. Kelkar and Dr. Byoung-Hee You for their assistance in every phase of this thesis. It was a great opportunity and pleasant experience learning from you all.

Thanks go to these unique people, Dr. Stephan Sprenger and Ms. Melissa King of nanoresins AG, Germany, Dr. Vedaraman Sriraman, Chair, Department of Engineering Technology, and Dr. Harold Stern, Director, Ingram School of Engineering.

I am indebted to several people that made this work a reality, especially my co-workers at Composite and Plastics Lab (CPL), Alex Herrera, Dmitri Kabakov, Ben Butler and Travis Hilbig. Also to lab supervisors, Shane Arabie, Ray cook, Evan Jensen, and Jason Wagner. I also thank Ms. Sarah Rivas, Administrative Assistant for her timely help in ordering equipment/materials. Thanks to Mr. Al Matinez and Dr. Pulin Patel of IEIS facility, and Dr. Hugo of NST facility at UT Austin for SEM training.

I cannot finish without saying thank you to my parents for their help and encouragement, my siblings, Emma and Bukky for their support. I am forever grateful to Bisime Akinola and Tunji Akinola for oiling the engine of my career.

This manuscript was submitted on April 8, 2008

TABLE OF CONTENTS

	Page
ACKNOWLEDGEMENTS.....	iv
LIST OF TABLES	ix
LIST OF FIGURES	xi
ABSTRACT	xiv
CHAPTER	
1. INTRODUCTION	1
1.1 Motivation and Background	1
1.2 Reinforcement Materials	7
1.2.1 Carbon Fiber	8
1.2.2 Glass Fiber	9
1.3 Reinforcement Forms.....	10
1.3.1 Roving and Tow.....	11
1.3.2 Mats.....	11
1.3.3 Woven Fabrics	12
1.3.4 Braided Fabrics	12
1.3.5 Knitted Fabrics.....	12
1.4 Different Weave Types	13
1.5 Resins.....	15
1.6 Epoxy Resin	18
1.7 Nanomodification of Polymers	21
1.7.1 Carbon Nanotubes.....	21
1.7.2 Nanoclay	24
1.7.3 Halloysite Nanotubes (HNT™)	27

1.7.4 Nanosilica	31
1.8 Manufacturing Methods.....	32
1.9 Fatigue of Composites	33
1.9.1 The Stress Life Approach	34
1.9.2 Fatigue Behavior in Polymers.....	36
1.9.3 Material Degradation due to Fatigue Loading	39
1.9.4 Fatigues under Loading Parallel to Fibers	39
1.9.5 Fiber damage Models.....	44
1.9.6 Matrix and Interfacial Damage	45
1.10 Problem Statement.....	46
1.11 Objectives of the research.....	48
2. MANUFACTURING	50
2.1 Manufacturing methods of composites.....	50
2.1.1 Wet Lay-up Method.....	50
2.1.2 Prepreg Method.....	51
2.1.3 Autoclave Processing.....	52
2.1.4 Pultrusion.....	54
2.1.5 Filament Winding	55
2.1.6 Resin Transfer Molding (RTM)	56
2.1.7 Vacuum Assisted Resin Transfer Molding (VARTM)	58
2.2 Material System	60
2.3 Dispersion of Nanoparticles in Epoxy	62
2.3.1 IKA® High Shear Mixer	63
2.3.2 Planetary Centrifugal Mixing: THINKY® ARV-310	66
2.3.3 Low-shear Mechanical Mixing: (Dispermat)	67

2.4 Steps in VARTM	70
2.4.1 Mold Preparation and Vacuum Bagging.....	70
2.4.2 Resin Formulation and Degassing	74
2.4.3 Resin Impregnation and Curing.....	76
2.5 Overall Fiber Volume Fraction.....	79
3. PERFORMANCE EVALUATION.....	80
3.1 Introduction.....	80
3.1.1 Dynamic/Fatigue Testing System.....	82
3.2 Static Tests.....	83
3.2.1 Static Tensile Test.....	83
3.2.2 Flexure Test	86
3.2.3 Inter laminar Shear Strength-ILSS Test (Short-Beam Test)	88
3.3 Tension-Tension Fatigue Tests	91
3.4 Stiffness Degradation.....	93
3.5 Static Tests on HNT-Epoxy Neat Resin	95
4. RESULTS AND DISCUSSION.....	100
4.1 Introduction.....	100
4.1.1 Static Tensile Test	100
4.1.2 Flexural Test	103
4.1.3 Inter laminar Shear Strength (ILSS) Testing	106
4.2 Axial Fatigue Tests	111
4.2.1 S-N Diagram	114
4.3 Stiffness Degradation Curves	116
4.4 HNT-Epoxy Neat Resin Static Tests	120
4.5 Analysis of variance (ANOVA).....	124

4.5.1 One-way ANOVA: Tensile Strength versus Nanosilica Percentage	124
4.5.2 One-way ANOVA: Flexural Strength versus Nanosilica Percentage	126
4.5.3 One-way ANOVA: Interlaminar Shear Strength versus Nanosilica Percentage	127
5.0 CONCLUSIONS.....	128
REFERENCES	135

LIST OF TABLES

Table	Page
1.1 Properties of Typical Fibers.....	8
1.2 Properties of Typical Polymer Matrix Materials	16
1.3 Advantages and Disadvantages of Thermosetting Resins	17
2.1 Material system for Nanosilica nanocomposites	60
2.2 Material system for HNT nanocomposites	61
2.3 Material system for HNT-epoxy neat resin	61
2.4 High Shear Mixer Shear Rates.....	64
2.5 Resin Dispersion Technique and processing	69
2.6 Resin formulations for Nanosilica Nanocomposites.....	75
2.7 Resin formulations for Halloysite nanotubes neat coupons.....	75
3.1. Test matrix for static test	81
3.2 Number of fatigue test specimens.....	93
4.1 Tensile Strength of Nanosilica Nanocomposites	101
4.2 Flexural Strength.....	104
4.3 Interlaminar Shear Strength (ILSS)	108
4.4 Fatigue life of control specimens, 5 Hz frequency	112
4.5 Fatigue life of control specimens, 2 Hz frequency	112
4.6 Average fatigue life on control specimens.....	112
4.7 Fatigue life of 6wt% nanosilica composite specimens, 2 Hz frequency.....	113

4.8 Average fatigue life on control and 6wt% nanosilica composite specimens (2 Hz)	113
4.9 Flexural, Izod-impact, and Tensile Test Results (High-shear mixing)	120
4.10 Flexural, Izod-impact, and Tensile Test Results (centrifugal planetary mixing)	119
4.11 Flexural, Izod-impact, and Tensile Test Results (low-shear mechanical mixing)	123
4.12 Flexural, Izod-impact, and Tensile Test Results for 2.5wt% HNT loading with three different mixing techniques	124
4.13 Univariate Analysis of Variance for Tensile Strength	125
4.14 Student Newman Keuls Test for Tensile Strength	125
4.15 Univariate Analysis of Variance for Flexure Strength	126
4.16 Student Newman Keuls Test for Flexural Strength	126
4.17 Univariate Analysis of Variance for Interlaminar Shear	127
4.18 Student Newman Keuls Test for Flexural Strength	127

LIST OF FIGURES

Figures	Page
1.1 Different Weave Patterns	14
1.2 Curing reaction of Epoxy.....	19
1.3 Morphology of Halloysite Nanotubes.....	28
1.4 Nomenclature for constant stress amplitude loading	35
1.5 S/N diagram	36
1.6 S/N Diagram for different R- values.....	38
1.7 (a) Stress controlled loading and (b) The strain response due to cyclic softening	39
1.8 Fatigue damage mechanisms in unidirectional composites under loading parallel to fibers	40
1.9 Fatigue Damage Mechanisms in Composite Laminate	43
1.10 Modulus Decay under Fatigue Loading in Woven Composites	44
2.1 Typical wet layup processing.....	51
2.2 Autoclave Processing.....	53
2.3 Pultrusion process	55
2.4 Filament winding	56
2.5 Resin Transfer molding.....	57
2.6 Schematic for VARTM.....	60
2.7 IKA [®] Labor Pilot 2000/4 High Shear Mixer with cooling jacket.....	65

2.8 Rotation and Revolution action in Centrifugal Planetary Mixer	66
2.9 Planetary centrifugal vacuum mixer	67
2.10 DISPERMAT® CC	68
2.11 Silicone mold with flexure specimens	70
2.12 Room Temperature VARTM Setup: Vacuum bagging	71
2.13 Resin Flow in VARTM Process	71
2.14 VARTM process - from layup to resin infusion to demolding	76
2.15 Micrograph of Nanosilica in Epoxy.....	77
2.16 EDS showing material constituents of Nanosilica in Epoxy	78
3.1 MTS servo hydraulic test system	82
3.2 Tensile Tests Specimen.....	84
3.3 Tension Test Specimen and Fixture.....	85
3.4 Typical Tensile Test Failure Modes	85
3.5 Flexure Test Specimen Loading	87
3.6 Flexure Test Specimen and Fixture	87
3.7 Short Beam Specimen Loading	89
3.8 Short Beam Test Fixture Loaded with Specimen	89
3.9 Specimen Geometry for Neat Resin Coupon.....	96
3.10 Notching cutter.....	97

3.11 Monitor/ Impact tester.....	97
3.12 Specimen Geometry for Neat Resin Coupon.....	98
4.1 Tensile stress-strain curves for control and nanocomposites.....	101
4.2 Chord modulus on control specimen	102
4.3 Front side micrograph of failed tensile specimen	103
4.4 Side micrograph of failed tensile specimen	103
4.5 Load vs displacement graph of control and nanocomposites	104
4.6 Slope of initial linear portion for control composites	105
4.7 Front and side micrographs of failed flexure specimen.....	106
4.8 Superimposed load vs cross-head displacement	108
4.9 Front and side micrographs of failed ILSS specimen.....	109
4.10 Bar chart of different strengths of control, 6, 7 and 8 wt% composites	110
4.11 Bar chart of Tensile and Flexural Modulus of control, 6, 7 and 8 wt% composites.....	110
4.12 Failed fatigue specimens of composite specimens	114
4.13 S-N Diagram for Nanomodified Neat Epoxy Resin	115
4.14 S-N Diagram for Glass reinforced composites	116
4.15 Stiffness degradation curve of Control specimens.....	118
4.16 Stiffness degradation curve of nanomodified specimens.....	119
4.17 Superimposed stiffness degradation curves for 46.6 MPa.....	119
4.18 HNT-epoxy mixture after high-shear mixing	121

ABSTRACT

FATIGUE PERFORMANCE OF GLASS/EPOXY NANOCOMPOSITES FOR WIND TURBINE BLADES

by

Adekunle Temitope Akinola, B.S.

Texas State University-San Marcos
May, 2010

SUPERVISING PROFESSOR: JITENDRA S. TATE

Wind power is capable of becoming a major contributor to America's electricity supply over the next three decades (Composite world, 2008). This desire is borne to create a sustainable energy that will be cheap and easily adapted by people irrespective of their geographical locations. Recently, there is a growing interest in designing cheap and efficient turbine blades. Polymer matrix composites (E-glass/Epoxy) dominate the wind turbine blade market because of their low-cost, superior fatigue characteristics, high specific stiffness, and ability to make complex geometries. Different sizes of wind turbine blades can be produced depending on the desired amount of power to be generated. The length of wind turbine blade is proportional to the energy generated by the turbine and

this is the simple reason why longer blades are commonly designed by most wind turbine blade designers. Wind turbine failure is a major issue as failure rates are as high as 20% within three years (Richardson, 2009). Major causes of wind turbine failures are bad bonds, delamination, voids and also manufacturing errors. Nanoparticles have been discovered to enhance mechanical properties of existing materials (Blackman et al., 2007). The overall objective of this research is to develop and manufacture glass/epoxy nanocomposites in conjunction with low cost vacuum assisted resin transfer molding (VARTM) for improved fatigue performance. EPIKOTE RIMR 135 epoxy resin was used which has been specially formulated for wind turbine applications by Hexion specialty Inc. Non-crimp E-glass $\pm 45^\circ$ stitched bonded fabric from Saertex, Germany was used as reinforcement because of its overall balanced properties and low cost.

Nanosilica and Halloysite nanotubes (HNT) were used to modify the epoxy resin system. Nanosilica did not pose any problem in dispersion because it was already dispersed in epoxy by the manufacturer, nanoresin AG, Germany. Three different loadings of Nanosilica (6, 7, and 8 weight percentages) were used in making composites and static tests were performed. Considerable improvements were recorded in tensile strength, tensile modulus, flexural strength, flexural modulus and interlaminar shear strength. Statistically, improvements in mechanical properties due to nanoparticle loading was found to be significant when compared to control (0 wt%) group.

However, 6 weight percent (wt%) nanosilica nanocomposites showed much improvement in tensile strength and interlaminar shear strength (ILSS) over control composites (0 weight percent nanosilica). Control and 6 weight percent nanosilica were

tested in axial tension-tension fatigue at 2Hz frequency and R ratio of 0.1. 6 weight percent. Nanosilica modification showed 10 and 3 times improvement in fatigue life in high-cycle and low-cycle fatigue, respectively.

Halloysite nanotubes (HNT) was another nanoparticle that was used in this research. The uniform dispersion of HNT in epoxy was a challenge. Three different dispersion methods were explored; centrifugal mixing, high shear mixing and low shear mixing. Dispersion with low-shear mixing was promising but it involved a very long and tedious process. More studies with different HNT percentages are required to confirm these improvements. There is also need to conduct detail SEM analysis especially on fractured surfaces to evaluate interfacial adhesion between epoxy and HNT particles.

CHAPTER 1

INTRODUCTION

1.1 Motivation and Background

The motivation of this work was borne out of the desire to create a sustainable energy that will be cheap and easily adapted by people irrespective of their geographical locations. Wind turbine blades are designed to meet and withstand complex loadings and harsh operational conditions; wind hits the turbine blades in different directions, wind turbines are mounted in the open at wind turbine farms and exposed to different temperatures. Basically, fatigue, tensile and shear failures are the few target areas researchers focus in designing turbine blades to withstand the exposed cyclic loads in their operating lives (Thomsen, 2009).

Different sizes of wind turbine blades can be produced depending on the desired amount of power to be generated. The length of wind turbine blade is proportional to the energy generated by the turbine and this is the simple reason why longer blades are commonly designed by most wind turbine blade designers. Wind turbine power of 5MW and rotor diameter of more than 60 m is a common feat in wind turbine industry. It has been observed that the total production cost per Kilowatt hour of electricity produced decreases with increasing wind turbine size (Thomsen, 2009). The present size of wind turbine blades is expected to increase in the nearest future with the level of interest and

research going on in this field. Modern wind turbine blades are being manufactured using polymer matrix composite materials (PMC). The manufacturing techniques used in making wind turbine blades may differ but the processes are commonly composite prepreg technology, vacuum assisted resin transfer molding (VARTM) and vacuum infusion process. Wind energy is a driving force in alternative and renewable sources of energy in the world according to some studies. The US installed capacity increased by 45% in 2007, has installation of more than 16,800 MW, which is capable of generating an estimated 48 billion Kilowatt-hours (KWh), enough to power 4.5 million homes (Scott J. Johnson, C.P Van Dam, & Dale E. Berg, 2008).

The probably most important load in turbine blade design is flap wise bending load that arises when the turbine has been brought to a standstill due to high wind and the blade is hit by extreme gust wind assuming a uniform wind profile. Epoxy-based composites are of great interest to composite manufacturers because of the environmental, production and cost advantage over other resin systems. Epoxy also has some distinct properties like shorter cure cycles, increased durability, and improved surface finish.

In order to make wind energy competitive with other sources of power, the weight and cost of the turbine blades have to be minimal. Several researchers have indicated ways of reducing overall weight of wind turbine through the reduction of the weight of the tower and rotor. Rotor in most of the modern wind turbines constitutes 37 to 77% of the total weight (Locks & Valencia, 2004).

It is necessary in designing turbine blades to design for good fatigue life, good stiffness property to achieve high operating lives. Due to exceptional good strength and modulus, lower weight to power ratio, composite materials are highly favored in making turbine blades. Different approaches have been adopted in designing good turbine blades but the most promising approach is the integrating of advanced composite materials $\pm 45^\circ$ stitch bonded non-crimp fiber glass because of the possibility of having good torsion and fatigue properties due to its stitch bonded pattern.

It is obvious that the growth of wind energy industry will be sustained in the presence of constant hike in fuel prices, pollutants emission, and depletion of ozone layers. Although, keeping wind energy competitive requires lowering the cost of its production which is the cheapest at the moment compared to other sources of power. Many avenues are being explored and different composite materials are being tested to achieve the target of reduction in turbine cost and weight.

Although, composite materials are highly favored in making wind turbine blades especially $\pm 45^\circ$ stitch bonded non-crimp fiber glass and epoxy, there are still some drawbacks in the areas of flexural and fatigue strength, as well as minimizing fatigue failures. This research is focused on ways of solving these current problems and potentially reduces the cost of fabricating turbine blades with exceptional flexural and fatigue strengths by minimizing blade failures which could be costly in terms of turbine down time and repairs.

The few problems facing the usage of composite materials in turbine blades application could be easily reduced by using carbon fabric because of its exceptional

flexural and fatigue strengths but it is really expensive and in solving the world energy need, a cheap renewable energy source is needed. Hybrid fabric of carbon and E-glass is also a potential means of fabricating composite materials with increase flexural and fatigue strengths, as well as minimizing the blade failures but it is also costly and the design is complex which makes it difficult to commercialize. The most feasible and cheap means of solving the underlined problems is through nanomodification of epoxy resin with carbon nanotubes, Hallosite nanotubes (HNT™) and nanosilica, which is the basis of this research.

The addition of carbon nanotubes (CNT) with epoxy as a structural element in nanocomposites has shown a great improvements in material properties. The applications range from devices in nanoelectronics to field emitters. There are two main types of carbon nanotubes that can have high structural perfection; Single walled nanotubes (SWNT), which consists of a single graphite sheet seamlessly wrapped into a cylindrical tube and Multiwall nanotubes (MWNT) which comprises an array of nanotubes that are concentrically nested like rings of a tree trunk. Research shows that polymers adhered well to CNT at the nanometer scale when examined through transmission and scanning electron microscopy, which explained why the properties of electrons inside matter and atomic interactions are influenced by materials variations on the nanometer scale (Yueping, Haibin, Jingshen, & Lin, 2007). Past research shows that the young's modulus and the yield strength have been doubled and quadrupled for composites with low loadings of nanotubes compared to the pure resin matrix samples. Many researchers have shown that fatigue strength of fiber reinforced composite can be improved if the fatigue

performance of the epoxy resin is improved; some literatures show how nanosilica, (HNTTM), and MWCNT have improved the mechanical properties of composite materials (Karapappas, Vavouliotis, Tsotra, & Kostopoulos, 2008, Deng, Ye, & Friedrich, 2007, Johnsen et al., 2007). Addition of 10 wt% of nanosilica showed 6 to 10 times improvement in high cycle fatigue life (Manjunatha, Taylor, Kinloch, & Sprenger, 2009). Based on the author's past research, HNT has shown tremendous improvement in mechanical properties (Tate, Akinola, Pulin, & Massingill, 2009).

Carbon nanotubes in polymer-matrix composites have already been shown to improve the mechanical, electrical, and thermal properties substantially over neat polymer. The increased thermal properties given by small weight percentages of carbon nanotubes could have applications in preventing heat damage to materials with especially low thermal conductivity as well as increasing the thermal conductivity of shape memory alloys and thus decreasing their activation time. Carbon nanotubes have a wide range of potential applications in various technological areas such as aerospace, energy, automotive, medicine, or chemical industry in which they can be used as gas absorbents, templates, actuators, composite reinforcements etc. but the major drawback of CNTs is their high cost.

Halloysite Nanotubes (HNTTM) has been discovered to be excellent in toughening of polymers because of its inherent properties. Impact resistance or damage tolerance of epoxy composites can be improved by improving the resin toughness, unlike thermoplastics where the toughening is achieved by a simple physical blending, in an epoxy resin the same is achieved exclusively through the chemistry. Polymer scientists

discovered some basic criteria for a modifier to be a toughening agent for epoxies; the modifier should be a low molecular weight to ensure miscibility with epoxy resin, it must have functionalities like carbon, amino etc. which can react with the epoxy resin and it must have borderline miscibility so that before curing it remains mixable with the epoxy and undergo a reaction-induced phase separation with the advancement of curing reaction, leading to the formation of a two-phase microstructure (Debdatta, 2007). Looking at the characteristics of (HNTTM), one could conclude that it does have the basic criteria to be a good toughening agent for epoxies.

Nanomodification of polymer helps in improving the fiber/matrix adhesion which reduces the tendency of composite laminate's delamination. This is one of the common failures of turbine blades, leading to low interlaminar shear strength (ILSS) of laminates. Earlier research shows that delamination prior to the gross failure under fatigue loading is one of the major reasons for blade failure (Pancasatya, Samborsky, & Mandell, 2008). In order to improve the fiber/matrix adhesion, almost all the fiber manufacturers have devised means of chemically treating (sizing) of their fibers to become more compatible with matrix, and the resin manufacturers have been toughening their matrix to adhere more with fiber. One of the economically convenient processes of improving matrix to enhance better adhesion is through nanomodification (Blackman, Kinloch, Sohn Lee, Taylor, Agarawal, Schueneman, & Sprenger, 2007; Johnsen, Kinloch, Mohammed, Taylor, & Sprenger, 2007; Yuan, & Van Hoa, 2007).

Polymer Matrix Composites (PMC) is the combination of polymer matrix and reinforcement to make a solid material. Polymer matrix can be thermoplastics or

thermosets. Thermosets are widely used in the industries because of its distinct properties. Reinforcement is in the form of fibers and there are varieties of fibers used in composite manufacturing.

1.2 Reinforcement Materials

Reinforcement for composites vary depending on their intended usage, it can be fibers, whiskers, or particles. Fiber is the most common on the market, and has a great impact that fibers especially long fibers are now being referred to as a new class of solid materials, other reinforcements are also used but due to fiber's distinct properties, it is preferred in the industries. Fibers have one very long axis compared to another with significantly higher strength in the longer direction, and are available in many diameters and lengths including continuous that can be used as is, or chopped to desired shape (Strong, 2008). The list of fiber types includes E-glass, S-glass, carbon and aramid. Their properties are shown in Table 1.1.

Table 1.1: Properties of Typical Fibers (Strong, 2008)

Fiber type	Diameter, micron	Density, g/cm³	Tensile, Strength, MPa	Tensile, Modulus, GPa	Elongation at break,%
E-glass	8-14	2.5	3447	69	4.9
S-glass	10	2.5	4585	83	5.7
Carbon (standard Modulus)	7	1.8	4137	228	1.6
Aramid (Kevlar 49)	12	1.45	3660	83	30

1 2 1 Carbon fiber

Carbon fiber is a very strong, light, and expensive material commonly used in making of composites, it has a very thin fibers with diameters ranging from 0.005 – 0.010 mm and consists carbon atoms which are bonded together in microscopic crystals that are aligned or almost to the long axis of the fiber which makes the fiber strong. Several thousands of carbon fibers are twisted together to form a yarn, which could be used directly or woven into a fabric. Carbon fiber could also be made into weave patterns and its combination with matrix form composite materials. Carbon fiber has been researched to be ideal in many applications due to its high strength-to-weight ratio (high specific strength), and also has a lower density than steel with considerable low weight. Processing temperature in making carbon fibers play a major role in determining carbon properties, heating carbon in the range of 1500 – 2000°C exhibits highest tensile strength while carbon heated from 2500 - 3000°C exhibits a higher modulus of elasticity.

1.2.2 Glass fiber

Glass fiber is made from completely fine fibers of glass. It is made from raw materials like silica sand, limestone, boric acid and other ingredients. It is usually formed from extruding thin strand of silica-based or other formulation glass into many fibers with small diameters. The most commonly type of fiber glass used in industries is E-glass, others like A-glass, C-glass, D-glass, R-glass and S-glass are also being used due to their various distinct properties. Nevertheless, E-glass still makes up most of the fiberglass production in the world. Its specific components may differ slightly in percentage, but usually fall within a particular range. The letter E in E-glass is used because the glass fiber was originally made for electrical applications. The letter S is used in S-glass because it has a high-strength formulation for use when tensile strength is the most important property desired, while C-glass was developed to resist attack from chemicals, mostly acids which destroy E-glass. A-glass was formed with alkaline lime glass with little or no boron oxide and R-glass is a high mechanical requirement glass made of alumino silicate without magnesium oxide and calcium oxide (Loewenstein, 1973).

Pure silica is a major constituent used in making glass fiber but requires a high temperature to work with which constitute a drawback for flexibility in manufacturing temperature but impurities can be introduced into the constituents by the addition of other materials in order to lower the working temperature and also impart other properties to the glass that may be advantageous in different applications. In addition, most glass fibers

are sparingly soluble in water and depend on pH, in most cases chloride ion will attack E-glass surfaces.

Glass fiber has high ratio of surface area to weight and the higher its surface area, the more susceptible it becomes to chemical attack. Glass fiber has a widely applications in making of components where high strength-weight, excellent molded surfaces, dimensional stability, high dielectric strength, and parts consolidation are important (Strong, 2008).

Although, it's optimal usage in corrosion-resistant and electrical products depends on the suitability as well as the performance strength of the matrix used in conjunction with the glass fiber. Glass fibers are fragile and could easily abrade when processing, this could cause a major problem during weaving. In order to avoid loss of strength, which depends on surface defects that might occur during handling, a temporary sizing is applied. Sizing is the process of applying chemicals to the fiber strands in order to protect the fibers during handling and also holds the individual filaments together. In most cases the size is removed after weaving, and finish is applied. Finish is usually added to fiber to enhance its compatibility with the matrix.

1.3 Reinforcement forms

Fibers are available in many oriented forms such as chopped strand mat (CSM), woven fabrics, braided, stitched and knitted fabrics.

1.3.1 Roving and Tow

Roving is the simplest and most common form of glass. It can be chopped, woven or processed and also used in creating secondary fiber forms for composite manufacturing. It is supplied by weight with specific filament diameter. Tows can be wound around a shape as commonly done in filament winding, it can also be twisted into a yarn, or several tows combined into a roving.

1.3.2 Mats

Mats are generally nonwoven fabrics derived from fibers and are held together by a chemical binder. Chopped mats consist of randomly distributed fibers with cut length of around 38mm to 63.5 mm (Composite world, 2010). They are isotropic because of the random nature of the fibers and possess equal strength in all directions. The chemical binder does not give much concern since it dissolves in styrene (a material contained in polyester and vinyl ester resins). Chopped-strand mats (CSM) conform easily to complex shapes, by providing low-cost plastic reinforcement, chopped-strand mats are primarily used in hand lay-up, continuous laminating, and some closed molding applications.

Stronger than chopped-strand, continuous-strand mats are formed by swirling continuous strands of fiber onto a moving belt, and finished with a chemical binder to hold fibers in place. A non-dense fiber arrangement accepts a high ratio of resin to fiber, which results in a thick, smooth, resin-rich finish. It is usually used in non-critical applications, as most applications of composites are non-critical (Composite world, 2010).

1 3.3 Woven Fabrics

Woven fabrics are usually made on looms with different weaves and widths. They are bidirectional and provide high strengths in yarn direction, but the tensile strength is always compromised because fibers are crimped as they pass over and under one another during the weaving process. This is commonly used in applications that require thick reinforcement especially in hand lay-up and VARTM. Several different weaves are used for bi-directional fabrics. In a plain weave, each yarn or roving alternately crosses over and under each warp fiber. Harness satin and basket weaves, in which the yarn or roving crosses over and under multiple warp fibers at a time, are more pliable and conform easily to curved surfaces. Due to its relatively coarse weave, woven roving wets quickly; it is relatively inexpensive and results in a thick fabric used for heavy reinforcement, especially in hand lay-up operations (Kelkar & Whitcomb, 2006).

1 3 4 Braided Fabrics

Braided fabrics are continuous weave process that has at least one of its axial yarns not crimped in the weaving process. This is commonly done by having intertwining three or more yarns and not twisting any two yarns around each other. This ingenious process gives braided fabrics stronger strength and greater strength-to-weight than woven. The quasi-isotropic formation within a single layer tends to eliminates problem associated with layering of multiple fabrics with other formations and it also reduces delamination which is the cause of most failures in composite. Braids are widely used in the industry

because of the possibility of maximizing properties in all directions of a part (Strong, 2008).

1.3.5 Knitted fabrics

Knitted fabrics are formed by simply placing yarns atop one another in practically any arrangement and stitching them. Orienting all strands in one direction, for example, results in a fabric with greater flexibility. Placing the yarns on top, rather than over and under each other, makes greater use of their inherent strength. Since they have no crimped fibers, knitted fabrics are more pliable than woven. Due to the wide variety of yarn orientations and fabric weights, knitted fabrics are tailored to individual customer requirements. They are much more elastic and are not available in lightweights (Strong, 2008).

1.4 Different weave types

The Figure 1.1 below displays some of the common types of weaves available. The fabric or long direction is commonly called warp direction while the cross or width direction is called the fill or weft direction.

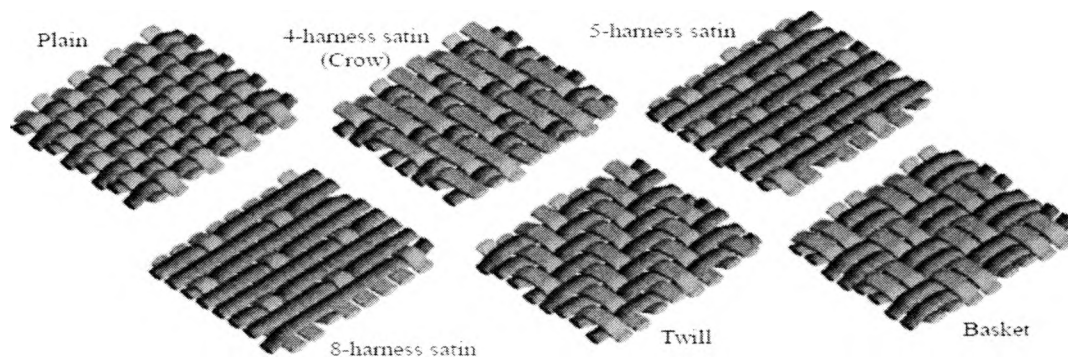


Figure 1.1: Different Weave Patterns: Plain, Twill, Satin and Basket (Whitcomb and Tang, 1999)

The Plain weave is the simplest of the weave patterns, the warp and weft are aligned, and are made by interlacing yarns in an alternating over-and-under pattern. There is usually one warp fiber for one fill fiber. It has a peculiar checker board like appearance. This pattern gives uniform strength in both directions when yarn size and count are similar in warp and fill. The weave is considered stiff and stable which usually left moderately open for good resin penetration and air removal.

In the crowfoot satin weave, one warp yarn is taken over three and then under one fill yarn. This produces a weave with improved unidirectional quality with more strength in the fiber directions than with plain weave. The fabric is more pliable and can comply with complex contours and spherical shape (Strong, 2008).

The long-shaft or 8-harness satin weave typically has one warp yarn weaving over 7 fill yarns then under one fill yarn. It has a high degree of drape and stretch in all directions. This weave is less stable and open than most weaves, therefore, it requires vacuum for resin impregnation and air removal. It is widely used in applications that

require complex shape formation and contoured surfaces. 5-harness satin weave follows the same pattern (Composite world, 2010).

Basket weave is similar to the plain weave except that two warp yarns are woven as one over and under two fill yarns. It is less stable than plain weave and has similar usages but it drapes on mild contours. Twill is formed with a diagonal parallel pattern. It is made by passing the weft yarn over one or more warp yarns. It usually has some form of offset between rows to create the characteristics diagonal pattern, it drapes because of this pattern. Twill fabrics usually have the front and the back sides unlike plain weave that both sides are the same. Twill recovers better from wrinkles than plain weave fabrics. It requires vacuum for good resin impregnation and air removal (Composite world, 2010).

1.5 Resins

Resins are one of the most important components of polymer matrix composites. While the loads are essentially carried by fibers, modulus and failure strain depends on resin/matrix adhesion in the performance of composites. It also determines the type of fabrication process, service temperature, and flammability and corrosion resistance of the composite. Many researchers have considered different resin systems, and it was proven that for wind turbine applications, epoxy is well suited. Thermosets and thermoplastics are commonly used matrix systems.

Thermoplastic resins become soft when heated, may be shaped or molded while in a heated semi-fluid state, and become rigid when cooled. Thermoset resins are usually liquids or low melting point solids in their initial form. When used in making finished

goods, these thermosetting resins could be cured at room temperature or under high heat depending on the desired properties. Unlike thermoplastic resins, once cured, solid thermoset resins cannot be converted back into their original liquid state. Cured thermosets will not melt and flow, but will soften when heated (and lose hardness), and once formed, they cannot be reshaped. Heat Distortion Temperature (HDT) and the Glass Transition Temperature (T_g) are used to measure the softening of a cured resin. Both test methods (HDT and T_g) measure the approximate temperature where the cured resin will soften significantly to yield (bend or sag) under load (MDA Composites, 2009).

Table 1.2: Properties of Typical Polymer Matrix Materials

Matrix type	Liquid Density g/ml	Tensile strength, MPa	Tensile modulus GPa	Coefficient of thermal expansion, 10 ⁻⁶ /°F	Glass transition temperature, T _g , °F
Unsaturated Polyester	1.1-1.5	5.8-13	0.46-0.51	33-110	50-110
Vinyl ester	1.23	12.5	1.5	212-514	220
Epoxy	1.20	60-75	2700-3200	59-212	140-176

Unsaturated Polyester: AROPOL 7241T15, Ashland Speciality Chemicals, Inc.
 Vinyl ester: Derkane Momentum 510-A40, Ashland Speciality Chemicals, Inc. Epoxy: Epikote RIM 135, Hexion Speciality Chemicals.

Table 1.3: Advantages and Disadvantages of Thermosetting Resins (Zac-Andrew, 2006)

Polyester	
Advantages	Disadvantages
Easy to use	Moderate mechanical properties
Cheap resin cost	Very high cure shrinkage
	Low working time before curing
Vinylester	
Advantages	Disadvantages
Very high chemical/environmental resistance	Possession of high styrene content
Higher mechanical properties than polyesters	Higher in cost than polyesters
	Very high cure shrinkage
Epoxy	
Advantages	Disadvantages
High mechanical and thermal properties	More expensive than vinyl esters
High water resistance	Critical mixing
Long working times available	Corrosive handling
Low cure cycle, Improved surface finish	

Thermosetting plastics have a number of advantages, unlike thermoplastics, they retain their strength and shape even when heated. This makes thermosetting plastics well suited to the production of permanent components and large, solid shapes. Additionally, these components have excellent strength attributes (although they are brittle), and will not become weaker when the temperature increases (Thomasnet, 2008). The most common thermosetting resins used in the composites industry are unsaturated polyesters, epoxies, vinyl esters, polyurethanes, and phenolics.

1.6 Epoxy Resin

The composite industry is dominated by thermosetting resins like epoxy, unsaturated polyester and vinylester because of their availability, relative ease of processing and low material cost. Thermosetting resins are available in oligomeric or monomeric low viscosity liquid forms, which have excellent flow properties to facilitate resin impregnation of fiber bundles and proper wetting of the fiber surface by the resin. They are characterized by cross linking reaction, and because of this reaction; thermoset composites offer better creep properties and environmental stress cracking resistance compared to many thermoplastics (Debdatta, 2007).

Thermoset composites also form a major portion of the interior finishing in modern commercial aircrafts and in semi conductor devices. Epoxy is one of the most widely used matrices for carbon fiber reinforced composite materials by virtue of its good impregnation and adhesion to carbon fiber. The development of 177°C cured epoxy systems can provide composite materials for structural applications in aircraft. (Yuan & Suong, 2008)

Epoxy is a thermosetting polymer formed from the chemical reaction of epoxide and polyamine; it consists of monomer with epoxide group at both ends. Epoxy resins are basically produced from a reaction between epichlorohydrin and bisphenol-A. Hardener consists of polyamine monomer and when they react together, the amine groups react with the epoxide groups to form a covalent bond. Each NH group can react with an epoxide group to result in high crosslinking and thereby become strong and rigid

polymer. The curing reaction of epoxy is shown in figure.1.2. Curing of epoxy can be performed at ambient temperature or can be controlled by temperature.

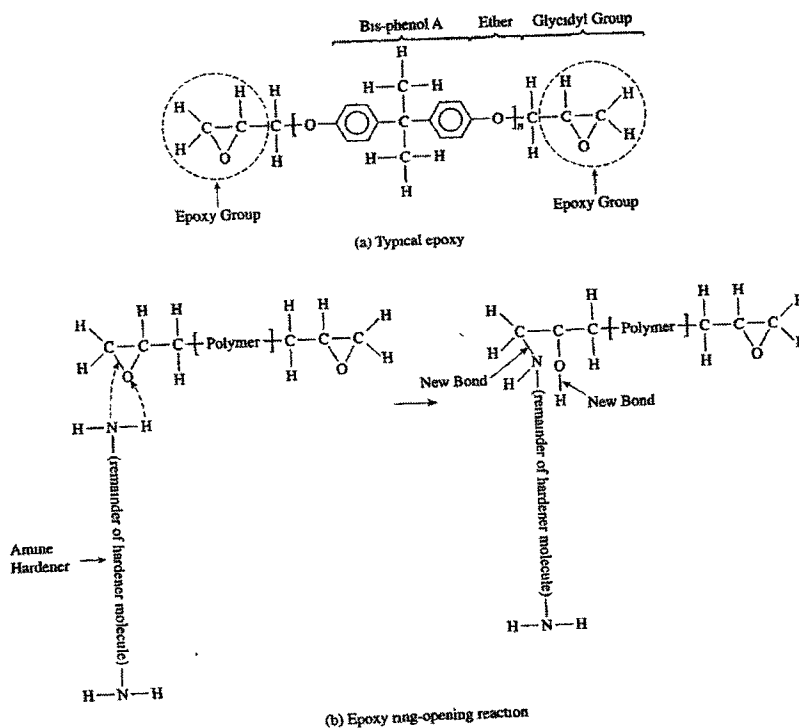


Figure.1.2 Curing reaction of Epoxy

Epoxyes have excellent adhesion, chemical and heat resistance. It possess excellent mechanical properties and very good electrical insulating properties, many of these properties can be easily modified which makes epoxy an ideal and frequently used resin amongst researchers and in general industrial applications. As of 2006, the epoxy industry amounts to more than US \$5 billion in North America and about US \$ 15 billion worldwide. Epoxyes are modified by formulators to be usable to smaller end users by adding; mineral fillers in improving its properties, adding flexibilizers to reduce the

viscosity, accelerators and thickeners to promote adhesion. Modifications on epoxy is basically done to reduce costs, improve performance, and to improve processing convenience. In the aerospace industry, epoxy is used as a structural matrix material which is then reinforced by fiber. Epoxies are also used as structural glue; materials like metal, wood, glass, stone and plastics are glued with epoxy. Epoxies are used as coating, which dries quickly and provides tough UV resistant and abrasion resistance. Fusion bonded epoxy powder coatings (FBE) are commonly used for corrosion protection of pipes in the oil and gas industry, pipes used in transferring household water are also coated with epoxy. Epoxy coatings are also used as primers in improving the adhesion of automotive and marine paints on structural surfaces where corrosion resistance is pertinent (May, 1987).

Lately, different kinds of nanoparticles have been discovered and added in the polymer to improve its performance. This improvement could be made possible because nanoparticles have very high surface-to-volume ratio, creating nanometer scale structures. It is possible to control fundamental properties of materials like their melting temperature, magnetic properties, charge capacity, and even their color. Epoxy nanocomposites is the combination of epoxy and bisphenol as the matrix and fiber as the reinforcement, the combination of epoxy and bisphenol could be enhanced with nanoparticles with resultant nanocomposites often having properties superior to conventional composites and this is usually achieved at a much lower weight-percent (loading) of nanoparticles compared to conventional micron-sized particles (Mingliang et al., 2006).

1.7 Nanomodification of Polymers

Nanotechnology is the understanding and control of matter at dimensions of roughly 1 to 100 nanometers, where unique phenomena enable novel applications. A nanometer is one-billionth of a meter. The introduction of inorganic nanoparticles as additives into polymer systems has resulted in polymer nanocomposites (PNCs) exhibiting multifunctional, high-performance polymer characteristics beyond what traditional filled polymeric materials possess (Koo, 2006). Polymer nanocomposites can also be more inclusively referred to as polymer nanostructured materials (PNMs). Uniform dispersion of nanoparticles produces ultra large interfacial area per volume between the nanoparticle and the host polymer. Carbon nanotubes, Nanoclay, Halloysite nanotubes (HNTTM) and Nanosilica are few of the commonly used nanoparticles in the industry and are discussed in the next section.

1.7.1 *Carbon nanotubes*

The addition of carbon nanotubes (CNT) with epoxy as a structural element in nanocomposites has shown a great improvements in material properties. The applications range from devices in nanoelectronics to field emitters. There are two main types of carbon nanotubes that can have high structural perfection; Single walled nanotubes (SWNT), which consists of a single graphite sheet seamlessly wrapped into a cylindrical tube. Multiwall nanotubes (MWNT), comprises an array of such nanotubes that are concentrically nested like rings of a tree trunk. Research shows that polymers adhered well to CNT at the nanometer scale when examined through transmission and scanning

electron microscopy, which explained why the properties of electrons inside matter and atomic interactions are influenced by materials variations on the nanometer scale (Yueping et al., 2007).

Past research shows that the young's modulus and the yield strength have been doubled and quadrupled for composites with low loadings of nanotubes compared to the pure resin matrix samples. There are many methods used to successfully synthesize carbon nanotubes like arc discharge, laser ablation, and chemical vapor deposition etc. The unique electrical properties of carbon nanotubes are to a large extent derived from 1-D character and the peculiar electronic structure of graphite; they have extremely low electrical resistance. Carbon nanotubes are expected to have high stiffness and axial strength as a result of the carbon-carbon SP^2 bonding. CNT have been shown to have a thermal conductivity at least twice that of diamond. The specific heat and thermal conductivity of carbon nanotubes systems are determined primarily by photons (Bose, Khare, & Moldenaers, 2010). CNT is also used in composites for thermal management. Pristine CNT are chemically untreated carbon nanotubes, they are used in their natural state or as produced with no alteration to enhance their properties while functionalized CNT are chemically treated to enhance their properties. Scanning electron image analysis by some authors have shown that chemically functionalized MWCNTs have higher interfacial bonding strength with epoxy matrix than as produced or pristine MWCNTs. A high electrical conductivity at low loading concentration of as produced SWCNTs and as produced (pristine) MWCNTs have been reported.

Direct dispersion of nanoparticles in a polymer matrix is one of the methods for synthesizing of nanocomposites. Technologies are available for synthesis of a wide range of nanomaterials such as silicon whiskers, carbon nanotubes and so on. Research shows that CNT tend to agglomerate as bundles in solvents or in the host resin and if dispersed, re-agglomerates quickly thereafter due to electrostatic attraction. Uniform dispersion within the polymer matrix and improved nanotubes/matrix wetting and adhesion are critical issues in the processing of these nanocomposites. Use of silane coupling agents and initiating the chemical bonding between CNT and the polymer matrix have been reported for improvement of the dispersion and the final properties of the nanocomposites (Debdatta, 2007). In composites, matrix-CNT interfacial bonding is a critical parameter which controls the efficiency of stress transfer from CNT to the matrix, and then dictates the mechanical properties of the composites. However, since the magnitude of CNT strength is very high; almost 10 times higher than typical carbon fiber, very high interfacial shear strength may be required for more efficient strengthening of polymer with CNTs.

Carbon nanotubes in polymer-matrix composites have already been shown to improve the mechanical, electrical, and thermal properties substantially over neat polymer. The increased thermal properties given by small weight percentages of carbon nanotubes could have applications in preventing heat damage to materials with especially low thermal conductivity as well as increasing the thermal conductivity of shape memory alloys and thus decreasing their activation time. Carbon nanotubes have a wide range of potential applications in various technological areas such as aerospace, energy,

automotive, medicine, or chemical industry in which they can be used as gas absorbents, templates, actuators, composite reinforcements etc. Cost is the major drawback of CNTs which limits its usage in the industry and for research purposes (Strong, 2008).

1 7.2 Nanoclay

The general interest in clay-polymer has been on increase ever since Toyota demonstrated commercial applications of nylon 6/clay nanocomposites (Balakrishnan & Raghavan, 2005). Polymer-clay nanocomposites (PCN) is one among very few areas in the field of polymer technology which has drawn considerable interest in recent years, which is mainly due to the low cost of clay and well developed intercalation chemistry which makes it possible to achieve a nanostructure from a micron size filler. Hence, PCN technology can avoid the potential health hazards involved in other nanomaterials technology (Debdatta, 2007).

Reinforcement of polymeric resin with nanoclay platelets has resulted in lightweight materials with enhanced mechanical and thermal properties. This improvement in properties of resin can be extremely useful given that traditional carbon fiber / organic matrix based composites have less desirable properties through the thickness or Z – axis direction because of the polymer matrix (Yueping et al., 2007). This idea of adding clay to matrix material is definitely appealing if cost reduction, high thermal inertness, and environmental friendly characteristics are desired. Poor dispersion of hydrophilic clay into organic polymer matrices has been a hindrance in the general use of nanoclay platelets in thermoset and thermoplastic polymeric materials. The clays are made up of a

crystal lattice (0.95 nm thick layer) stacked together. A layer consists of two tetrahedral sheets fused to one octahedral sheet of either aluminum or magnesium hydroxide (2:1 layers). These 2:1 layers are not electro statically neutral (Debdatta, 2007).

The nanoscale particles possess enormous surface area. Hence, the interfacial area between the two intermixed phases in a composite is substantially larger than the traditional composites, which results in better adhesion between the matrix and the particle. Therefore, several mechanical, thermal, and electrical properties of nanocomposites are observed to be better than those of conventional micro composites or the neat matrix resin (Yueping et al., 2007). Currently, nanoclay – filled composites account for almost 25% by volume of total nanocomposites usage and their market share is rapidly increasing. The relatively low cost of nanoclay, rising energy and polymer prices are contributing to the increase use of clays as filler to achieve savings of matrix polymers.

Clay-Epoxy nanocomposites have attracted considerable technological and scientific attention because it offers a wide array of property improvements at very low filler content. Epoxy-organoclay nanocomposites have been studied by some researchers and their results include; significant increase of modulus at a low clay loading, improvement of both stiffness and toughness, increase of elongation-at-break while increasing tensile strength, decrease of glass transition (T_g) for some aromatic amine cured epoxies and increase of T_g for an aliphatic amine cured epoxy (Yueping et al., 2007). Agglomeration occurs in polymer nanocomposites by the clumping together of the clay platelets in the polymer, this does not improve the properties of the polymer. Intercalation is the process

of inserting nanoparticle in nanoscale level into polymer; which usually results in enhanced properties of the polymer, the platelets are still close together in a similar pattern and could increase the properties of the polymer but not as much as when it is randomly dispersed while exfoliation is the breaking of the nanoparticles into tiny nanoscale layers and randomly dispersed in the polymer (Koo, 2006).

In-situ synthesis is a very common method for making thermoset/clay nanocomposites. Organoclay is first intercalated with monomers then the clay layers are expanded in subsequent polymerization. In – situ synthesis, the nanocomposites morphologies are largely determined by the relative rates of intra-gallery and extra-gallery reactions. The interlayer distance increases with the progress of the intra-gallery reaction, and is suppressed by the extra gallery reaction. Faster diffusion of the reactive species into clay galleries might enhance the intra-gallery polymerization (Balakrishan & Raghavan, 2005).

Clay containing polymeric nanocomposites has several advantages over the matrix polymer or classical composites. The main improvements are in; modulus, impact strength, heat resistance, dimensional stability, barrier properties, flame retardancy, optical properties, ion conductivity, and thermal stability. However, complete exfoliation of nanoclay pose a significant challenge in various types of polymers. The development of simple and cost effective processing methods that lead to the complete exfoliation will result in the widespread application of these composite materials. Nanocomposites have many applications in aerospace, automotive structure, food packaging, electronics, and bio-medical applications. Although, it has been proved by many researchers that adding

some clay could enhance the nanocomposites properties but adding more clay might not guarantee a further improvement, which is basically due to increase in viscosity of the epoxy on the addition of the clay and the augmentation of the amount of air bubbles during the mixing process (Xu & Hoa, 2008).

1.7.3 Halloysite Nanotubes (HNTTM)

Halloysite nanotubes (HNTTM) are naturally formed in the earth over millions of years, they are unique and versatile nanomaterials that are formed by surface weathering of aluminosilicate materials and unlike carbon nanotubes are composed of aluminum, silicon, hydrogen and oxygen. HNTTM are ultra tiny tubes with diameter typically smaller than 100 nanometers (100 billionths of a meter) with lengths typically ranging from about 500 nanometers to over 12 microns (Naturalnano, 2009).

According to Natural Nano, Inc., Halloysite nanotubes might one day be used for odor masking in household products or to add scents to cosmetics, to create light weight durable plastics and polymers for cars, air planes, and computers, to developing timed release drug delivery using non-synthetic delivery vehicles and to create radio frequency blocking paints. Furthermore, HNTs have been embraced in the composite world due to its easy process ability, HNTs do not require large amounts of chemical modifications or complex chemical process such as intercalation and exfoliation in order to produce stable nanoparticle dispersion in the melt, this makes it possible to obtain performance improvements without the complexity and processing cost associated with many clays.

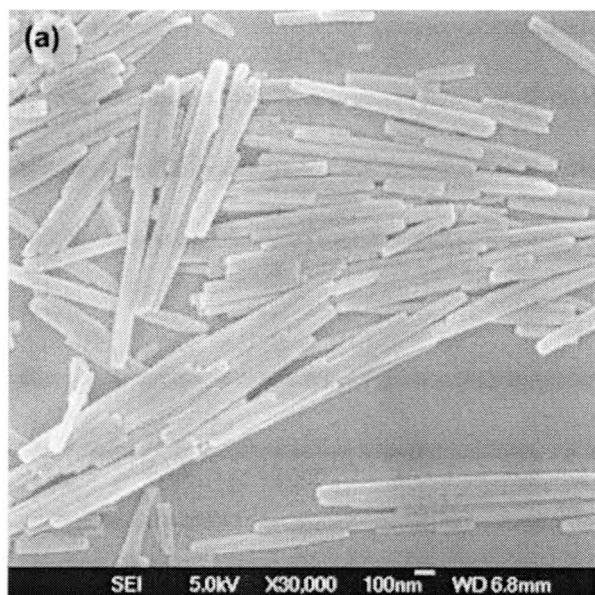


Figure 1.3 Morphology of Halloysite Nanotubes (Yueping et al. 2007)

Halloysite nanotubes provide a new avenue for the preparation of nanocomposites with promising improvements, the functional characteristics desired for specific application can be controlled and influenced through selection of nanotube diameter and length. HNTTM could be modified and add to other materials to achieve a wide range of electrical, chemical and mechanical properties. Chemically, the outer surface of the halloysite nanotubes has properties similar to SiO₂ while the inner cylinder core is related to Al₂O₃ (Cuiping, Jiguang, Xiaozhong, Baochun, & Zhenzhong, 2008).

The charge behavior of halloysite particles can be roughly described by superposition of mostly negative (at pH 6 – 7) surface potential of SiO₂ with a small contribution from the positive Al₂O₃ inner surface. The positive (below pH 8.5) charge of the inner lumen promotes loading of halloysite nanotubes with negative macromolecules, which are at the same time repelled from the negatively charged outer surface

(Naturalnano, 2009). HNTs are chemically similar to kaolinite. A range of active agents, including drugs, nicotinamide adenine dinucleotide (NAD), and marine biocides can be entrapped within the inner lumen as well as within void spaces of the multilayered aluminosilicate shells. This entrapment can be followed by retention and release of the agents, making the halloysite a nanomaterial well suited for macromolecular delivery applications. Both hydrophobic and hydrophilic agents can be entrapped after an appropriate pre-treatment of the halloysite surface (Naturalnano, 2009). HNTs are aluminosilicates with predominantly tubular structure at nanoscale and the surface of HNT is composed of siloxane and has only a few hydroxyl groups which indicate that HNTs possess much better dispersion property than other natural silicates such as montmorillonite and kaolinite (Mingliang et al., 2006). Research shows that halloysite nanotubes appear to perform as well as clay composites with the added benefit that you can load them with various materials to add additional function with minimal impact.

Several researches have shown that HNT modified polymers show tremendous increase in material strength and modulus without sacrificing ductility and to provide highly uniform compounds with reduced weight and better heat resistance. Substantial toughening of brittle polymers without sacrificing other important properties is a long time challenge in manufacturing of composites. Toughening of polymers is achieved by adding rubbery modifiers, where fracture energy is dissipated via plastic deformation of the matrix induced by rubber particles (Yueping et al., 2007).

HNTs have been discovered to be excellent in toughening of polymers because of its inherent properties. Looking at the characteristics of halloysite nanotubes, one could

conclude that it does have the basic criteria to be a good toughening agent for epoxies. It is also cheap; however, it has a time consuming dispersion process. Past researches indicate that epoxy resins can be toughened effectively by rubber, but addition of rubber also results in decrease of the desired mechanical and physical properties like modulus, strength, and thermal stability. Toughening efficiency of rigid micro-sized particles is much lower than that of rubbers due to various reasons including that rigid particles cannot effectively stabilize or stop crack propagation (Yueping et al., 2007). The coefficient of thermal expansion (CTE) of HNTTM with epoxy/cyanate has been found to be substantially lower than that of the neat resin and the module of the hybrids in the glassy state and rubbery state were significantly higher than the neat epoxy resin (Mingliang et al., 2006).

Ye et al. (2004) have studied that the morphology of the HNTTM was geometrically similar to multi-walled carbon nanotubes. They blended epoxy with HNTTM in different loadings 0.8, 1.6, and 2.4%. The results demonstrated that blending epoxy with 2.3 wt% HNTTM increased the impact strength by 4 times without scarifying flexural modulus, strength and thermal stability. In last 3-4 years, researchers have reported mechanical and thermal properties improvement in thermoplastics nanocomposites and elastomeric nanocomposites using HNTTM (Ye et al., 2004; Li et al., 2008). There are very few attempts made to use HNTTM in reinforced composites.

Tate et al. (2009) used both nanosilica and HNTTM (Haloysite Nanotubes) to modify polyurethane matrix. This nanomodified polyurethane was further used to make glass

reinforced composites. For 0.8 wt% loaded HNT™ modified composites, flexural strength, flexural modulus, and ILSS were increased by 6%, 28% and 82%, respectively. For 7.5 wt% loaded nanosilica modified composites, compressive strength, flexural strength, flexural modulus, and ILSS increased by 135%, 64%, 34%, and 120%, respectively. These results are very promising even considering complex formulation of polyurethane resins.

1 7.4 Nanosilica

The introduction of nanoparticles in low viscosity reactive resins such as epoxies, vinyl ester, and phenolic results in a rapid increase in viscosity as the nanoparticle content is increased to 5 to 7 wt% by weight and leads to limited use in processes that demand “low-to –medium” viscosity such as VARTM. A novel technique developed by Hansie Chemie of preparing “macrosurfaced silica” appears to avoid the increased viscosity problem with ≥ 10 wt % nanosilica (Koo, 2006). The spherical silica particles (typically 20 nm), when combined with the right monomers or prepolymers give Nanopox F400 a significant lower viscosity yield even with particle loading up to 50 percent. It has been observed that Nanopox F400 could improve fatigue performance ten folds in composites (McConnell, 2010).

Manjunatha et al. (2009) performed tension-tension fatigue studies on nanomodified epoxy resin system. They used predispersed nanosilica; micron-rubber; and both nanosilica and micron rubber from Nanoresins AG, Germany to modify epoxy resin.

Addition of 9 wt% of micron-rubber, 10 wt% of nanosilica, and combination of both showed 6 to 10 times improvement in high cycle fatigue life. Tensile strength and modulus with 10 wt% nanosilica were improved by 18% whereas tensile strength and modulus decreased when only micron-rubber or combination of micron-rubber and nanosilica was used. These results are very promising and clearly show that the use of such particle- toughened epoxy polymers as matrix materials in PMCs could improve fatigue behavior without sacrificing on in-plane properties. There are very few attempts made to use nanosilica in reinforced composites.

This research used Nanopox F400 nanosilica that is specially designed for epoxy resin. Nanopox F400 contains 40% of SiO_2 dispersed in epoxy resin by the producer; Nanoresin AG. Germany. Nanopox technology is designed to boost not only the performance of epoxy but also vinyl ester, acrylic and other chemistries as well (McConnell, 2010).

1.8 Manufacturing Methods

There are many methods available such as layup processes and VARTM. VARTM is a closed mold and low-cost process with the capability of making complex and huge parts such as wind turbine blades. Each of these fabrication processes has distinct characteristics that suit different types of composites. This is advantageous because the

best solution process can be used for a specific desired material application.

Manufacturing methods are explained in details in chapter 2.

1.9 Fatigue of Composites

Almost 70% of structural failures are due to fatigue. The fatigue mechanism in composites is much more complex than that of metals. The damage may be in one or more forms, such as failure in a fiber-matrix interface, a matrix cracking, delaminations, and final fiber breakage. Both matrix cracking and delamination reduce stored energy and stiffness. Detectable damage can be found very early in the fatigue life. The damage causes a reduction of elastic properties such as stiffness. There is always a correlation between damage and stiffness reduction. Since the reduction of stiffness (or damage) occurs long before the composite is in danger, the definition of fatigue failure in composite materials may change from one application to another. The following section discusses the fatigue mechanism in composite materials.

Fatigue usually occurs in composite laminates through the progressive localized defect in materials when exposed to increase in both stresses and strains. Materials under some form of load could return to its initial condition or shape when the load is removed and the maximum stress observed is lower than the ultimate tensile limit of the tested material. Fatigue of composite materials subjected to cyclic loading depends not only on the maximum stress observed but also on the number of times or cycles the same load is repeated. Static loading has been observed to be less severe in material failure than cyclic

loading which involves repeated loading. Moreover, materials especially composites tend to fail quickly under cyclic loading than static loading. Ruptures usually occur when loadings are thousands or millions of times on the same material. However, it is possible to expose a particular material to loadings repeatedly few or hundreds of times without failure provided the ultimate tensile limit of the material has not been reached.

It is therefore pertinent for designers to have good knowledge of composite materials and the techniques of predicting material failures in order to avert failure in their designs; increase their productivity and also have dependable end products.

1 9 1 The Stress Life Approach

Some good knowledge of fatigue characteristics for material or its combination is important to be certain about the durability of composite material and its performance. Wohler introduced the concept of endurance limit; in which the applied stress amplitude and materials with stresses below it could have an infinite fatigue life. Wohler's empirical method is widely acceptable in fatigue analysis. However, it did not account for plastic deformation during cyclic loading (Talreja, 1987).

Wohler's curves or S/N curves is constant amplitude testing in which specimens are tested between maximum and minimum stress, or strain level until failure. Total life could be defined as the total number of load cycles needed to initiate fatigue cracks in the sample specimen plus the number of cycles to propagate the dominant fatigue crack to failure. In the S/N curves, S is the applied strain, strain is chosen because both matrix and reinforcement would be subjected to the same strain but different stresses, and N is the

number of load cycles. S is usually in linear scale while N is in logarithm or semi logarithm. In this research, constant amplitude stress loading was used as per ASTM 3479. The fatigue parameters are shown in figure.1.4

$$S_{amp} = \frac{S_{max} - S_{min}}{2}$$

$$S_{amp} = \frac{S_{max} + S_{min}}{2}$$

Where,

S_{max} is the maximum stress

S_{min} is the minimum stress

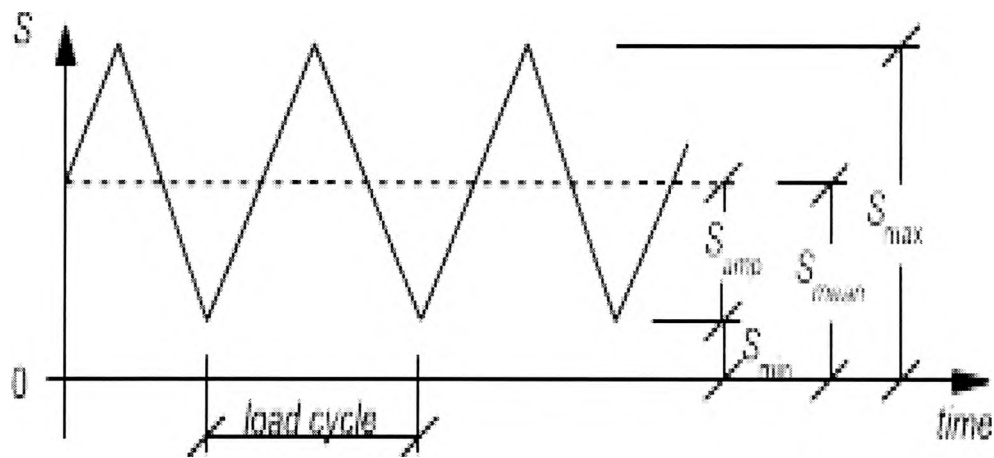


Figure.1.4 Nomenclature for constant stress amplitude loading

1.9.2 Fatigue Behavior in Polymers

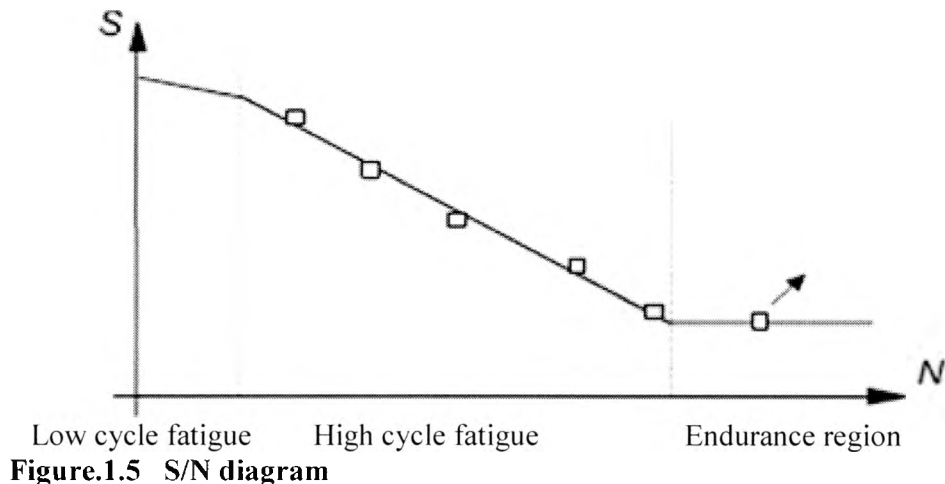


Figure.1.5 S/N diagram

In composite materials under constant amplitude loading, it shows high stress life plot above 10^6 fatigue cycles and below this level, the material exhibits infinite fatigue life with little or no crack propagation. The stress level at which materials show infinite fatigue life is called “endurance limit”.

According to Talreja (1987) S/N diagram could be successfully divided into three regions where by the first region is called the low cycle fatigue; it is a region with maximum stress level in the load cycle and also with low number of cycles to failure. It is craze dependent and in the absence of maximum tensile stress large enough to form craze, this first region may not exist. The middle region is the region with high cycle fatigue and the graph exhibits a straight line, this region is usually around 10^6 and 10^7 load cycles before failure. The slow growth of crazes and their transformation into cracks usually occur at the high end of the middle region. The third region is called the

endurance region which could withstand 10^6 to 10^9 numbers of cycles. Fatigue life in the third region is controlled by the incubation time for the nucleation of microscopic flaws. Most engineering materials are designed based on stress level close to the endurance limit but it is unfortunate that some materials do not have endurance limit which make their stress level to be different.

Fatigue life of a material is usually different under constant amplitude loads and maximum applied load with vary minimum load.

$$R = \frac{S_{min}}{S_{max}}$$

Whereby,

R is the changed amplitude

S_{Min} is the minimum load

S_{Max} is the maximum load

The fatigue life of most materials will decrease with increasing mean stress level which decrease R – value. The interval $0 < R < 1$ represent tests under tension/tension loads and $R > 1$ represents compression/ compression loading. The nucleation and formation of small cracks are the two common phases involved in a material before fatigue failure. Damage nucleation is a major part of fatigue life and nucleation phase varies between specimen samples regardless of materials. In this research R ratio of 0.1 is used. The stress level corresponding to 10^6 cycles is evaluated. It is observed that the material system used in this research (Glass/Epoxy) does not have endurance limit.

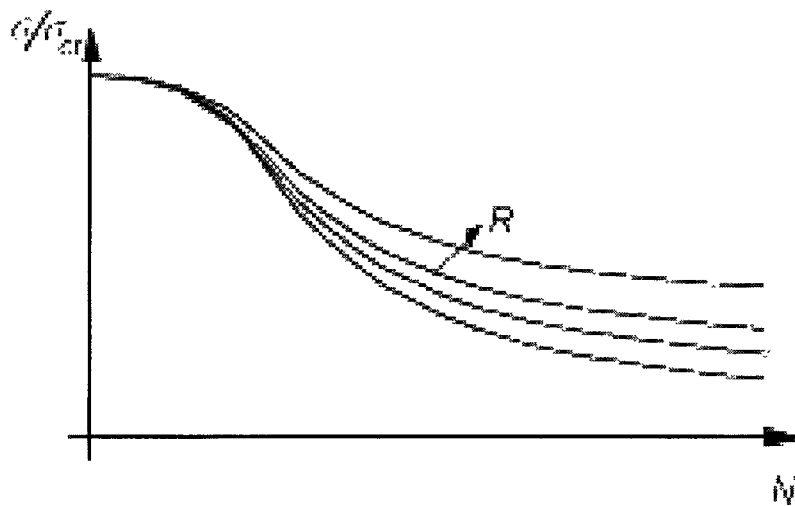


Figure 1.6 S/N Diagram for different R- values

Fatigue damage modeling is difficult because of several damage mechanisms (matrix cracking, fiber/matrix debonding, delamination, and fiber breakage) and the heterogeneity in test specimens. It is impossible to produce specimens with identical microstructural features. Therefore, a material damage model including all the damage states is difficult to establish.

Fawaz & Ellyin (1995) proposed a semi-log linear relationship between applied cyclic stress S and the number of cycles to failure N for laminated composites:

$$S = S_u (m \log N + b) \text{ where,}$$

S_u is the mean static strength, and m and b are constants. Low values of m and high values of b indicated higher fatigue strength. This is the most popular linear model used in conventional laminated composites.

1.9.3 Material Degradation due to Fatigue Loading

There is an increase in strain under constant amplitude stress loading. This phenomenon is typically known as creep. This increase in strain ultimately reduces stiffness of the composite. The stiffness reduction is a means of evaluating fatigue damage in composites.

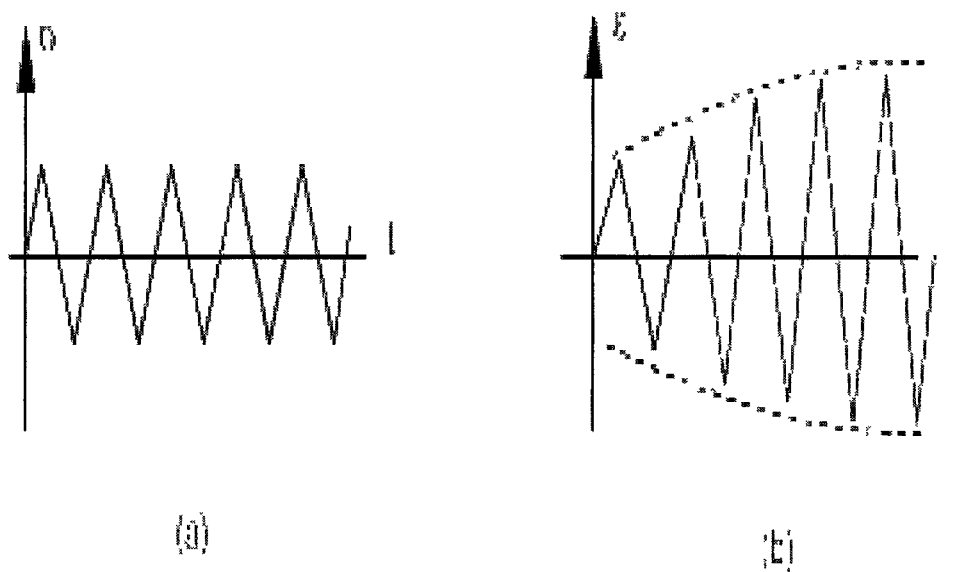


Figure 1.7 (a) Stress controlled loading and (b) The strain response due to cyclic softening

1.9.4 Fatigues under Loading Parallel to Fibers

The microscopy damage mechanism in tensile fatigue of fiber reinforced composites are divided into three parts namely (a) Fiber breakage, interfacial debonding (b) matrix cracking (c) interfacial shear failure. It has been observed that the three types of damages

may occur simultaneously and different modes of damage interact with each other (Owen, 1974).

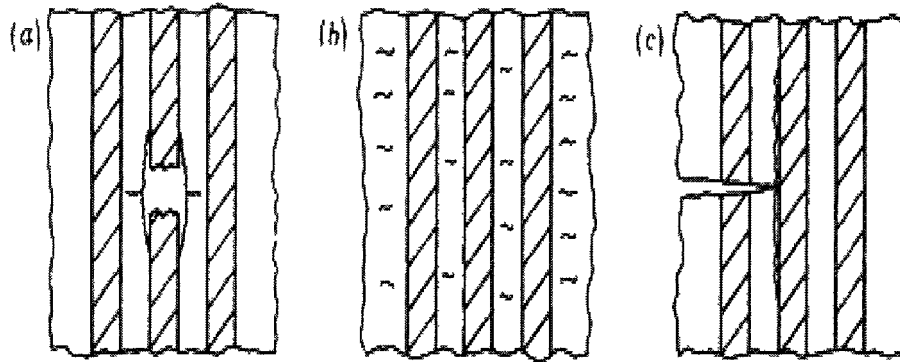


Figure 1.8: Fatigue damage mechanisms in unidirectional composites under loading parallel to fibers: (a) fiber breakage, interfacial debonding; (b) matrix cracking; (c) interfacial shear failure (Talreja, 1987).

Fiber breakage usually occurs at stresses that exceed the strength of fiber with the least strength from the array of fibers in composite. Stress distributions in matrix and fibers differ for different fiber arrangements and contribute significantly to the failure of fibers.

The breaking of an isolated fiber causes shear-stress concentration at the interface close to the broken fiber which may cause failure of the interface leading to debonding of the fiber from the matrix that surrounds it. Longitudinal tensile stress usually concentrates at the debonded area which leads to a transverse crack in the matrix whenever the magnified tensile stress exceeds fracture stress (Talreja, 1987).

Matrix cracking is the first damage observed in fatigue failure (Talreja, 1987). They do not necessarily change mechanical properties of materials but create an accessible

pathway for corrosive agents that cause degradation. Adequate knowledge of matrix cracking is essential for designers in designing durable materials because micro cracks are the starting points of events that lead to potential failures.

It is often difficult to verify micromechanics damages because of the interaction between interface debonding and matrix micro-cracking. In detecting micro mechanics damages, researchers have been using appropriate sizing on fibers to suppress interface debonding in composite materials. Transverse cracks usually start at the specimen's free edges, then increases and expands towards the specimen center. In the early life of specimen, the numbers of cracks are always few and short in size and as the number of cycle increases, the cracks become larger and closer to each other. A substantial analysis of crack development in fatigue tests can be done through microscopic and radiographic observations (Talreja, 1987).

Interfacial shear failure - An interface is a thin layer in composites that comprise of matrix and fiber materials that are bonded together. Interface is a region where size and matrix diffused into each other's domain; it is responsible in transferring load from the matrix to the reinforcement (Strong, 2008).

The optimal performance of a composite material depends solely on the reinforcement/matrix interface (Mallick, 1993). Good adhesion of reinforcement and matrix is essential in improving the properties of the matrix by the reinforcement; the matrix of a composite material usually transfers the load to the reinforcement. Most matrix materials are brittle and the use of reinforcements strengthen them and make them applicable for their various multi function usages.

The strength of the interface is greatly influenced by the weakest phase of its constituents which make the weakest phase the region of crack initiation. Interfacial shear failure usually occur by crack initiation parallel to the fibers and the failure modes are basically tensile and shear modes caused by the mode I and the mode II of crack growth (Talreja, 1987).

Fatigue in multidirectional laminates is a well-understood phenomenon. The damage takes place in three stages as shown in Figure 1.8. There are three main stages in the fatigue life: cross-ply cracks with large initial stiffness reduction, initiation and propagation of delamination of plies with slow stiffness reduction, and complete delamination and fiber failure (Reifsnider, 1990).

Fujii, Amijima, & Okubo (1993) proposed the Modulus Decay Mechanism for woven composites as shown in Figure 1.10.

Stage I: Debonds (between fiber and the matrix) in the weft occur near the cross-over points. The number of matrix cracks also increases rapidly. At a cycle ratio (n/N) of 0.1 debonds in the weft do not progress very much and the matrix crack density does not increase significantly. This stage is termed the meta-characteristics damage state (meta-CDS). The modulus decreases rapidly.

Stage II: In this stage, debonds occur in the warp direction. The debonds in warp and meta-delamination mainly cause gradual modulus decay in an almost linear fashion. This stage constitutes more than 75% of the total fatigue life.

Stage III: Final failure occurs with the breakage of fibers. However, the final stage is sometimes hardly distinguishable. The stiffness decreases rapidly again during the last few cycles before the specimen fails

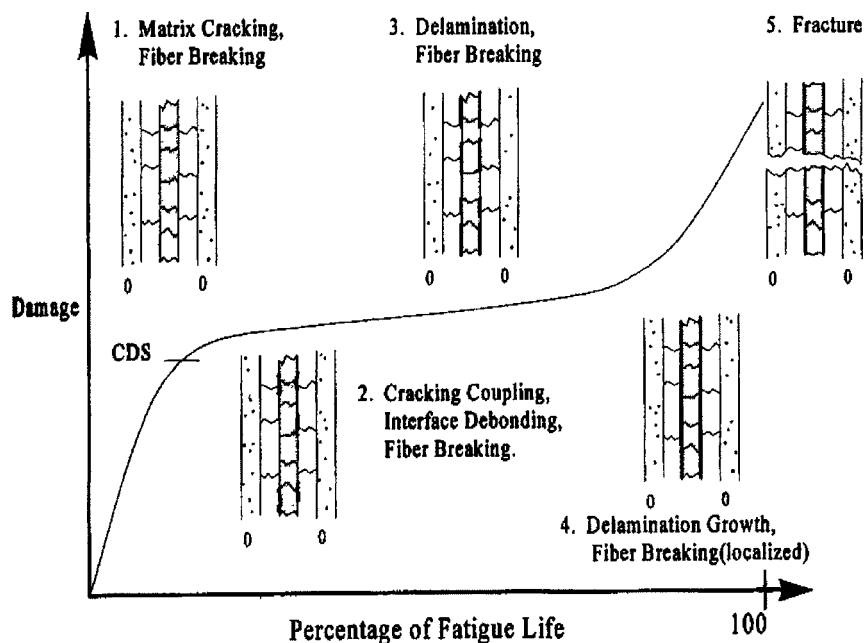


Figure 1.9: Fatigue Damage Mechanisms in Composite Laminate (Talreja, 1987)

The fatigue damage in composites can be evaluated by measuring the residual stiffness or strength. Measurement of the residual strength is a destructive test and thus cannot be used to predict or track the fatigue damage. On the other hand, stiffness can be measured non-destructively. Therefore, the stiffness degradation model is much more applicable to the practical design of composite structures (Lee, Fu, & Yang, 1996).

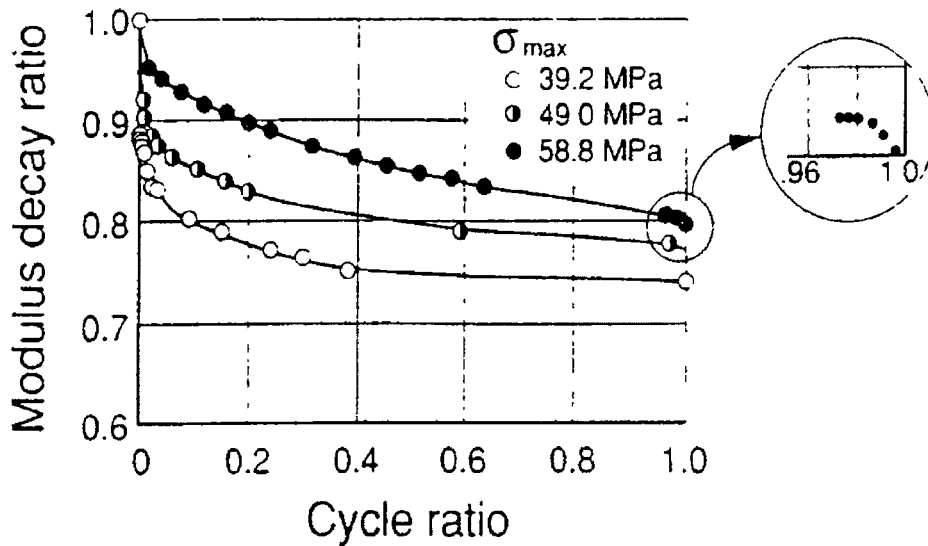


Figure 1.10: Modulus Decay under Fatigue Loading in Woven Composites

1.9.5 Fiber damage Models

Glass fibers that are under slow or steady crack growth does not suffer fatigue damage but environmental condition which deteriorate the strength overtime in the presence of oxidation and stress corrosion. This mode of fiber damage depends on the matrix behavior and properties.

There are two types of models that have been used by researchers in predicting the strength of fiber damage in composites namely (a) loose fiber bundle model (b) Chain of bundle model.

In loose fiber bundle model, fibers are placed parallel to one another and are arranged by gripping the fibers at each end, they are considered linearly elastic and when there is a fiber breakage, the surviving fibers jointly carry the additional load. This concept of equal load sharing between fibers is limited in composite materials in situations of matrix crack growth, the cross sectional area thereby exposing fibers to environmental attack. It has been observed that fiber breakage and intact matrix could lead to a local failure of matrix and interface.

In chain of bundle models, a large number of fibers are joined in series whereby the fibers within each bundle observe some form of load sharing rules. The strength of fibers in a chain of bundle is greatly affected by the fiber within the weakest strength and this model has been used to evaluate composite strength in static loading (Talreja, 1987).

1 9 6 Matrix and Interfacial Damage

There are two possible matrix damage modes namely: dispersed and localized modes. From past researches, it has been observed that interfacial damage is always localized (Talreja, 1987). In dispersed; the average crack size is smaller than the average crack spacing of the fiber distributed throughout the composite. Materials under fatigue tends to undergo a number of cycles which make the crack density to increase as the number of cycle increases and become localized at a critical value. In a dispersed failure mode, the composite may be homogeneous and its strength properties may not be affected but as the damage become localized, the strength properties are thereby affected. Failure in composites occurs when the localized failure zone grows to a critical size.

1.10 Problem Statement

With wind installed capacity growing at a rate of 35% per year, wind turbines are the composite industry's fastest growing application. The wind turbine blade industry is working hard to improve manufacturing efficiency and address blade failure issues, but challenges remain great, with failure rates as high as 20% within three years.

Replacement of wind turbine blades takes 2-weeks to 2-months. It is considerable downtime in the energy production. Major causes of wind turbine blades are Manufacturing errors such as waviness and overlaid laminates; Bad bonds, delamination and voids; Leading-edge erosion; Trailing-edge splits; and Lightning strikes (Richardson, 2009).

The loading on a wind turbine blade is primarily aerodynamic pressure loads. Loading is also applied at the root of wind turbine. The overall pressure field on the blade causes a "bending moment" and torque at the root. A "bending moment" refers to the tendency of wind turbine blades to bend and twist during operation. This constant and variable amplitude cyclic bending and twisting of wind turbine blades is termed as **fatigue**. Blades are designed with a high level of bending stiffness and fatigue-resistant characteristics (Richardson, 2009).

The major causes of blade failure are related to manufacturing errors and design of blades. Besides manufacturing and design, inherent performance of existing material system is also a key factor. Current wind turbine blades are fabricated with 2D woven glass fabric reinforcement stacked layer-by-layer to achieve required thickness. Such 2D components have limited life in fatigue environments due to inherently low matrix

dominated interlaminar shear strengths (ILSS). Low ILSS leads to poor bond between two layers, delamination, and splitting of laminates.

This weakness is not of a serious concern when composites are used in thin form and as flat plates. The weakness is serious when composites are used in thin form and/or for complex shapes. In such applications component is subjected to triaxial stresses and the weak ILSS results in fatal fracture even at low loadings (Yamashita, Takei, & Sugano, 1991).

There are few solutions to deal with blade failures due to fatigue.

1. Use of three-dimensional (3D) fiber architectures that enhances ILSS and through-thickness mechanical properties and in turn will perform better in fatigue (Bolick, 2005).
2. Use of high performance S2 glass and carbon fabric as reinforcement.
3. Use of hybrid composites (combination of glass and carbon fabric).
4. Nanomodification of polymer matrix to enhance fracture toughness and ILSS that would improve fatigue performance.

First two solutions are cost prohibitive. Third solution poses challenge in design and prediction of failure mechanisms. Fourth solution is economical and easy to implement without much changes in design and manufacturing methods.

Popular polymer matrix for large wind turbine blades is epoxy. The epoxy polymers are amorphous and highly cross-linked materials, because of which they have many useful structural properties such as a high modulus and failure strength, good creep resistance, and good thermal properties. However, they are relatively brittle and have

poor resistance to crack initiation and growth. This, in turn, may adversely affect the overall performance of the reinforced composites under static and cyclic-fatigue loads (Manjunatha et al., 2009). The initiation and propagation of matrix cracks and interlaminar delaminations are the dominant and progressive fatigue damage mechanisms in a quasi-isotropic lay-up FRP composite employing a typical brittle epoxy matrix (Reifsnider, 1990; Talreja, 1987). The fatigue strength of fiber reinforced composites can be improved if the fatigue performance of the epoxy matrix itself is improved. A fair amount of studies have been performed in last 5 to 6 years using different nanoparticles to modify epoxy matrix in PMCs to improve mechanical and fatigue properties as discussed in earlier sections.

Low-cost material system and low-cost manufacturing method are key factors in wind turbine market. This research proposes to nanomodify popular epoxy resin using low-cost nanoparticles by using simple dispersing techniques and then use this nanomodified epoxy resin to manufacture glass reinforced composites using low-cost vacuum assisted resin transfer molding process and then mechanically characterize these composites especially for fatigue.

1.11 Objectives of the research

The specific objectives of this research are as follows:

1. To establish effective mixing technique/s to uniformly disperse nanoparticles into epoxy resin.
2. To perform SEM analysis to evaluate degree of dispersion of nanoparticles.

3. To conduct mechanical characterization on neat resin specimens under tensile, flexural, and impact loadings.
4. To develop a low cost VARTM process to produce high quality E-glass reinforced epoxy nanocomposites.
5. To evaluate the mechanical performance of composite specimens under static tensile, flexural, and interlaminar shear loadings.
6. To compare the performance selected nanocomposites from step 5, under tension-tension fatigue loadings.
7. To establish S-N diagrams (Max stress vs fatigue life) for control (0wt% nanoparticles) and selected nanoparticle loading composites.
8. To study stiffness degradation (also called modulus decay) mechanism in these composites.

CHAPTER 2

MANUFACTURING

2.1 Manufacturing methods of composites

The tremendous weight reduction offered by composite laminates over metal has made composite parts attractive, also due to their durability and resistance to fatigue. Advanced composites are composites made by optimizing the relationship of mechanical properties and weight, or optimizing thermal performance and weight while Engineering composites are composites made for superior properties but focus on cost reduction. There are many methods used in making engineering and advanced composites like wet lay-up, prepreg method, autoclave processing, filament winding, Resin Transfer Molding (RTM), and Vacuum Assisted Resin Transfer Molding (VARTM). In the following section, a brief description of these methods, their advantages and disadvantages are explained.

2.1.1 Wet lay-up Method

It is a method that involves laying of reinforcement into the mold followed by applying the resin system. The wet composite is usually rolled by hand for evenly distribution of the resin and air pockets removal. Another layer of reinforcement is placed on top of the wet composite and resin poured on it. This same process is repeated until the desired thickness is achieved; the composite is then allowed to dry through curing.

Wet lay-up is a simple method which does not require any special handling of wet fabrics, it allows the resin to be applied only in the mold which helps in maintaining a neat working environment but variations in resin viscosity affects the curing process and also cause problems in having good wet- out of reinforcement. A mold release is usually applied to the mold thereby preventing the composite from sticking to the mold and allows easy removal of the composite from the mold (Strong, 2008).



Figure 2.1: Typical wet layup processing
(<http://sunsetters.ndsu.nodak.edu/indivcontent/whatsnew/2003-2005/03.09.2005.html>)

2.1.2 Prepreg Method

Prepreg method can be viewed to a great extent as an extension of the wet lay-up method. The fibers are usually arranged in a unidirectional tape or a woven fabric, it is impregnated with partially cured resin and stored in a way to avoid complete cure of the resin. Prepregs are made in different rolls which could later be put or cut to fit into mold depending on its desired usage. It is usually stack up in layers until the desired thickness

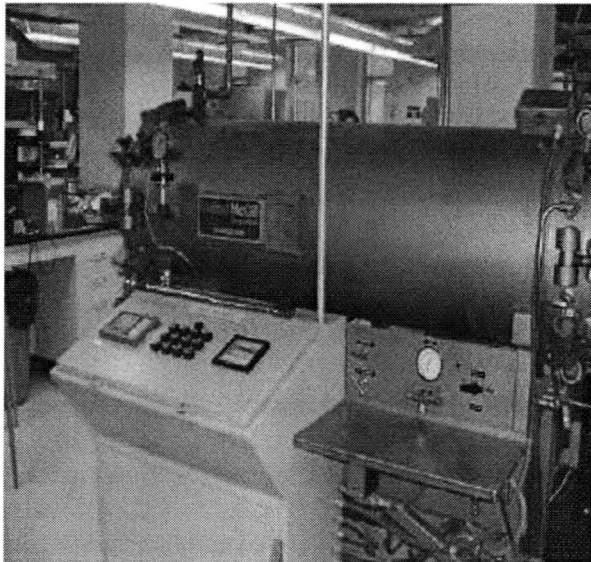
is achieved. Prepregs are always made to be comfortable on molds so that complex shapes can be produced.

Prepregs usually have a limited shelf-life because its resins have already been initiated when the prepreg is made. The shelf-life is usually several days to weeks and stored at room temperature but it can be extended by storing the prepreg in freezer. It is a common practice to record the time out of freezer in order to determine the remaining shelf-life. If prepregs are not well stored, they turn out dry and rigid which is always difficult to use. Although, this method is slow and labor intensive but it offers better part definition, higher fiber content and better consolidation than wet lay-up (Strong, 2008).

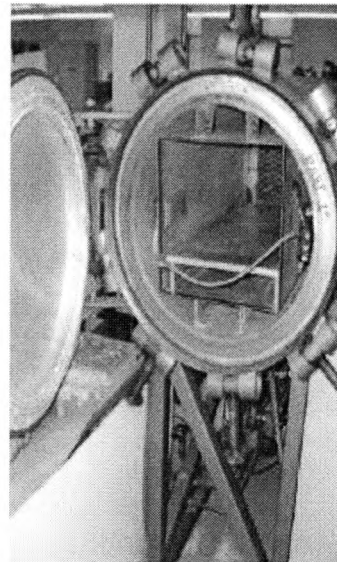
2 1 3 Autoclave processing

This is the most common method used for curing thermoset prepregs (composite world, 2010). It involves applying high pressure and heat to the part through the autoclave atmosphere. Autoclave consists of a vessel that can be pressurized internally up to 5 bar (~ 75 psi), before its contents are heated. The vessel used for component curing is usually large to accommodate large components. They are pressurized with gas, usually nitrogen that is circulated through the heaters to maintain a uniform temperature throughout the vessel. Attaining proper airflow is essential in achieving uniform temperature in the vessel. Heat enters through the end side of the autoclave and circulates the entire area of the vessel through series of ducts and fans. This whole unit of the part in this case; composite is kept in a vacuum bag to maintain vacuum pressure on the laminate. The outer membrane is pressed against the laminate by atmospheric pressure.

The part is then placed in the autoclave where the bagged molding may be reconnected with the evacuation system to maintain the vacuum. The autoclave is pressurized which augments the consolidated pressure. The temperature of the autoclave is reduced when the resin is adequately cured. The major advantage of autoclave is the manufacturing of composites with high fiber volume fraction and uniform thickness of the structure. However, high cost of the equipment is a huge set back as well as stringent pressure code regulations in using autoclave processing (Strong, 2008).



Front view



Side view

Figure 2.2: Autoclave Processing

(Courtesy: NC A&T State University, Greensboro, NC 27411)

2.1 4 Pultrusion

This is a continuous molding process that combines fiber reinforcements and thermosetting resin. It is widely used in making composite parts that have a constant cross-section profile which is also automated. It is a process by which reinforcements are positioned in a specific location using shapers to form a profile. It involves passing of reinforcement through a resin bath where the reinforcement is thoroughly coated with the resin before passing through a heated metal pultrusion die (Composite world, 2010).

The dimension and shape of the die usually define the finished shape of the part being fabricated. Heat is transferred by temperature control to the die which cures the combination of the reinforcement and the resin passing through it, and heat energy transferred changes the resin from liquid to solid. Solid laminates emerges from the pultrusion die having the exact shape of the die cavity; the laminates usually solidifies when cooled and continuously pulled through pultrusion machine by tandem pullers between the die exit and cut to the desired length.

However, the initial capital investment on pultrusion is exceedingly high than most other manufacturing processes which limits its common application but has low cost to high volume production that justifies its usage in the industry (Stróng, 2008).

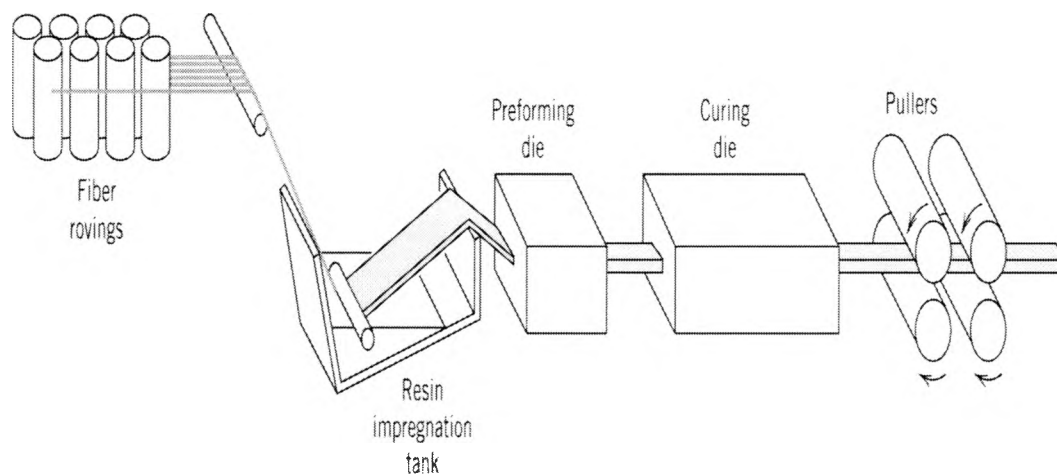


Figure 2.3: Pultrusion process (Callister, 2008)

2.1.5 Filament Winding

This is a process of winding resin-impregnated fiber on a mandrel surface in a precise pattern. It is usually done by rotating the mandrel while a delivery head precisely position fiber on the mandrel surface to form the part. Successive layers could be added using the same or different winding angles until the required thickness is achieved.

Filament winding machines operate on the principles of controlling machine motion through various axes. The basic motions are the spindle or mandrel rotational axis, the horizontal carriage motion, and the cross or radial carriage motion axis. The mandrel or the application head can rotate to give the fiber coverage over the mandrel and transverses longitudinally giving the coverage.

In addition, Filament winding does not use prepreg materials but incorporates the impregnation of the fiber tows as part of the filament winding process. The use of more

than one type of reinforcement materials may have some advantages in terms of cost and product performance like a vessel wound with carbon fiber for strength and modulus, and then overwound with aramid to protect the vessel from impact damage when in use.

Defining the relative speed of the mandrel and the head are important in successful filament winding. The two motions determine the wrapping angles and the overlap as well as the mechanical properties of the part (Strong, 2008).

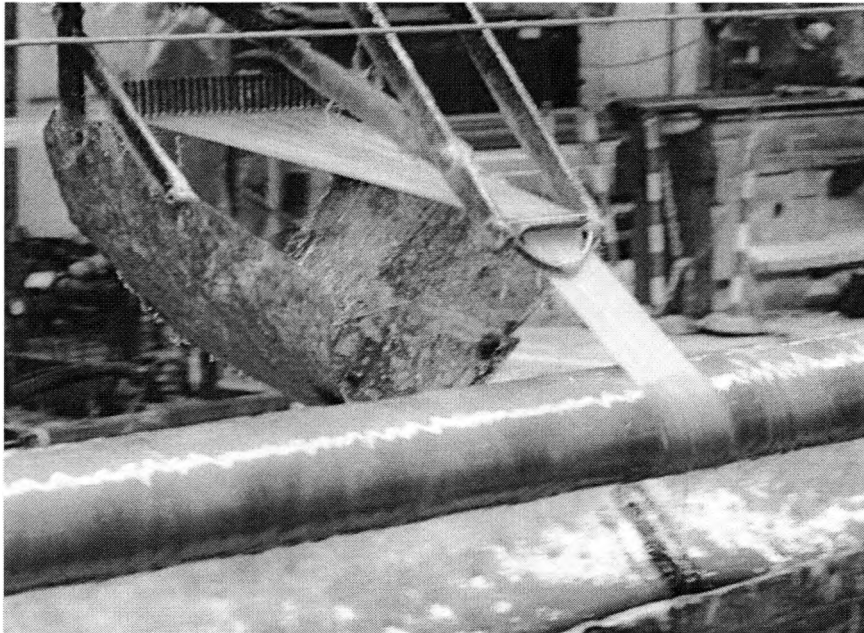


Figure 2.4: Filament winding
(<http://www.david-briggs-software-services.co.uk/images>)

2.1.6 Resin Transfer Molding (RTM)

This is a process that involves placement of reinforcement materials between two matching mold surfaces, these matching mold surfaces are commonly called male and

female molds usually closed in molding processes, clamped and a low-viscosity resin system is injected into the mold cavity through one or series of ports under moderate pressure. Vacuum is usually used in enhancing the flow of the resin and reducing void formation.

Design of the mold is the most critical factor in proper resin transfer. The mold is usually fabricated and ensures that resin reaches all areas with the same concentration. RTM molds are usually made of composite materials but other materials may also be used, very large and complex shapes can be made efficiently and inexpensively (Strong, 2008). Molds are vented in such a way that air is pushed out of the mold by the resin but the vent is too shallow to allow passage of resin outside. It is arguably one of the widely used manufacturing processes in making composite laminates but control of resin uniformity is always difficult, radii and ends are usually resin rich (Strong, 2008).

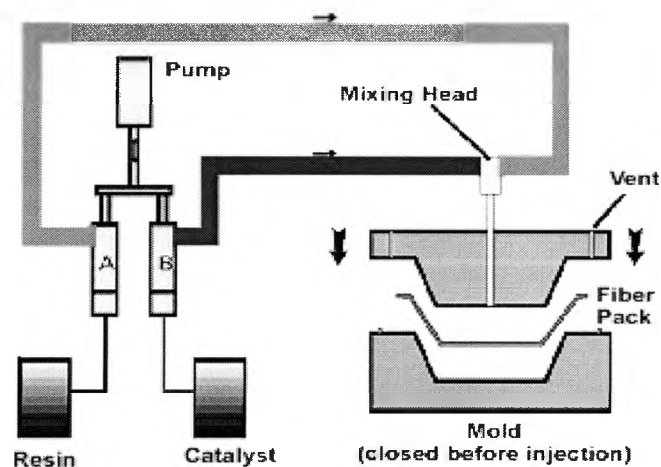


Figure 2.5 Resin Transfer molding
 (<http://www.ctihuatai.com/index.files/rtmstatic.gif>)

2.1.7 Vacuum Assisted Resin Transfer Molding (VARTM)

VARTM is an adaptation of the RTM process and is very cost-effective in making large structures such as boat hulls. In this process, tooling costs are cut in half because one-sided tools such as open molds are used to make the part. In this infusion process, fibers are placed in a one-sided mold and a cover, either rigid or flexible, is placed over the top to form a vacuum-tight seal. A vacuum procedure is used to draw the resin into the structure through various types of ports. This process has several advantages compared to the wet lay-up process used in manufacturing boat hulls. Because VARTM is a closed mold process, styrene emissions are close to zero. Moreover, a high fiber volume fraction (70%) is achieved by this process, and therefore, high structural performance is obtained in the part (Mazumdar, 2002).

Distribution media aids the proper distribution of the resin over the reinforcement while peel ply which is usually used in covering both top and bottom of the stacked fabrics helps in easy removal of the composite part from the mold. This method also allows visual monitoring of the resin amongst other things while impregnating and defects could be easily spotted.

Generally, VARTM is an attractive and affordable method of fabricating composite laminates and lends itself to the production of large scale and high quality parts provided the resin system has low viscosity in the range of 1000cP and less for proper wet out of the fabrics. During VARTM, dry fabric is placed into a tool and vacuum bagged in conjunction with the resin distribution line, the vacuum distribution line, and the distribution media. A low viscosity resin is drawn into the fabric through the aid of a

vacuum. Resin distribution media ensures resin infiltration in the through-the-thickness direction. The key to successful resin infiltration of the fabric is the design and placement of the resin distribution media which allows complete wet-out of the fabric and eliminates voids and dry spots. Properly designed and properly placed resin distribution media eliminate race tracking and resin leakage around the fabric (Seeman, 1990 and 1994). The schematic for the fabrication is shown in Figure 2.6.

Although, autoclave and RTM processes are the most widely used in aerospace and some other industries due to their regular high fiber volume fractions and uniform thickness of the composite structures but autoclave is expensive and VARTM process has various advantages; the process is relatively low cost for low volume production, and tools used are relatively simple and inexpensive. It can be used to make large and complex parts which make it suitable in making turbine blades, with considerable high fiber volume fraction and on-site manufacturing and repair is possible with negligible environmental concerns unlike hand lay-up process. Open molding is a method used longest in the polymer-matrix composite industry to make thermoset products. The molding process involves placing of reinforcements and liquid resin onto the surface of an open mold. It uses basic materials technology and processing methods. Closed molding is a molding process that usually involves two matched molds that provides a good inside and outside surfaces, it generates lesser emission and it is less labor intensive than open molding process. VARTM is closed molding process and hence it has less environmental concerns. Styrene emission is major concern in open molding processes when using unsaturated polyester and vinyl ester resins.

Most turbine blades are extremely long which might cost some fortune in transferring to turbine farms but VARTM process could be set up on the farm in making these blades and in case of repairing, blades could be easily repaired on the farm and return to active service with very little down time. This process was used in manufacturing composite panels in this research. VARTM process is explained in detail in the next section.

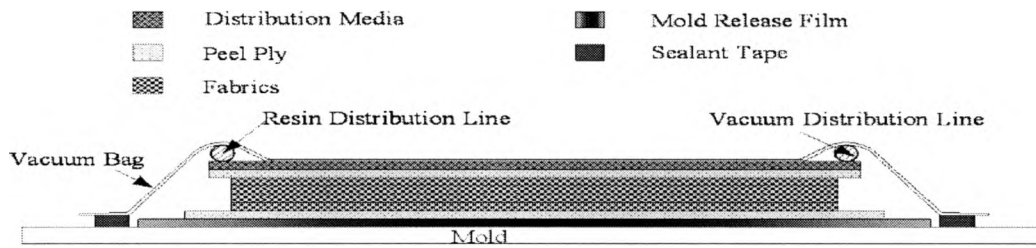


Figure 2.6 Schematic for VARTM (Tate, 2004)

2.2 Material System

Table 2.1: Material system for Nanosilica nanocomposites

Reinforcement	E-glass $\pm 45^\circ$ stitched bonded fabric (Bidiagonal glass fabric, areal weight 989 g/m^2)	Saertex USA, LLC.
Nanoparticle	Nanopox TM F400 nanosilica predispersed in epoxy resin	nanoresins AG, Germany
Epoxy resin system	EPIKOTE MGS TM RIM 135 epoxy resin EPIKOTE MGS TM RIMH 1366 hardener	Hexion Specialty Chemicals, Inc.

Table 2.2: Material system for HNT nanocomposites

Reinforcement	E-glass $\pm 45^\circ$ stitched bonded fabric (Bidiagonal glass fabric, areal weight 989 g/m ²)	Saertex USA, LLC.
Nanoparticle	Untreated Halloysite Nanotubes (HNT)	NaturalNano, Inc.
Epoxy resin system	EPIKOTE MGS™ RIM 135 epoxy resin EPIKOTE MGS™ RIMH 1366 hardener	Hexion Specialty Chemicals, Inc.

Table.2.3: Material system for HNT-epoxy neat resin

Nanoparticle	Untreated Halloysite Nanotubes (HNT)	NaturalNano, Inc.
Epoxy resin system	EPIKOTE MGS™ RIM 135 epoxy resin EPIKOTE MGS™ RIMH 1366 hardner	Hexion Specialty Chemicals, Inc.

In this paper glass reinforced composites will be referred as HNT nanocomposites and Nanosilica nanocomposites. Further these composites will be referred as 0.8 wt% HNT nanocomposites or, 7 wt% Nanosilica nanocomposites to indicate the wt% loading of nanoparticles. Control nanocomposites means there are no nanoparticles. When no glass reinforcement is added then such materials are referred as HNT-epoxy neat resin and Nanosilica- epoxy neat resin. Control neat resin means there are no nanoparticles. Nanosilica-epoxy neat resins have been studied very extensively under static and fatigue tests by many researchers (Karapappas et al., 2008; Deng, Ye, & Friedrich, 2007;

Johnsen et al., 2007). Therefore, nanosilica-epoxy neat resins would not be studied in this research. Nanosilica nanocomposites were studied under static and fatigue loading.

HNT is a new material and very few attempts are made to use it in epoxy (Cuiping et al., 2008; Mingliang et al., 2005). The test results are inconsistent and dispersion techniques used are very time consuming. Therefore attempts are made to finalize better and economical dispersion technique for HNT epoxy neat resin. The various dispersion techniques studied are centrifugal mixing, mechanical low shear mixing, and high shear mixing. HNT epoxy neat resins are tested under tension, flexure, and impact loading. The test results indicate that neither centrifugal mixing nor high shear mixing provides uniform dispersion on HNT in epoxy. The mechanical test results are very inconsistent. Therefore, no research work has been conducted for HNT nanocomposites.

2.3 Dispersion of Nanoparticles in Epoxy

Different nanoparticles are mixed with polymers to improve mechanical performance. Moreover, evenly dispersion and exfoliation of nanoparticles in polymers increases fundamental properties drastically. Properties are usually enhanced when the nanoparticles are present in polymer in nanometer scale. Therefore, proper understanding of dispersive and distributive mixing mechanisms is vital. Dispersive mixing involves the reduction in size of a cohesive minor component such as clusters of solid particles or droplets of a liquid. Distributive mixing is the process of spreading the minor component throughout the matrix in order to obtain a good spatial distribution in any good mixing

device; these two mechanisms must be achievable. The conditions under which dispersive mixing occurs are determined by the balance between the cohesive forces holding agglomerates or droplets together and the disruptive hydrodynamic forces (Manas-Zloczower, 2009).

The different mixing techniques used are sonication, high shear mixing, low-shear mechanical stirring, centrifugal planetary mixing, and simple hand stirring. The following section explains different mixing techniques that were used in this research.

2.3.1. IKA[®] High Shear Mixer

High shear mixing is a very effective technique to disperse solid nanoparticles in liquid polymer resins. Koo and coworkers have successfully used high-shear mixing techniques to incorporate carbon nanotubes, layered silicates, nanosilicas, carbon nanofibers, and POSS to form polymer nanostructured materials in several of their research programs (Koo, 2006).

High Shear Mixer (IKA[®] Labor Pilot 2000/4) with a DR module was used in this research. This configuration of mixer was previously used for successful dispersion and exfoliation of nanoclay in different resin systems. It is 3-stage disperser for application with high shear requirements. It has 3 generators (stator and rotor together are known as generator), 2 medium and 1 fine. The motor speed is controlled using digital controller by changing motor frequencies. Shaft speed depends on the belt drive that connects motor and shaft. According to manufacturer's data, the radial (grinding) gap between stator and

rotor is fixed to 0.2 mm. The diameter of rotor (D) was 57mm. Shaft speed determines the shear rate. The rotational speed of shaft was measured with tachometer at different motor frequencies to calculate the real ratio of drive and shaft. .

Table 2 4 shows motor and shaft speed; circumferential speed and shear rate.

Previous study indicates that, shear rate is in the order of 45,000 to 110,000 s^{-1} provides good mixing in terms of intercalation and exfoliation of nanoclays (Cheng, 2006). It was found that there is no recirculation occurrence if the frequency of the motor is set lower than 35 Hz. According to technical data, the output speed ranges from 3,160 to 13,750 RPM. That means the maximum shear rate can theoretically be about 200,000 s^{-1} . In this research, 40 Hz frequency was used which provided a shear rate of 76,906 s^{-1} . (Tate J. S., Kabakov, Koo, & Lao, 2009).

Table 2.4: High Shear Mixer Shear Rates

Motor Freq. (Hz)	Motor Speed (RPM)	Shaft speed (n) (RPM)	Circumferential speed (πDn) (m/s)	Shear rate (circumferential speed/ grinding gap) (S^{-1})
0	0	0	0.000	0
10	600	1221	3.645	18223
20	1200	2536	7.570	37849
24	1440	3057	9.126	45632
30	1800	3848	11.486	57429
40	2400	5153	15.381	76906
50	3000	6455	19.268	96338
60	3600	7768	23.187	115935

High shear mixer was one of three techniques used for blending HNT into epoxy resin. High shear mixing has proved to provide good dispersion and exfoliation of nanoclays. Halloysite nanotubes was washed in acetone and dried in vacuum oven at 75°C. Only the resin (no hardener) was mixed with HNT in the high shear mixer. HNT was mixed for 20 min at 40 Hz frequency that gave shear rate of 76906 sec^{-1} . The arrangement of setup is displayed in Figure 2.7.

The temperature of the resin and the mixing chamber was constantly monitored with IR thermometer. The temperature was maintained below 50°C. Epoxy resin was mixed in batches with HNT in 3 different proportions: 2.5, 5.0, and 10% by weight.

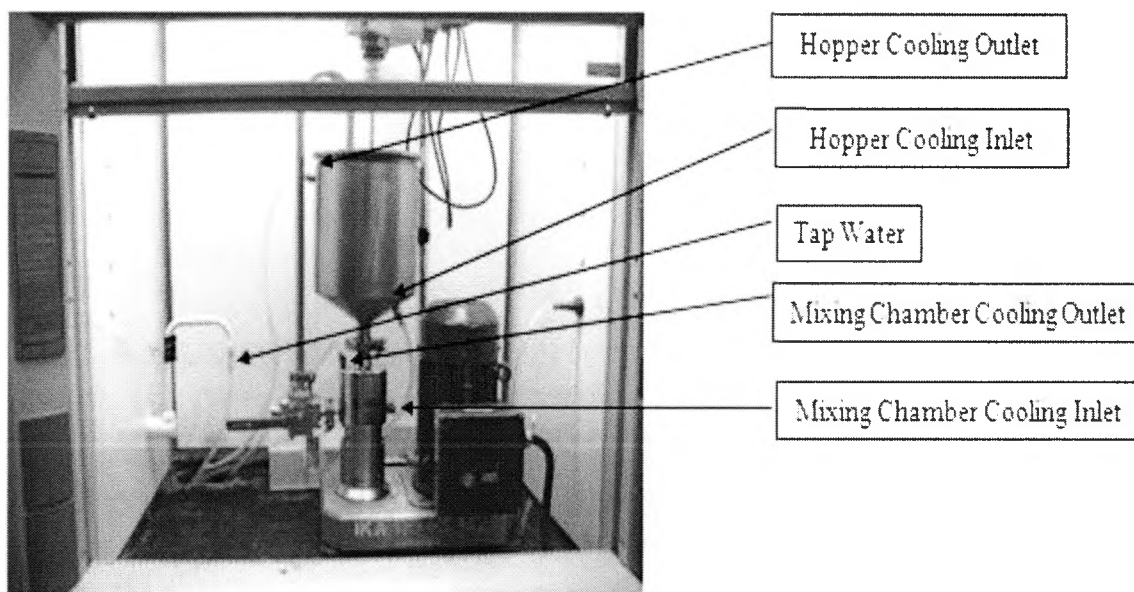


Figure 2.7: IKA[®] Labor Pilot 2000/4 High Shear Mixer with cooling jacket (Tate, Kabakov, Koo, & Lao, 2009)

2.3.2 Planetary Centrifugal Mixing: THINKY® ARV-310

Planetary Centrifugal Vacuum Mixer, THINKY® ARV-310, was another mixing techniques used in HNT-epoxy neat resin study. According to the manufacturer, the mixer's maximum centrifugal power is 400G, which is produced from 2,000 RPM and the 9 cm diameter arc of the container rotation. The speed of revolution can be adjusted in a range of 200-2000 RPM. The ratio of the revolution to the rotation of the cup holder is fixed at a 2:1. The mixer can also apply vacuum while mixing. The vacuum pressure can be programmed to a maximum of 0.67Kpa. The following Figure 2.8 shows the operational principle of the mixer.

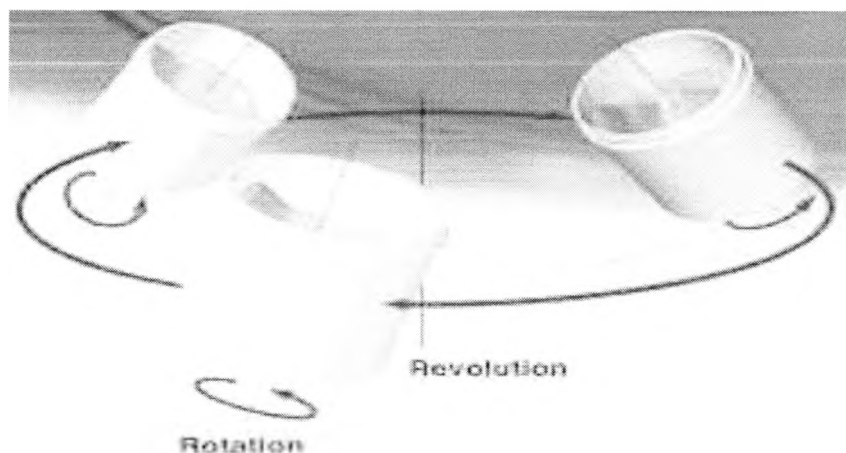


Figure 2.8: Rotation and Revolution action in Centrifugal Planetary Mixer (Kabakov, Tate, Koo, 2010)

Planetary centrifugal mixers are simple in use. It provides uniform stirring during rotation and revolution, concurrent defoaming and deaeration.

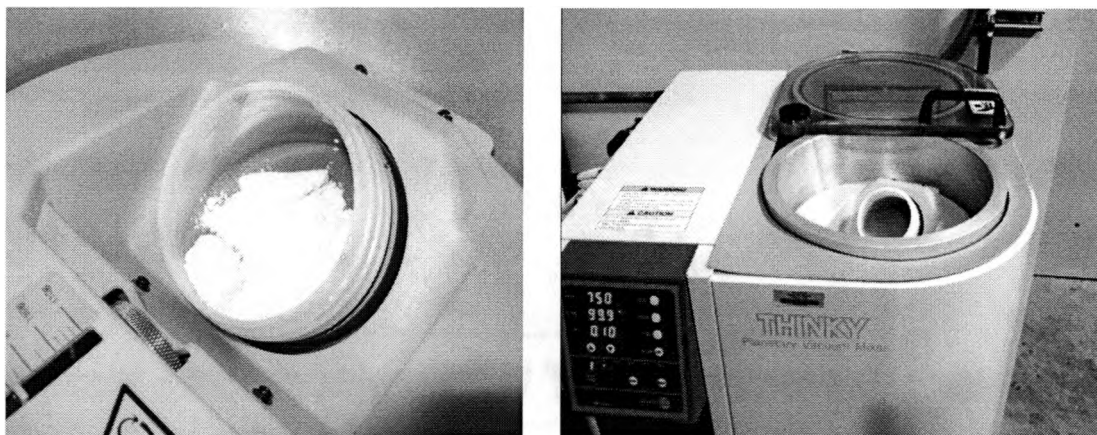


Figure 2.9: Planetary centrifugal vacuum mixer: Phenolic resin with nanoclay before and after mixing (Kabakov, Tate, Koo, 2010)

Halloysite nanotubes was dispersed in epoxy using centrifugal mixer for 20 minutes at 2000 rpm without vacuum, hardener was added to the mixture and mixed with centrifugal mixer at the 2000 rpm with vacuum (4 kPa) for another 5 minutes.

Nanosilica (Nanopox F400) which contains 40% nanosilica well dispersed in epoxy that was produced by nanoresins, AG was added to EPIKOTE RIMR 135 epoxy resin, placed in the centrifugal mixer for 5 minutes without vacuum at 2000 rpm. Hardener; RIMH 1366 was added to the mixture and mixed in centrifugal mixer with 4 kPa vacuum at 2000 rpm for another 5 minutes.

2.3.3. Low-shear Mechanical Mixing: (Dispermat)

Low-shear mixing was another method used for blending HNT in Epoxy in this study. According to the manufacturer, DISPERMAT® CC has a counter rotating power of 0.135 kW, speed of up to 16.000 rpm, the shearing action is 1067 s^{-1} and it could

handle product of 0,05 – 1 kg at a time. The container for mixing could be 50 – 250 mm in diameter and maximum of 300 mm in height. Figure 2.10 shows DISPERMAT® CC when blending nanoparticles in epoxy.

The mixing procedure that was used for HNT is as follows:

1. HNT was mixed with acetone and solution was stirred using Dispermat for 30 minutes
2. The solution (acetone and HNTs) mixed with epoxy resin (RIM 135) using Dispermat for 2 hours at 75 C.
3. This nanomodified epoxy resin was degased in vacuum oven for 10 minutes at 75 C and 4 kPa vacuum gage pressure. The purpose of degassing was to remove the remaining acetone.
4. Nanomodified epoxy resin was removed from vacuum oven and hardener (RIMH 1366) was added. The resin was gently stirred for 5 minutes at 75C.
5. Later nanomodified epoxy resin was put THINKY mixer for 3 minutes, 1000 rpm with vacuum.

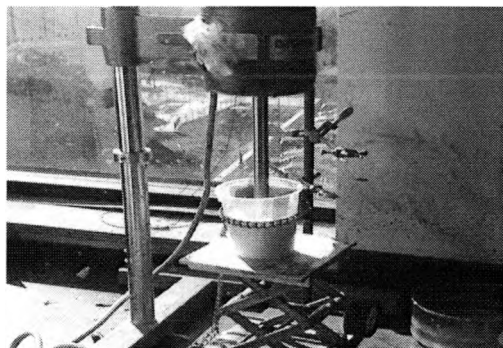


Figure 2.10: DISPERMAT® CC

The following table summarizes the mixing procedures adopted in this research.

Table 2.5 Resin Dispersion Technique and processing

Mixing technique	Nanosilica (Nanopox F400)	Halloysite nanotubes (HNT)
Centrifugal planetary mixer (THINKY)	<ul style="list-style-type: none"> • Resin + nanosilica mixed at 2000 rpm for 5 minutes • Nanomodified resin + hardner mixed for 5 minutes at 2000 rpm with 4 kPa vacuum. 	<ul style="list-style-type: none"> • Resin + HNT mixed at 2000 rpm for 20 minutes • Nanomodified resin + hardner mixed for 5 minutes at 2000 rpm with 4 kPa vacuum.
High shear mixer (IKA)		<ul style="list-style-type: none"> • Resin + HNT mixed in high shear mixer at 40 Hz frequency corresponding to shear rate of 76906 sec^{-1} for 20 minutes • Nanomodified resin + hardner mixed for 5 minutes at 2000 rpm with 4 kPa vacuum using THINKY mixer.
Mechanical low-shear (Dispermat)		<ul style="list-style-type: none"> • Acetone + HNT stirred at 750 rpm for 30 minutes • Acetone +HNT+Resin mixed at 750 rpm for 2 hours at 75°C • Nanomodified resin was degassed for 10 minutes at 75°C and 4KPa • Nanomodified resin + hardner stirred for 5 minutes at 75°C • Nanomodified resin in THINKY for 3minutes at 1000 rpm and 4KPa

The resin was poured into silicone molds for tension, flexure and izod impact test specimens. Figure 2.11 shows silicone mold for flexure specimens. Silicone molds were kept at 25°C for 24 hours. Specimens were removed from the molds and post-cured at 60 °C for 15 hours.



Figure 2.11: Silicone mold with flexure specimens

2.4 Steps in VARTM

Typically, the VARTM process at room temperature involves the following steps

1. Mold Preparation and Vacuum Bagging
2. Formulation and Degassing of Resin
3. Resin Impregnation and Curing

2.4.1 Mold Preparation and Vacuum Bagging

In VARTM, there is a typical sequence of vacuum bagging. The sequence of lay-up from bottom to top is mold, mold surface protection film, bottom release fabric (also called

bottom peel ply), fabrics, top release fabric (also called top peel ply), resin distribution media, vacuum and resin distribution lines, and vacuum bag. The vacuum bag is sealed using sealant tape. This procedure is depicted in Figures 2.12 and 2.13.

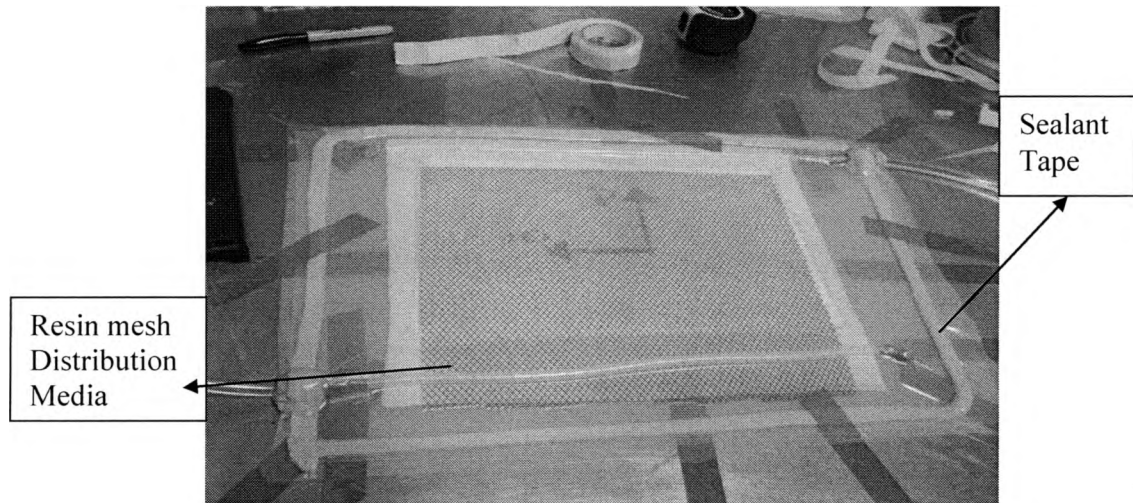


Figure 2.12: Room Temperature VARTM Setup: Vacuum bagging

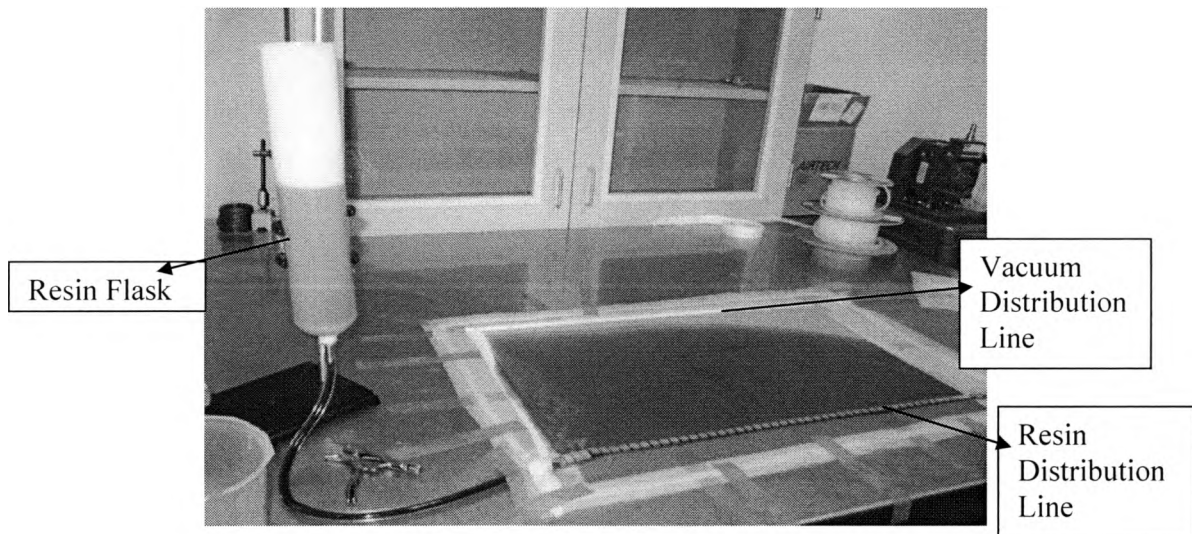


Figure 2.13: Resin Flow in VARTM Process

The purpose of each of these items is as follows:

1. Mold: The flat plate mold used for the fabrication is a Polycarbonate one.
2. Bottom Peel Ply: This is a porous nylon fabric, which leaves an impression on the part suitable for secondary adhesive bonding (like tabbing) without further surface preparation. Its use is optional.
3. Fabric Lay-up: In this research, 8-layers of Non-crimp E-glass $\pm 45^\circ$ stitched bonded fabric from Saertex, Germany was used.
4. Top Peel Ply: This is the same material as the bottom release fabric. It is laid on top of the braided fabrics to facilitate the flow of resin through it. It also leaves an impression on the part suitable for secondary bonding without further surface preparation.
5. Distribution Media: The distribution media is polyethylene mesh laid on top of the top release fabric. This helps maintain an even distribution of resin and facilitates the flow of resin through the thickness of the panel.

The use of distribution media is a patented technology termed as SCRIMP (Seemann Composite Resin Infusion Manufacturing Process) that was invented by W. H. Seemann. Seemann also patented different patterns of distribution media and the placement technique for these patterns (Seemann, 1990 and 1994). Distribution media control the flow of resin through the thickness. Resin flows quickly through the media and then remains in the mesh pockets. It then travels through the thickness.

6. Resin and Vacuum Distribution Lines: Spirally cut HDPE (High Density Polyethylene) tubes are used for this purpose. These lines are laid above the distribution media at two sides of the fabric lay-up and can run along its length or along its width.

One end of the resin line is closed, and the other end is connected to the resin supply through the flow control device (if used). The vacuum line is closed at one end and connected to the vacuum pump through the vacuum gage.

7. Breather: The breather material acts as a distributor medium for the air and escaping volatiles and gases. It is placed over the resin distribution media and the resin and vacuum lines. It also acts as a buffer between the vacuum bag wrinkles and the part surface. It is a highly porous material composed mostly of fiberglass, polyester felt, and cotton. The use of a breather is optional. It was not used in the present research.

8. Vacuum Bag: This is made from 25 μm nylon film. The film is placed completely over the mold area and sealed firmly using a special sealant tape. The sealant seals the vacuum bag and helps maintain a uniform vacuum throughout the molding process.

The other equipment used in the processing are a vacuum pump, flow control devices (optional), a vacuum gage, a degassing chamber, a temperature and humidity gage, and a stop watch. Flow control devices like valves, clamps, and peristaltic pumps are used with certain material systems. These devices deliver a controlled amount of resin according to the unit time in the mold. Thus, the resin has a chance to flow through the thickness and complete wet-out of the fabrics is ensured. A peristaltic pump delivers a fixed amount of resin in the mold per unit of time. The quantity of resin (e.g., cm^3/min) is dependent on the pump speed. The pump speed is selected according to the fabric-resin system and the thickness of the panel.

Once the fabrics and other relevant materials are laid over in the required sequence, the entire mold is sealed with sealant and a vacuum bag. The vacuum pump is then used

to maintain the lowest possible vacuum pressure throughout the process. Care should be taken that vapor pressure of ingredients should not exceed in the mold. Bag leaks are the most common problems that occur in VARTM. One of the reasons for leaks is a damaged vacuum bag. A vacuum bag is typically made of nylon film. The moisture level in the surrounding environment affects the nylon film. Dry and brittle film can cause cracking when handled frequently. Another common reason for bag leak is foreign material entrapped between the vacuum bag and the sealant tape. Once the leaks have been removed and the vacuum bag is completely sealed, the vacuum pump remains running for at least 1 to 2 hours to achieve a good vacuum in the bag. The typical vacuum achieved is in the order of 28" of Hg for epoxy resin system. The vacuum pump is then shut off, and the vacuum line is clamped. If the bag remains tight and holds almost the same vacuum after 1 to 2 hours, the mold is ready for resin impregnation.

The vacuum plays a vital role in the VARTM process. The pressure differential between the atmosphere and the vacuum provides the driving force for infusing the resin into the mold. The vacuum also removes all of the air from the mold before and during the introduction of resin.

2.4.2 Resin Formulation and Degassing

The following tables provide formulation details for Nanosilica nanocomposites and HNT nanocomposites.

Table 2.6 Resin formulations for Nanosilica Nanocomposites

SiO ₂ (Wt %)	RIMR 135 (g)	NANOPOX F400 (g)	RIMH 1366 (g)
0	100	0	30
6	81	19	24.7
7	78	22	24.5
8	75	25	24.13

Table 2.7 Resin formulations for Halloysite nanotubes neat coupons

HNT (Wt %)	HNT (g)	RIMR 135 (g)	RIMH 1366 (g)
0	0	100	30
0.8	1.04	100	30
2.5	3.25	100	30
5	6.5	100	30
7.5	9.75	100	30
10	13	100	30

After the formulation of the resin, degassing is the important step because the resin had to be free from entrapped air and/or gases that could cause voids in the composite panels. THINKY centrifugal planetary mixer was used for degassing as explained in detail in section 2.3.2 Degassing was a crucial step in the VARTM process and had to be performed very carefully to ensure high quality composite panels. Degassing resin for too short a period of time could not ensure complete removal of the entrapped air and/or gases. If the resin was degassed for too long a period of time, some of the ingredients (mainly styrene) in the resin could evaporate during processing. This

would change the final formulation of resin and also create voids. Five to ten minutes is the sufficient amount of time to remove all the entrapped air and/or gases.

2.4.3 Resin Impregnation and Curing

The resin impregnation process was the same for all types of resins used in this research. The resin was poured in the container that connects to the resin line in Figure 2.12. The resin was allowed to flow in the mold until the whole panel was soaked. There was no need to use a flow control device with this design. The driving force created by the vacuum alone was sufficient for complete wet-out of the fabric. Properly designed and properly placed resin distribution media eliminate race tracking and resin leakage around the fabric (Seeman, 1990 and 1994). Figure 2.12 displays the resin impregnation set-up. Panels remained in the mold for 24 hr at room temperature for curing, which is termed as the ‘Green Cure.’ Panels were removed from mold and were post cured.

Composite panels were cured in the mold at room temperature for 24 hours and post cured at 80°C for 15 hours in the oven. Figure 2.14 displays the different steps in making composites panels using VARTM.

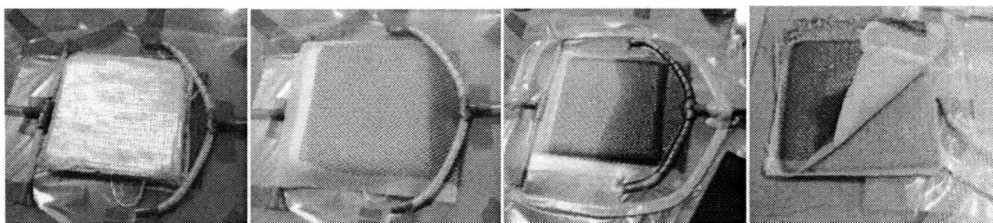


Figure 2.14 VARTM process - from layup to resin infusion to demolding

Scanning electron microscopy (SEM) was performed to evaluate quality of dispersion of nanosilica in epoxy resin. Figure 2.15 shows SEM micrograph showing uniform dispersion of nanosilica. EDS analysis was performed to evaluate chemical composition. Figure 2.16 shows uniformity of silica throughout the epoxy matrix.



Figure 2.15: Micrograph of Nanosilica in Epoxy

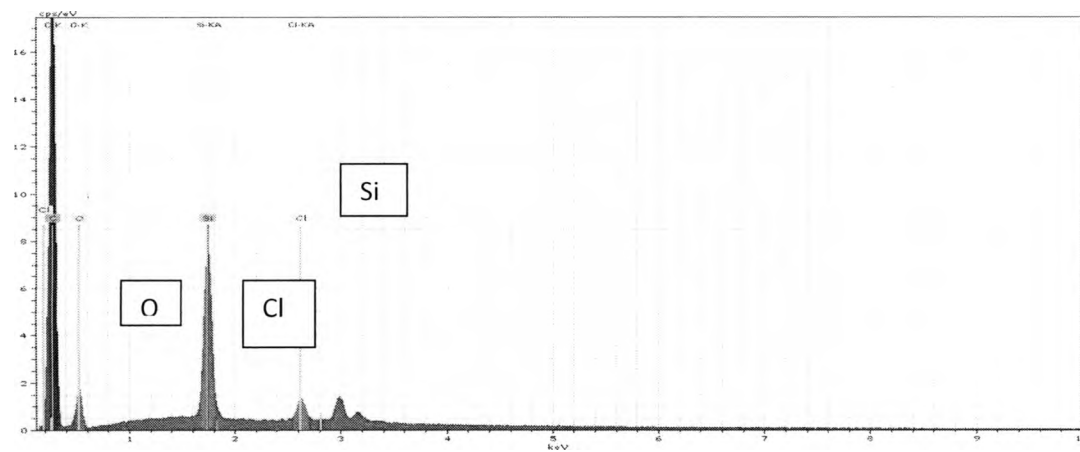


Figure 2.16a: EDS showing material constituents of Nanosilica in Epoxy

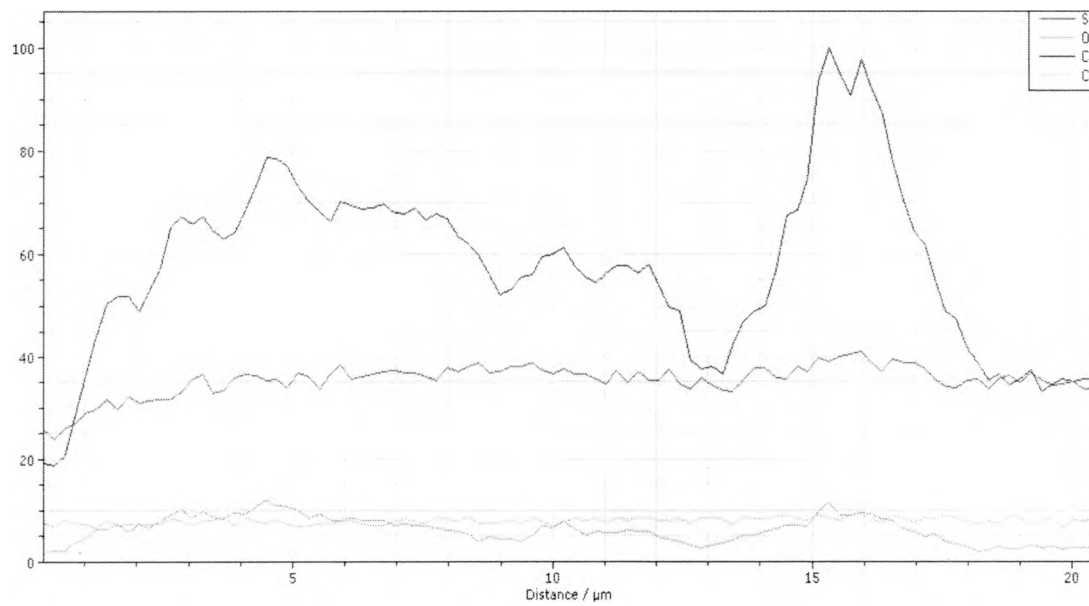
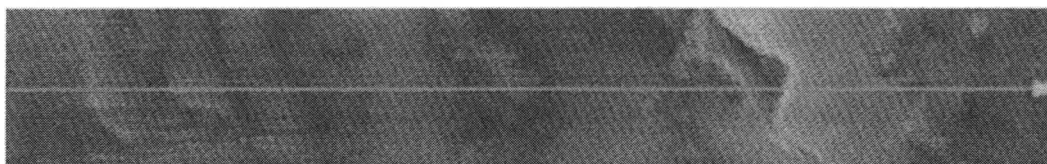


Figure 2.16b: EDS showing material constituents of Nanosilica in Epoxy

2.5 Overall Fiber Volume Fraction

Fiber volume fraction is important in composite manufacturing. Fiber is the main load carrying component of composite. Hence, the overall fiber volume fraction V_f^{overall} has a direct effect on mechanical properties of the composites. Different methods are used in determining the overall fiber volume fraction in composite materials like:

- Area Weight Method (ASTM D792-86)
- Ignition Method
- Density method (ASTM 2584-68)

Density method is the most widely used method for fiber volume fraction and it is only useful when there are negligible micro voids. This method is easy to apply because it deals with the density of the composite materials.

$$V_f^{\text{overall}} = \frac{\rho_c - \rho_m}{\rho_f - \rho_m}$$

Where:

ρ_c = density of composite

ρ_m = density of matrix

ρ_f = density of fiber

The densities of glass fiber and EPIKOTE RIM R 135 were 2.6 g/cm^3 and 1.17 g/cm^3 respectively. The average fiber volume fraction for composites was found to be 0.52.

CHAPTER 3

PERFORMANCE EVALUATION

3.1 Introduction

Chapter 2 discussed the low-cost VARTM manufacturing process for stitched bonded glass composites in detail. Different dispersion techniques used to disperse nanoparticles in liquid thermoset resins were also elaborated. This chapter discusses the performance evaluation of these composites under static and tension-tension fatigue loading. All the static and fatigue tests were performed according to the ASTM standards discussed below.

Static tensile tests were performed according to ASTM D3039/D3039M titled ‘Standard Test Method for Tensile Properties of Polymer Matrix Composite Materials.’ The in-plane tensile properties (viz.,) ultimate tensile strength (UTS or, S_u), strain at UTS, and longitudinal tensile modulus were evaluated. The axial strain was measured by an extensometer. Tensile strength is fiber dominant property but matrix materials do have effect on tensile modulus and failure strain. Flexure tests were performed according to ASTM D 790-92 titled ‘Standard Test Methods for Flexural Properties of Unreinforced and Reinforced Plastics and Electrical Insulating Materials’ to evaluate flexural strength and flexural modulus. Flexural properties are dependent on both fiber reinforcement and

matrix. Short Beam tests were performed according to ASTM D 2344/D 2344M titled ‘Standard Test Method for Short-Beam strength of Polymer Matrix Composite Materials and their Laminates’ to evaluate interlaminar shear strength (ILSS). ILSS is major of fiber/matrix adhesion and matrix dominant property. Current wind turbine blades are fabricated with 2D woven glass fabric reinforcement stacked layer-by-layer to achieve required thickness. Such 2D components have limited life in fatigue environments due to inherently low matrix dominated interlaminar shear strengths (ILSS). Low ILSS leads to poor bond between two layers, delamination, and splitting of laminates. This test was chosen to evaluate effect of nanomodification on interlaminar shear properties.

All static tensile tests were conducted in the displacement control mode with a cross lead rate as specified in the ASTM standard. Five specimens in each category were tested. The test matrix for static tests is shown in the table below.

Table 3.1. Test matrix for static test

Material System	Control 0wt% Nanosilica	6wt% Nanosilica	7wt% Nanosilica	8wt% Nanosilica
ASTM D3039: Tensile Test	5	5	5	5
ASTM D790: Flexure Test	5	5	5	5
ASTM D2344: Short Beam Test	5	5	5	5

Tension-tension fatigue tests were performed according to ASTM D3479/D3479M titled ‘Standard Test Method for Tension-Tension Fatigue of Polymer Matrix Composite

Materials.’ This test method is limited to unnotched test specimens subjected to constant amplitude uniaxial in-plane loading that is defined in terms of a test control parameter.

3.1.1 Dynamic/Fatigue Testing System

All the static and fatigue tests were performed on a MTS Servohydraulic Testing System as shown in Figure 3.1. The controller on this machine was Flex Test SE v4.0A. The capacity of the load frame was 110 kN (22 kips). The hydraulic grips in which the specimen was clamped could apply a maximum pressure of 10 ksi (69 MPa). The machine was capable of conducting static tensile, compression, flexural or bending, and fatigue tests. It was controlled by the use of “Multipurpose Testware” software developed by the MTS Corporation.

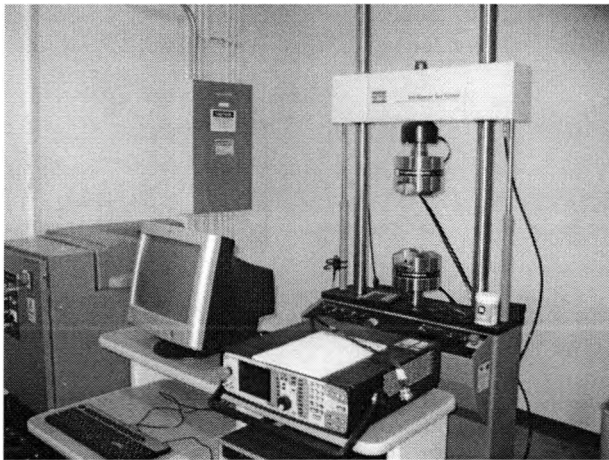


Figure 3.1 MTS servo hydraulic test system

3.2 Static Tests

The following sections provide details on static tests performed.

3.2.1 *Static Tensile Test*

Static tensile tests were performed according to ASTM D3039/D3039M titled ‘Standard Test Method for Tensile Properties of Polymer Matrix Composite Materials.’ This test method determines the in-plane tensile properties of polymer matrix composite materials reinforced by high-modulus fibers. The shape of the specimen is rectangular as shown in Figure 3.2. The specimens were 254 mm and 25.4 mm, respectively. The thickness varied between 5.7 mm to 6.2 mm. The specimens which met the requirements of the ASTM standard were selected. The critical requirements of the specimens were a width tolerance of $\pm 1\%$ and a thickness tolerance of $\pm 4\%$. The specimen should be tabbed at the ends to ensure failure occurs in gage area. Tabs are made of glass/polyester composite and are glued to specimen using high-strength 2-part epoxy adhesive DP-460 (manufactured by 3M, Inc.). Tabs strengthen the specimen at ends to ensure that failure doesn’t occur in grip area. The in-plane tensile properties, such as ultimate tensile strength (UTS or, S_u), strain at UTS, and longitudinal tensile modulus were evaluated. The axial strain was measured by an extensometer. All static tensile tests were conducted in the displacement control mode with a cross head rate of 2.0 mm/min.

In this test method a flat strip of material having a constant rectangular cross section was mounted in the hydraulic grips and loaded in tension while recording the load, displacement and time. The ultimate tensile strength of the material can be determined from the maximum load carried before failure. After the collection of data the stress vs.

strain graph was plotted from which the ultimate tensile strength (UTS or, S_u), strain at UTS, longitudinal tensile modulus were determined for that particular material.

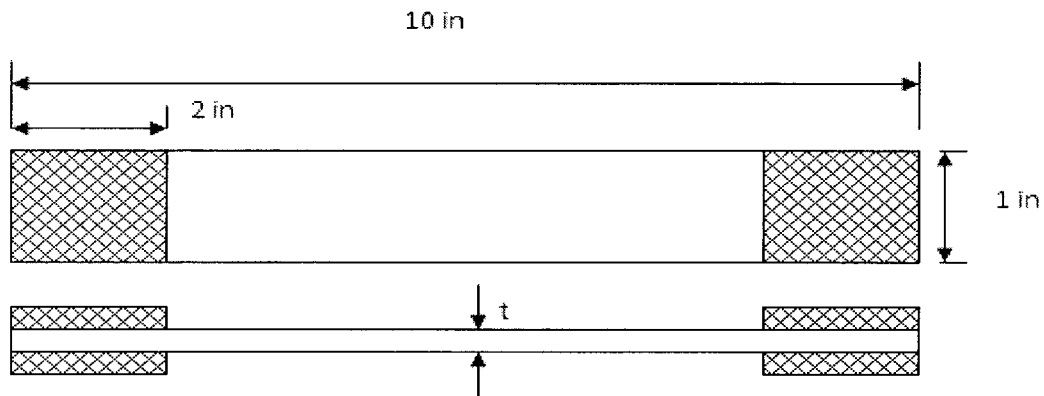


Figure 3.2 Tensile Tests Specimen

The tensile stress is the highest engineering stress that develops in the material before rupture. The tensile stress, also known as the ultimate tensile strength (UTS), can be determined by dividing the maximum load by the un-deformed area of the specimen. The equation below shows the UTS, which is the maximum stress

$$\sigma_{\max} = \frac{P_{\max}}{A_o}$$

Where, P_{\max} = maximum load, A_o = un-deformed cross-sectional area.

As per ASTM standard, the slope of the initial linear portion of the stress-strain graph is termed as chord modulus. The chord modulus of elasticity in tension is computed within strain range of 0.001 mm/mm to 0.003 mm/mm absolute strains.

$$E^{chord} = \frac{\Delta\sigma}{\Delta\varepsilon}$$

Figure 3.3 shows tension test specimen and a fixture during test. The failure modes of tensile specimens were noted as per the ASTM standard (Refer to Figure 3.4).

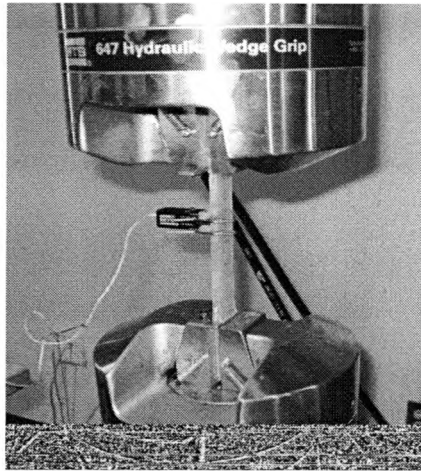


Figure 3.3 Tension Test Specimen and Fixture

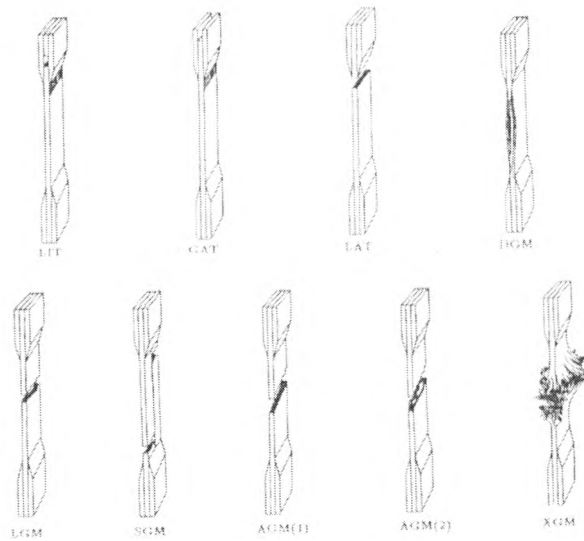


Figure 3.4 Typical Tensile Test Failure Modes (ASTM D3039)

3.2.2 Flexure Test

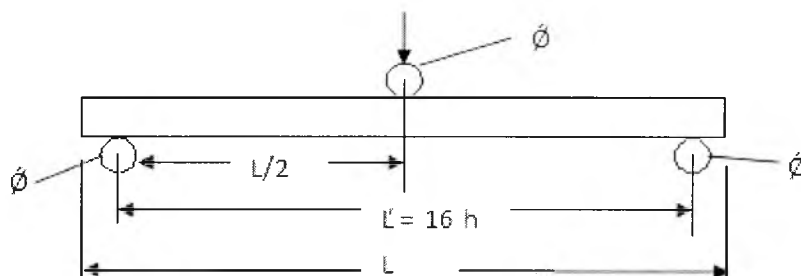
Flexure tests were performed according to ASTM D 790-92 titled 'Standard Test Methods for Flexural Properties of Unreinforced and Reinforced Plastics and Electrical Insulating Materials.' These test methods determine the flexural properties of unreinforced and reinforced plastics, including high-modulus composites and electrical insulating materials in the form of rectangular bars molded directly or cut from sheets, plates, or molded shapes.

The main use of the Flexure test is as a quality control test and for determining resistance of composite laminates to environmental factors. During the test, the top of the sample under the loading force is in compression and the bottom opposite the loading force is in tension (Strong, 2008). Depending on span-to-thickness ratio and strengths in tension/compression/shear, the beam may fail in tension at bottom or compression at top or in shear. Failures in shear requires very short span (span-to-thickness ratio 4:1) and failure in tension and compression occurs for longer spans (span-to-thickness ratio 16:1 and above). Flexural tests in this research are conducted with span-to-thickness ratio 16:1. In flexure test load is applied out-of-plane that imposes both compression and tensile stresses.

The specimen rests on two supports and was loaded by means of a loading nose midway between the supports. The proportions of specimen geometry are shown in Figure 3.5. Specimens were loaded under 3-point loading as shown in Figure 3.6. The ratio of loading span to depth of specimen was 16. The density of each specimen was measured to compute overall fiber volume fraction. The test specimen thickness and

width were measured. The specimens that meet ASTM requirement were selected. The specimen is placed in the testing machine such that the loading nose and two support cylinders were parallel and straight as shown in Figure 3.6.

As per thickness of the specimen, loading span was 80 mm and width was 13 mm. The specimen was loaded at a rate of crosshead movement of 2 mm/min., while recording load and the displacement. From the load and displacement data we can find the flexural strength and flexural modulus of the composite materials.



Where h =thickness, Specimen Length = L , Span Length (L') = $16h$, width= b
Figure 3.5 Flexure Test Specimen Loading

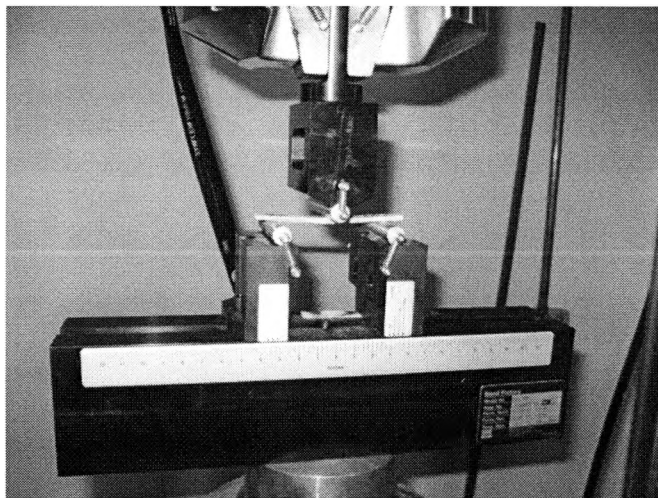


Figure 3.6 Flexure Test Specimen and Fixture

Flexural strength is calculated by using the formula,

$$\sigma_{fs} = \frac{F_{max}.L}{b.d^2}$$

Where, F_{max} = Maximum load, L= Loading span of the specimen, b= width of the specimen, d= thickness of the specimen.

Maximum strain is calculated by using the formula, $\epsilon = \frac{(6.D d)}{L^2}$

Where D = maximum deflection, d= Thickness, L= Loading span length

Flexural modulus is calculated by using formula, $E_{fs} = \frac{m.L^2}{(4.b.d^3)}$

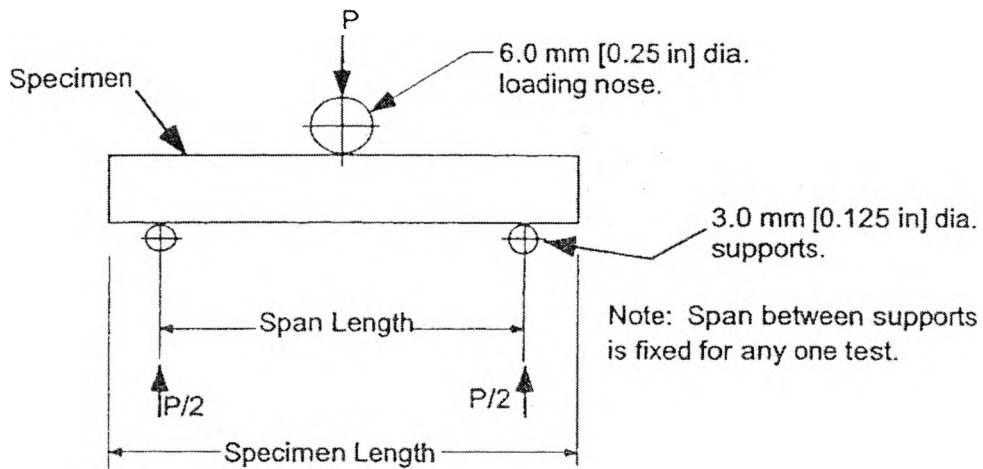
Where, m slope of initial linear portion on load-deflection curve, L= Length of the specimen, b= width of the specimen, d= thickness of the specimen.

3 2 3 *Inter laminar Shear Strength-ILSS Test (Short-Beam Test)*

Short Beam tests were performed according to ASTM D 2344/D 2344M titled ‘Standard Test Method for Short-Beam strength of Polymer Matrix Composite Materials and their Laminates.’ This test method determines the short-beam strength of high-modulus fiber-reinforced composite materials. The specimen is a short beam machined from a flat laminate up to 6.3 mm. thickness. The beam is loaded in three-point bending.

The size of the specimen depends on the thickness of the specimen. The proportions of specimen geometry are shown in Figure 3.7. The specimen is loaded at a rate of crosshead movement of 1 mm/min, while recording load and the displacement. From the

load and displacement data we can find the short-beam shear strength which is also referred to as inter-laminar shear strength (ILSS). The specimen geometry is shown in Figure 3.7 and related fixture is displayed in Figure 3.8.



Where h =thickness, Specimen Length (L)= $6h$, Span Length (L^1)= $4h$, width (b)= $2h$
Figure 3.7 Short Beam Specimen Loading (ASTM D 2344/D 2344M)

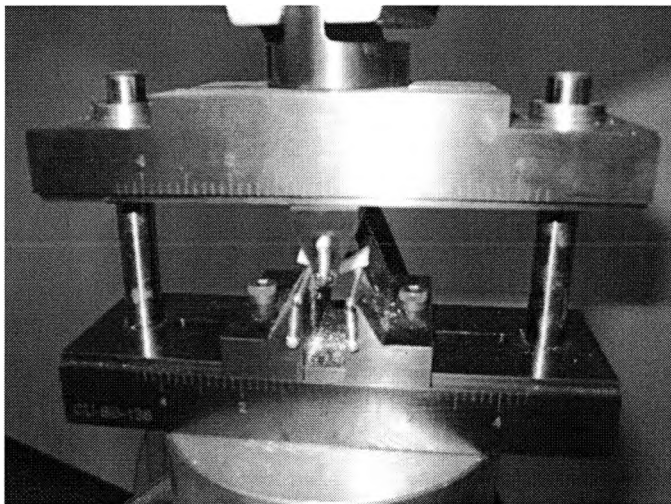


Figure 3.8 Short Beam Test Fixture Loaded with Specimen

The short-beam shear test (also called as inter laminar shear strength-ILSS) is used to determine the fiber/matrix adhesion of the composite materials. The most important of the tests for these materials view shear as a peel phenomenon (shearing along an adhesive plane). Short-Beam shear test is used as a quality control test of the lamination process and related matrix-dominated properties of the composite. The specimen span-to-thickness ratio is constrained to 4:1, forcing the shear stress to attain failure levels before tension and compression stresses reach their ultimate values (Strong, 2008).

This ILSS (Short Beam) testing is similar to the flexure testing except that the sample-to-thickness ratio is much less-approximately 4:1, for ILSS. The density of each specimen was measured to compute overall fiber volume fraction. The test specimen thickness and width were measured. The specimens that meet ASTM requirement were selected. The beam is loaded in three-point bending as shown in the Figure 3.11.

Short Beam strength is calculated by using the formula, Short Beam strength,

$$F_{sbs} = \frac{(0.75 * P_{max})}{b * h}$$

Where, Pmax= Maximum load observed during the test,

b= specimen width, h=specimen thickness.

3.3 Tension-Tension Fatigue Tests

Tension-tension fatigue tests were performed according to ASTM D3479/D3479M titled ‘Standard Test Method for Tension-Tension Fatigue of Polymer Matrix Composite Materials.’ This test method is limited to unnotched test specimens subjected to constant amplitude uniaxial in-plane loading that is defined in terms of a test control parameter (defined by Procedure A and B).

Procedure A (Load Controlled) — A system in which the test control parameter is the load (stress) and the machine is controlled so that the test specimen is subjected to repetitive constant amplitude load cycles.

Procedure B (Displacement Controlled)— A system in which the test control parameter is the strain in the loading direction and the machine is controlled so that the test specimen is subjected to repetitive constant amplitude strain cycles. All tension-tension fatigue tests were conducted according to procedure A.

In constant amplitude load controlled tests, stress is applied as a percentage of UTS. The stress was applied from 80% of UTS and reduced in steps of 10% until specimens survived 1 million cycles. Typically, the stress level at infinite life is referred to as endurance limit, but for most engineering purposes, “infinite life” is usually considered between 1 million and 10 million cycles. In the present research, endurance limit refers to the stress level at 1 million cycles. The other test parameters selected were sinusoidal waveform, 2 Hz frequency, and 0.1 stress ratio. Stress ratio (R) is defined as

$$R = \frac{\sigma_{\min}}{\sigma_{\max}} = \frac{P_{\min}}{P_{\max}} \quad \text{Where,}$$

σ_{\min} = Minimum stress and corresponding load is P_{\min}

σ_{\max} = Maximum stress and corresponding load is P_{\max}

Fatigue testing is very time-consuming study. Therefore very often researchers perform 'Accelerated Testing.' Accelerated testing consists of test methods that deliberately shorten (in a measured way) the life of the tested product or accelerate the degradation of the product's performance. Most accelerated testing is performed on materials or products to characterize their degradation mechanisms (e.g., fatigue, creep, cracking, wear, corrosion/oxidation, weathering (Battat, 2001). In accelerated fatigue testing, the frequency is limited to 5-10 Hz for polymer composite materials because of their viscoelastic nature. These materials may show dramatic change in fatigue life and different failure mechanisms at lower temperatures. Two sets of tests were performed one at 2 Hz frequency and one at 5 Hz frequency. There was dramatic decline in fatigue life especially in high-cycle fatigue when 5 Hz frequency was used. Besides maximum temperature of 52 °C was observed at the surface of the specimen. Therefore all fatigue tests are conducted at 2 Hz frequency. It should be noted that it took almost 6 days to complete 1 million cycles at 2 Hz frequency.

The geometry of the test specimens was identical for both tension and fatigue tests as shown in Figure 3.1. The specimens were 254 mm and 25.4 mm, respectively. The thickness varied between 5.7 mm to 6.2 mm. All the specimens were tabbed to avoid

failure in the grip. The specimens which met the requirements of the ASTM standard were selected. The critical requirements of the specimens were a width tolerance of $\pm 1\%$ and a thickness tolerance of $\pm 4\%$. Fatigue tests were performed only on control (0 wt% nanosilica) and 6 wt% nanosilica. The maximum stress was applied as percentage of ultimate tensile strength on control composites. These percentages were 80%, 70%, 60%, and 50% of UTS and magnitudes of 74.5, 65.2, 55.9, and 46.6 MPa, respectively. The control composites survived 1 million cycles at maximum stress of 50% of UTS. Three tests were performed at each stress level. Same maximum stresses 74.5, 65.2, 55.9, and 46.6 MPa were applied on 6wt% nanosilica composites. It should be noted that the objective of this research is to evaluate improvement in fatigue life when nanosilica is added. Table 3.2 exhibits test matrix. Total 24 specimens were tested.

Table 3.2: Number of fatigue test specimens

Maximum stress applied, MPa	Control Composites (0 wt%)	6 wt% Nanosilica Composites
74.5	3	3
65.2	3	3
55.9	3	3
46.6	3	3

3.4 Stiffness Degradation

The fatigue damage mechanism of composites is highly complex and may be in one or more forms such as fiber/debonding, matrix cracking, delaminations, and fiber breakage. Some of these damage mechanisms may interact simultaneously. Damage

during fatigue is reflected in strength, stiffness, and fatigue life reduction. Different damage mechanisms such as matrix cracking and delamination reduce stored energy, which in turn reduces stiffness. There is always a correlation between damage and stiffness reduction. Thus, stiffness reduction is the only parameter that can be monitored to evaluate the useful life of a component. Stiffness reduction is often referred to as “stiffness degradation” or “modulus decay” or “modulus reduction” in the literature.

The evaluation of residual strength and fatigue life involves destructive testing, whereas stiffness can be measured using nondestructive techniques such as ultrasound. It is well-known that the wave speed of sound in a material is related to its stiffness. The presence of defects (e.g., voids, cracks, micro damages, etc.) changes the effective stiffness of a material. When a wave is propagated through a material, the change in stiffness is manifested as a change in the sound velocity. Furthermore, the defects act as wave scatterers. As a result, the defect population also manifests itself in an attenuation of the wave that passes through the material. Many researchers have used the changes in wave speed and attenuation due to damage as a nondestructive tool for stiffness measurement.

Axial extensometer was used to monitor axial strain during entire fatigue tests on all tests specimens. Fatigue secant modulus is defined as maximum stress at particular cycle divided by corresponding axial strain. For example, $E(1)$ and $E(n)$ represent fatigue secant modulus at 1st and nth cycle, respectively.

Fujii & Amijima (1993) proposed the Modulus Decay Mechanism for woven composites as shown discussed in detail in chapter 1 and Figure 1.11. The modulus decay mechanism for $\pm 45^\circ$ stitched bonded composites exhibited similar pattern. There were 3 distinct zones. The stiffness degradation curves are explained in detail in the next chapter.

3.5 Static Tests on HNT-Epoxy Neat Resin

Static tests were conducted on control-epoxy neat resin (no nanoparticles) and HNT-epoxy neat resin specimens. The primary goal of these tests was to establish right dispersion procedure for HNTTM and to evaluate right weight percentage of HNTTM. These tests can be considered as screening tests. As discussed in detail in Chapter 2, three different techniques were used to disperse HNTTM in liquid epoxy resin. These techniques were centrifugal planetary mixing (THINKY), high shear mixing (IKA), and low-shear mechanical mixing (Dispermat). HNTTM loadings used were 2.5 wt%, 5 wt% and 10 wt%. Mainly tension, flexure, and Izod-impact tests were conducted. These tests were selected as they provide good knowledge about whether HNTTM helps in toughening epoxy resin. It will be reflected in percentage elongation at break in tension; flexural strength and modulus; and impact toughness.

The tensile properties of epoxy resin were evaluated according to ASTM D638 titled “Standard Test Method for Tensile Properties of Plastics” This standard recommends selecting a test speed to produce rupture in $\frac{1}{2}$ to 5 minutes. The selected speed of testing

was 5 mm/min. The axial strain was measured using an extensometer. The geometry of the test specimens is shown in Figure 3.4.

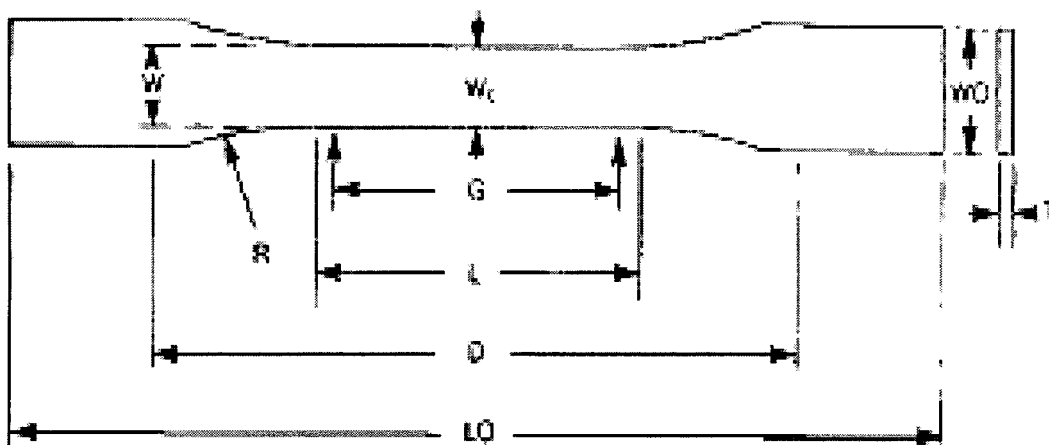


Figure 3.9: Specimen Geometry for Neat Resin Coupon (ASTM D638)

Where, W_0 is width overall, W is the width of the narrow section, G is gage length, L is the length of narrow section, D is the distance between grips, and R is the radius of the fillet.

The flexural properties of epoxy resin were evaluated according to ASTM D 790. This standard is same as that was used for glass reinforced composites as discussed in section 3.2.3. The length to thickness ratio selected was 16. The specimen dimensions were 100 mm overall length, 13 mm width, and 6.20 mm thickness. The loading span was 80 mm and rate of cross-head movement was 2 mm/min.

Izod-impact tests were conducted according to ASTM D256 titled “Standard Test Method for Determining the Izod Pendulum Impact Resistance of Plastics”. Impact toughness evaluated. Notches were made on the specimens with notching cutter shown in

Figure 3.10 before testing while monitor/impact tester was used to test the specimens as per ASTM D256. The impact/ monitor tester is shown in Figure 3.11.

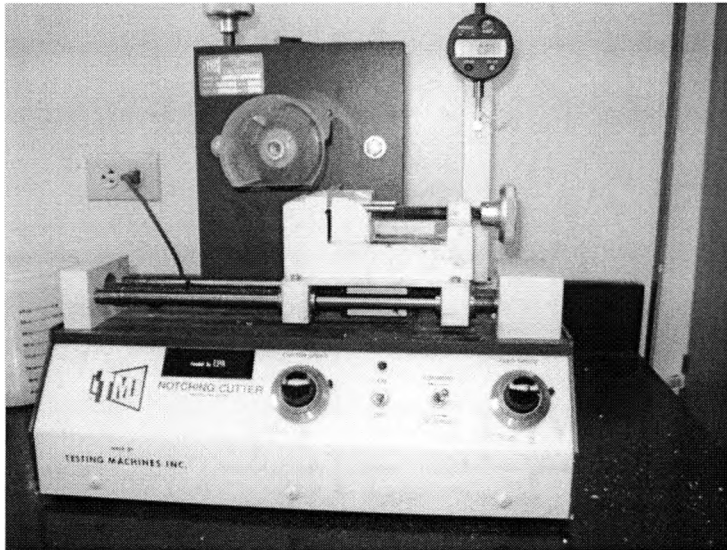


Figure 3.10: Notching cutter

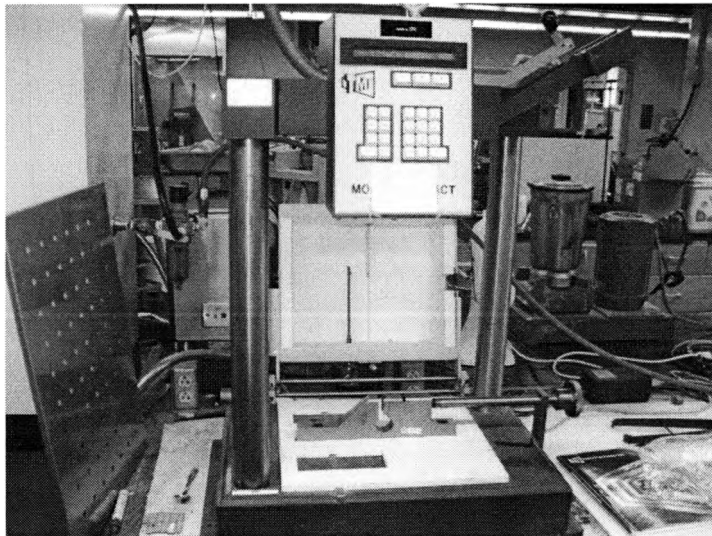
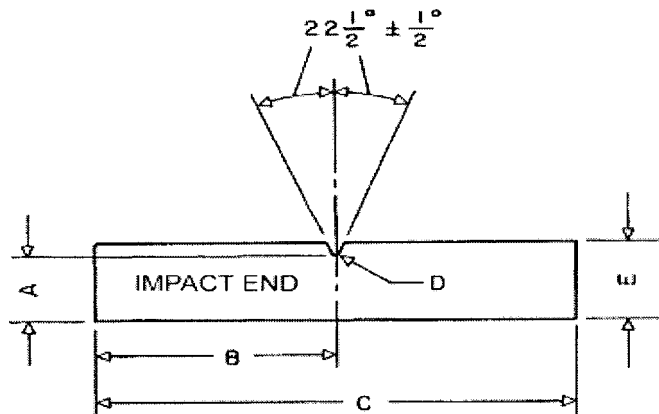


Figure 3.11: Monitor/ Impact tester

A range of pendulum having energies from 2.7 to 21.7 J has been found to be sufficient for use with most plastic specimens. Commonly used hammers have mass that range from 0.55- 4.5 kg, but due to the nature of the specimens, 550 g was used in this study on TMI impact tester. The vertical distance of fall of the pendulum from its latched height to its lowest point was around 610 mm. The cutting speed was constant throughout the cutting operation. Breaking energy is determined by detecting the height of rise of the pendulum beyond the point of impact in terms of energy removed from that specific pendulum.

Impact energy is expressed in Joules while impact strength is calculated by dividing impact energy by the thickness of the specimen (J/m). The geometry of test specimen is shown in Figure 3.12.



A= 10.16 mm, B= 31.8 mm, C= 63.5 mm, D= 0.25R, 12.70mm.

Figure 3.12: Specimen Geometry for Neat Resin Coupon (ASTM D256)

HNT-epoxy composites showed great inconsistency in results. It was concluded that further research is required on establishing right procedure for dispersing HNT. There is also need to conduct detail SEM analysis especially on fractured surfaces to evaluate interfacial adhesion between epoxy and HNT particles. Therefore, HNT nanocomposites (reinforced with glass) were not studied under static mechanical and fatigue loadings.

Chapter 4 deals with results and discussion on static tests, fatigue tests, S-N diagram, and stiffness degradation curves.

CHAPTER 4

RESULTS AND DISCUSSION

4.1 Introduction

In this chapter would elaborate on results of static tests, fatigue tests, S-N diagram, and stiffness degradation curves and would discuss it. The following section deals with tensile test, flexural test and inter laminar shear strength (ILSS) results.

4.1.1 Static Tensile Test

As mentioned earlier, 5 tests in each category were conducted according to ASTM D3039. Table 4.1 consolidates tensile test results which include ultimate tensile strength (UTS), tensile chord modulus (E), and failure strain at UTS. The numbers in the parenthesis indicate standard deviation. Figure 4.1 displays superimposed stress vs strain curves for control (0wt %), 6wt%, 7wt%, and 8wt% nanosilica loadings. Figure 4.2 shows how chord modulus was computed between strain values of 0.001 to 0.003 as stated in ASTM 3039 standard.

Composite materials are heterogeneous in nature. There is always variation in orientation of fibers between layers and fiber volume percentage. Tensile strength is fiber dominant property. It is true that majority of the load is carried by fibers but matrix carry small amount of load. The results indicate that there is improvement in tensile strength in

nanomodified composites. This improvement is mainly because of improved properties of epoxy resin itself and improved fiber/matrix adhesion. **Table 4.1: Tensile Strength of Nanosilica Nanocomposites (fiber volume fraction 0.52 ± 0.04)**

Nanosilica wt%	0	6	7	8
Tensile strength (MPa)	92.08 (1.91)	112.35 (6.14)	109.49 (11.57)	101.40 (1.09)
Tensile modulus (GPa)	10.26 (0.96)	11.19 (0.38)	12.75 (0.81)	11.66 (0.78)
Failure strain at UTS (%)	8.49 (0.64)	11.12 (1.44)	7.25 (2.60)	9.76 (0.84)

Standard deviations are in parenthesis

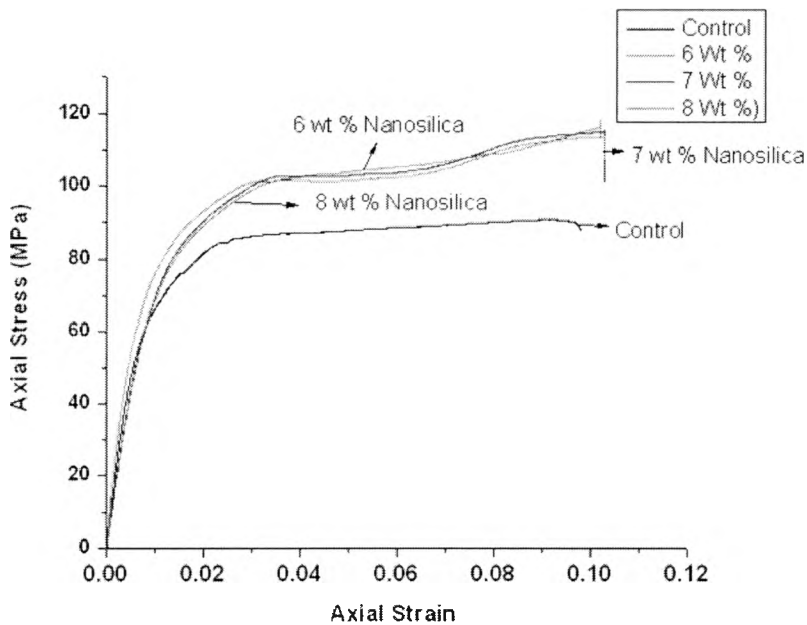


Figure 4.1: Tensile stress-strain curves for control and nanocomposites

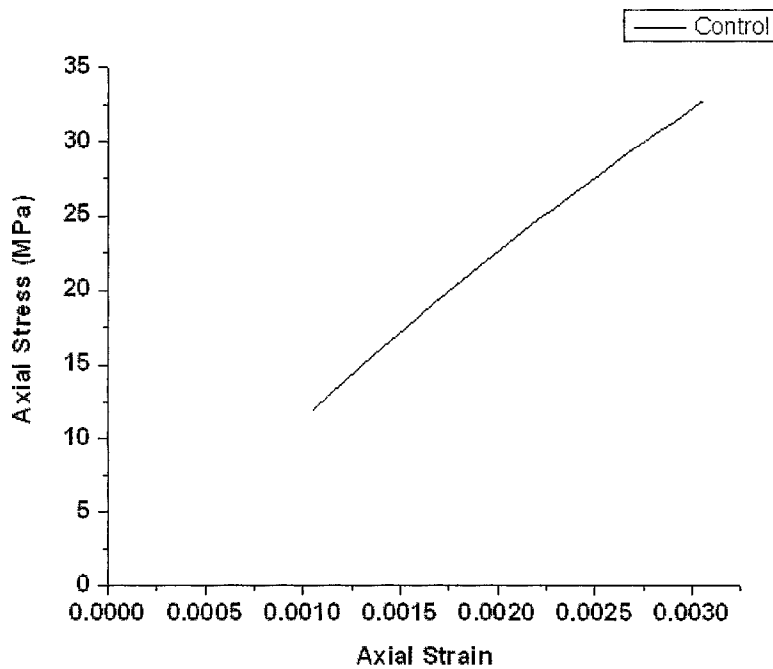


Figure 4.2: Chord modulus on control specimen

It is evident that with 6wt% and 8wt% nanosilica there is improvement in tensile strength, tensile modulus, and percentage elongation. It is very impressive that nanomodification improved tensile modulus at the same time toughened the composites which is indicative from increased area under stress-strain curve. 6wt% nanosilica nanocomposites showed 22% improvement in tensile strength. Tensile modulus and percentage elongation (failure strain at UTS) are affected by matrix material. 7wt% nanosilica showed highest improvement in tensile modulus but at the expense of percentage elongation. Decrease in percentage elongation indicate loss of ductility and thereby toughness. 6wt% nanosilica nanocomposites showed 10% improvement in tensile modulus over control and this improvement is along with 30% improvement in percentage.

Figure 4.3 and 4.4 shows failed specimens in tensile tests.

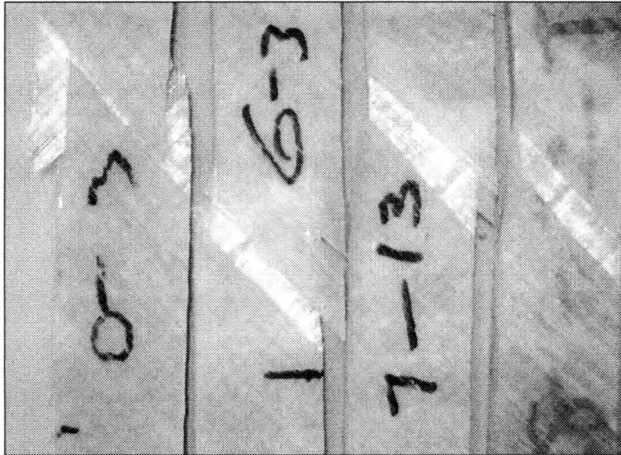


Figure 4.3: Front side micrograph of failed tensile specimen

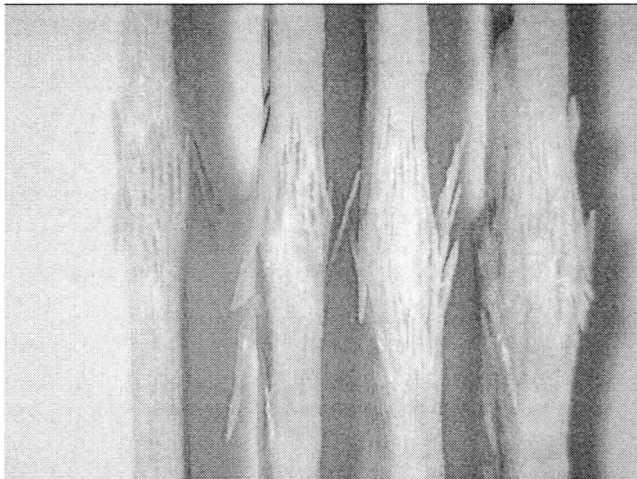


Figure.4.4: Side micrograph of failed tensile specimen

4.1.2 Flexural Test

As mentioned earlier, 5 tests in each category were conducted according to ASTM D790. Table 4.2 consolidates flexural test results which include flexural strength and flexural modulus. The numbers in the parenthesis indicate standard deviation. Figure 4.5

displays superimposed load vs cross-head displacement curves for control (0 wt%), 6wt%, 7wt%, and 8wt% nanosilica loadings. Figure 4.6 shows how slope of initial linear region (m) was computed, that is required for computation of flexural modulus.

Table 4.2: Flexural Strength

Nanosilica wt%	0	6	7	8
Flexural strength (MPa)	145.66 (10.41)	176.61 (7.90)	180.60 (3.91)	179.78 (1.58)
Flexural Modulus (GPa)	25.04 (2.11)	29.45 (2.15)	30.45 (1.15)	30.70 (0.85)

Standard deviations are in parenthesis

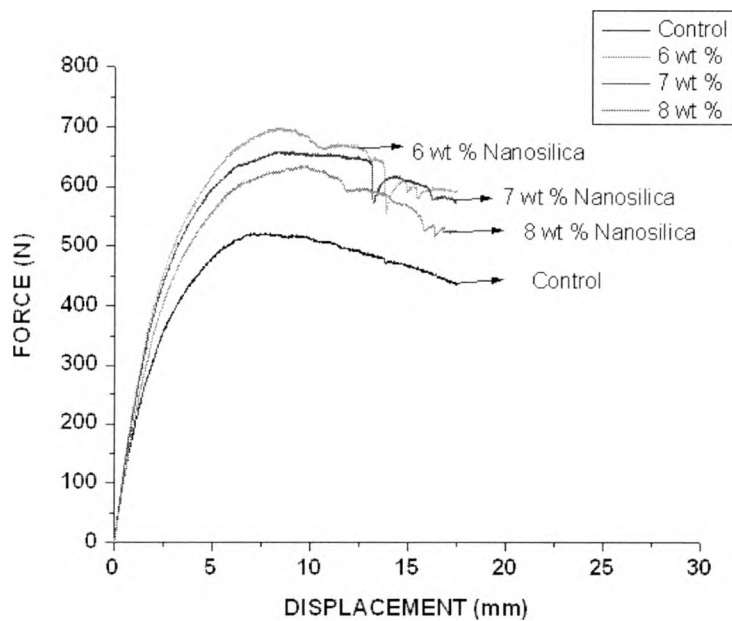


Figure 4.5: Load vs displacement graph of control and nanocomposites

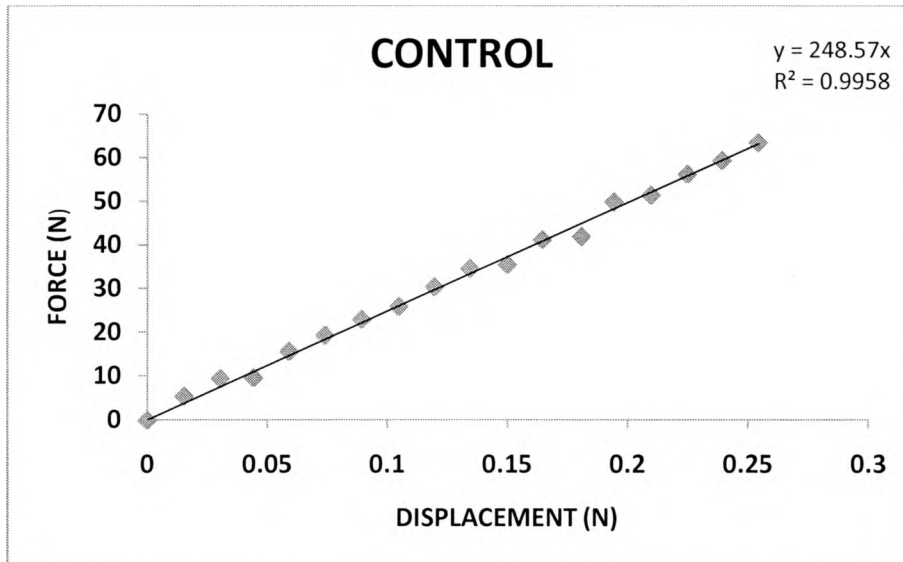


Figure 4.6: Slope of initial linear portion for control composites

For isotropic ductile materials such as carbon steels, flexural strengths are almost same as that of tensile strength. Composites are anisotropic materials and hence exhibit different strengths under tension, compression, and bending loads. Flexural properties are dependent on both fiber reinforcement and matrix. The main use of the Flexure test is as a quality control test and for determining resistance of composite laminates to environmental factors. They also can be used to compare relative increase or decrease between different materials systems. These tests are fairly easy to conduct and hence are very popular in composite industry. In flexure testing top layer is subjected to compression whereas bottom layer is under tension. Thus this test applies combination of tensile and compressive loadings. Flexural properties cannot determine basic material properties that are useful in theoretical design. But these properties play very important

role if the component is subjected to bending loads as in case of beams, truck beds, floor beds in airplane, and bath tub.

Table 4.2 indicates that 6wt%, 7wt%, and 8wt% nanosilica composites showed almost similar improvement in both flexural strength and flexural modulus. 6wt% nanosilica composites showed 21% and 17% improvement in flexural strength, and flexural modulus respectively. Figure 4.7 shows failed flexure specimens.

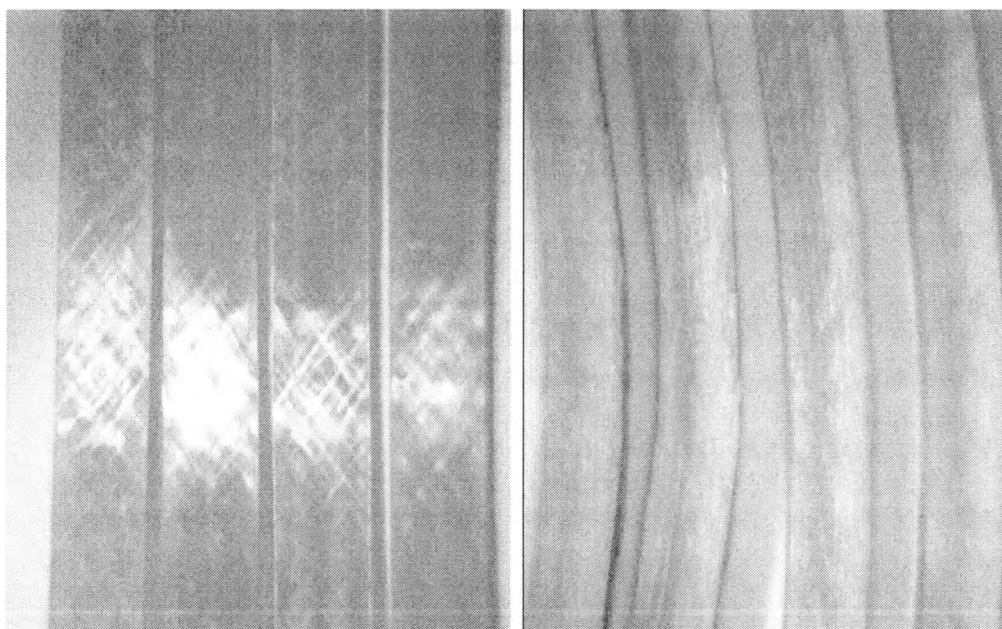


Figure 4.7: Front and side micrographs of failed flexure specimen

4.1.3 *Inter laminar Shear Strength (ILSS) Testing*

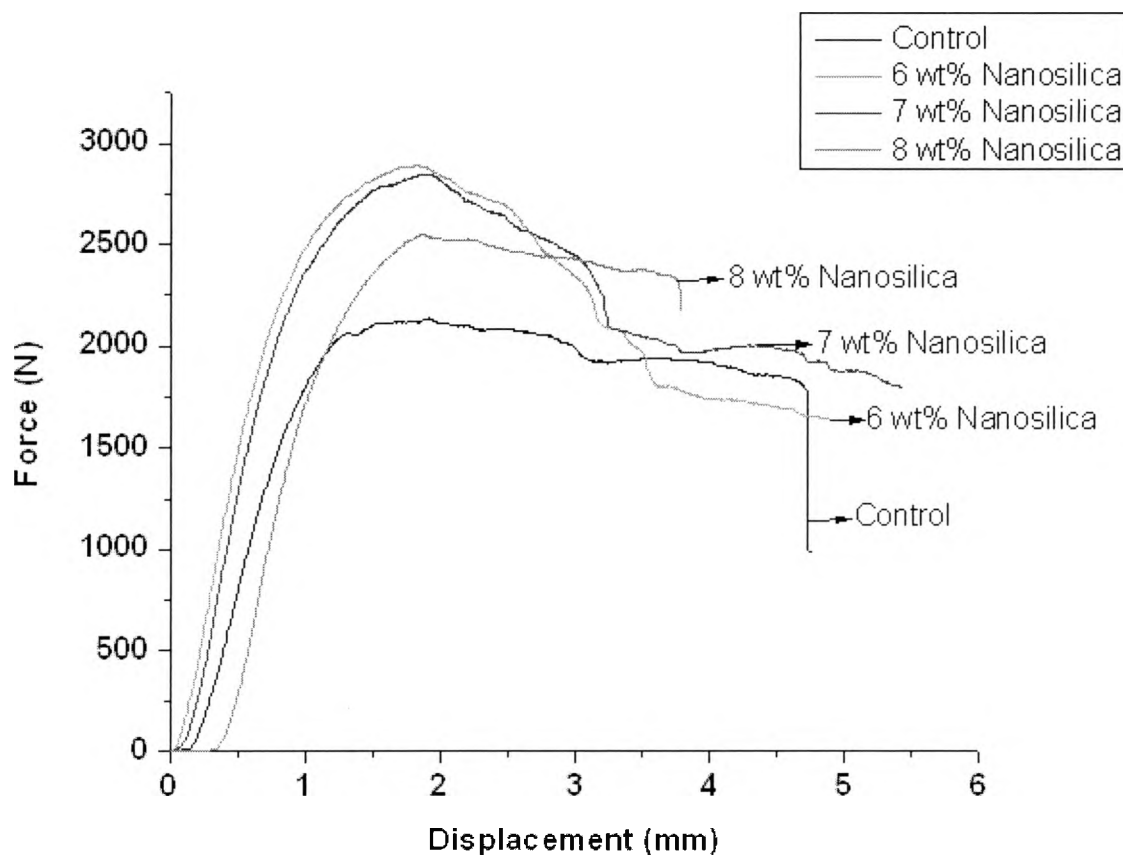
The short-beam shear test (also called as inter laminar shear strength-ILSS) is used to determine the fiber/matrix adhesion of the composite materials. Short-Beam shear

test is used as a quality control test of the lamination process and related matrix-dominated properties of the composite. As discussed earlier in chapter 3, the specimen span-to-thickness ratio is constrained to 4:1, forcing the shear stress to attain failure levels before tension and compression stresses reach their ultimate values. ILSS plays dominant role in products that are subjected to cycling loads leading to fatigue. Current wind turbine blades are fabricated with 2D woven glass fabric reinforcement stacked layer-by-layer to achieve required thickness. Such 2D components have limited life in fatigue environments due to inherently low matrix dominated interlaminar shear strengths (ILSS). Low ILSS leads to poor bond between two layers, delamination, and splitting of laminates. Thus the improvement in ILSS would lead to improved fatigue performance.

As mentioned earlier, 5 tests in each category were conducted according to ASTM D2344. Table 4.3 consolidates ILSS results. The numbers in the parenthesis indicate standard deviation. Figure 4.8 displays superimposed load vs cross-head displacement curves for control (0wt %), 6wt%, 7wt%, and 8wt% nanosilica loadings. Nanosilica modification showed improvement in ILSS at all loadings that shows improvement in fiber/matrix adhesion and in turn improvement in fatigue performance. At 6 wt% of nanosilica loading there was 26% improvement in ILSS. Figure 4.9 shows failed specimens in interlaminar shear loading.

Table 4.3: Interlaminar Shear Strength (ILSS)

Nanosilica wt%	0	6	7	8
ILSS (MPa)	24.50	31.02	30.12	29.79
Stdev	(1.05)	(0.84)	(0.48)	(0.76)

**Figure 4.8: Superimposed load vs cross-head displacement**

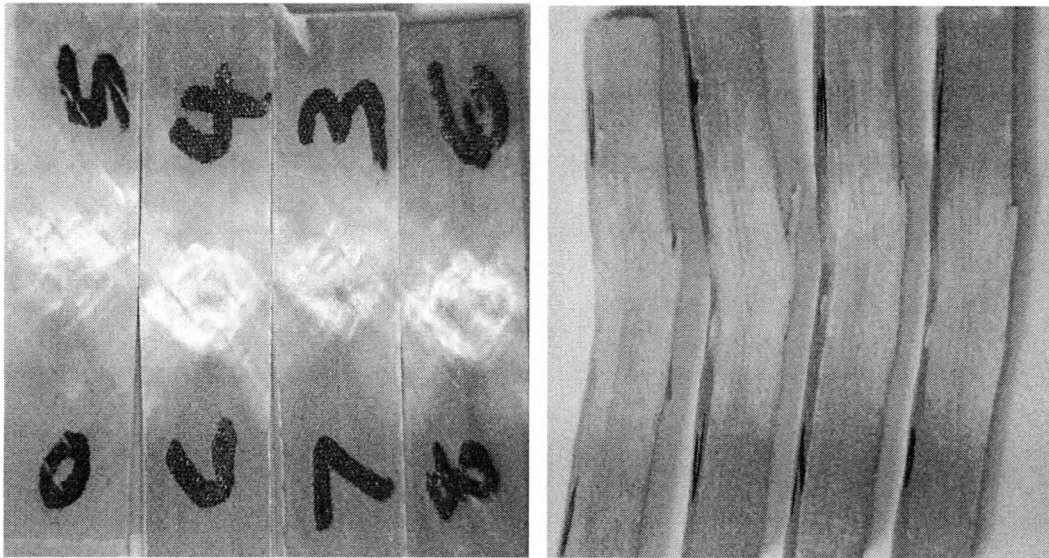


Figure 4.9: Front and side micrographs of failed ILSS specimen

Figure 4.10 below shows comparison of tensile, flexural, and interlaminar shear strengths, while Figure 4.11 shows comparison of tensile and flexural modulus.

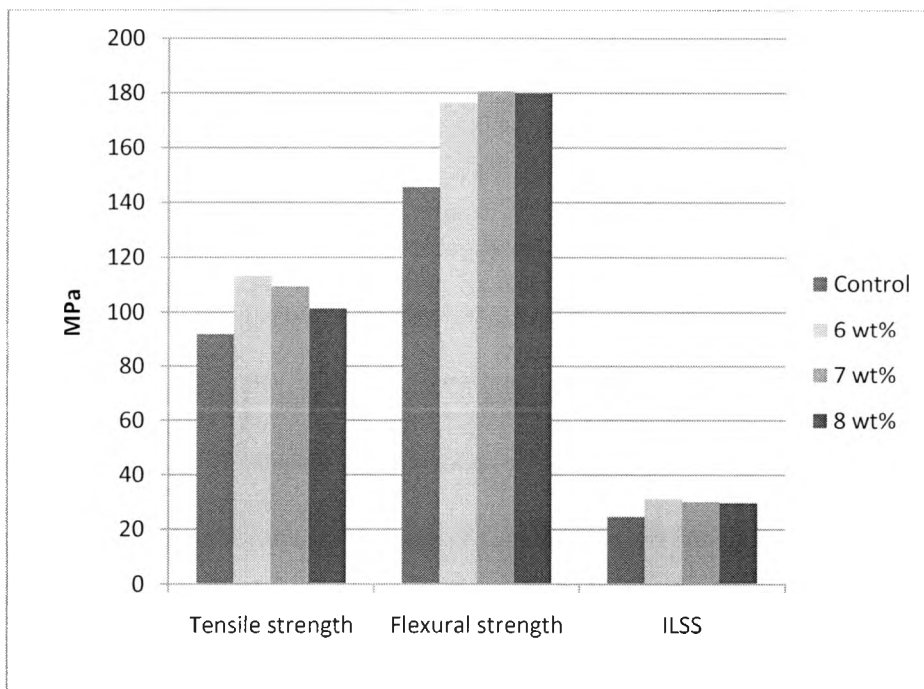


Figure 4.10: Different Strengths of control, 6, 7 and 8 wt% Composites

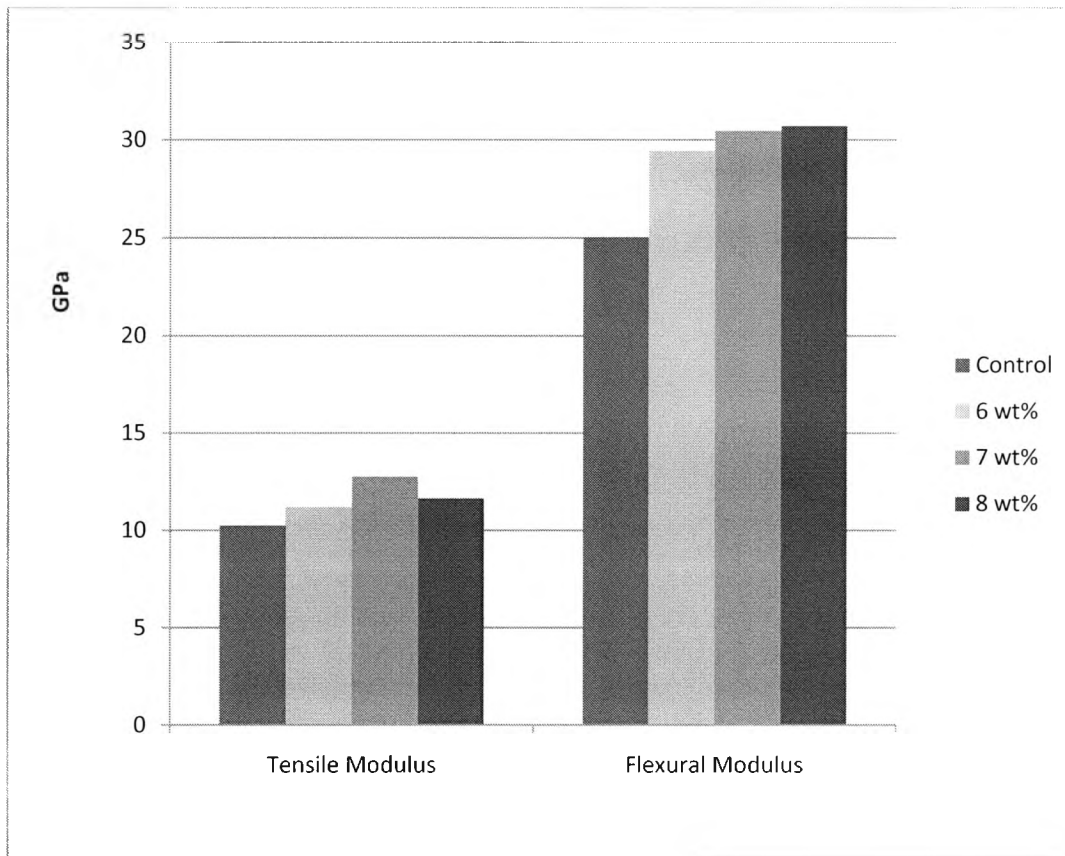


Figure 4.11: Tensile and Flexural Modulus of control, 6, 7 and 8 wt% Composites

When component is subjected to flexural cycling loading (flexural fatigue) the two sides of components alternately experience tensile and compressive loadings. Compressive loading closes cracks whereas tensile loading opens the cracks. In this research axial tension-tension fatigues tests are conducted that would simulate adverse loading compared to flexural fatigue loading. It would be expected that if material survives in axial fatigue then it would outperform in flexural fatigue. Wind turbine blades are designed with a high level of bending stiffness and fatigue-resistant characteristics. In

summary overall 6wt% nanosilica loading has shown impressive improvement in ILSS, flexural, and tensile properties. Therefore, axial fatigue tests were conducted only on 6wt% nanosilica composites.

4.2 Axial Fatigue Tests

Accelerated fatigue tests (higher frequencies) considerably reduce the time required for fatigue studies. Most of the polymeric materials show certain degree of viscoelasticity even at lower temperatures. Therefore frequency in fatigue tests should be selected very cautiously. Fatigue tests on control composites were conducted at 2 Hz and 5 Hz frequency. Three load-controlled tests were conducted at each load level according to ASTM D3479. The maximum stress was applied as percentage of ultimate tensile strength on control composites. These percentages were 80%, 70%, 60%, and 50% of UTS and magnitudes of 74.5, 65.2, 55.9, and 46.6 MPa, respectively. Same maximum stresses 74.5, 65.2, 55.9, and 46.6 MPa were applied on 6wt% nanosilica composites. All tests were continued until specimen breaks or survives 1 million cycles. Numbers of cycles required for failure (also called fatigue life) are shown in Tables 4.4 and 4.5 at 2Hz and 5Hz frequencies for control composites. Table 4.6 shows average number of cycles for failure at 2Hz and 5Hz frequencies for control composites. It is observed that frequency has dominant effect on fatigue life especially in high-cycle fatigue. Therefore, tests on 6wt% nanosilica composites were conducted at 2 Hz frequency. Table 4.7 shows fatigue test results for 6 wt % loading of nanosilica. Table 4.6 summarizes average

number of cycles for failure and average surface temperature on the specimens for control and 6wt% nanosilica composites at 2Hz frequency.

Table 4.4: Fatigue life of control specimens, 5 Hz frequency

Maximum stress applied, MPa	1	2	3
46.6	15820	N/A	N/A
55.9	15300	8974	4566
65.2	2158	2033	1001
74.5	919	355	165

Table 4.5: Fatigue life of control specimens, 2 Hz frequency

Maximum stress applied, MPa	1	2	3
46.6	1000000*	1000000*	1000000*
55.9	23598	21553	7590
65.2	1112	3220	1790
74.5	656	630	360

*run-out

Table 4.6: Average fatigue life on control specimens

Maximum stress applied, MPa	2 Hz	Average Temperature, °C	5 Hz	Average Temperature, °C
46.6	1000000*	33	15820	34
55.9	17580	35	9613	43
65.2	2041	51	1731	45
74.5	549	53	480	58

*run-out

Table 4.7: Fatigue life of 6wt% nanosilica composite specimens, 2 Hz frequency

Maximum stress applied, MPa	1	2	3
46.6	1000000*	1000000*	1000000*
55.9	166675	71420	55000
65.2	6058	7187	5672
74.5	1683	1444	1062

*run-out

Table 4.8: Average fatigue life on control and 6wt% nanosilica composite specimens (2 Hz)

Maximum stress applied, MPa	Control	Average Temperature, °C	6 wt% nanosilica composite	Average Temperature, °C
46.6	1000000*	33	1000000*	30
55.9	17700	35	166675	33.5
65.2	1832	51	6306	45.5
74.5	549	53	1396	51

*run-out

Both control and 6wt% nanosilica composites survived 1 million cycles at maximum stress of 46.6 MPa. It should be noted that tests were stopped at 1 million cycles. It is quite possible that 6wt% nanosilica nanocomposites would have much higher fatigue life remaining compared to control composites. This fact would be evident from stiffness degradation curves as discussed in the following section. When stress level is high specimens survive fewer number of fatigue cycles. This is very often called as low-cycle fatigue. At low stress levels specimens survive large number of fatigue cycles,

which is termed as high-cycle fatigue. Figure 4.12 shows failed fatigue specimens for control composites for 46.6, 55.9, 65.2, and 74.5 MPa maximum stress.



Figure 4.12: Failed fatigue specimens of control composites at 46.6, 55.9, 65.2, and 74.5 MPa maximum stress

4.2.1 S-N Diagram

Maximum fatigue stress applied vs number of fatigue cycles at failure diagram is very well-known as S-N diagram. This diagram can be used as fatigue life prediction tool at particular maximum stress.

Manjunatha et al. (2009) have conducted fatigue studies on neat epoxy resin (no glass reinforcement). They used same nanosilica Nanopox F400 as was used in this research. Figure 4.13 shows the linear trend in S-N diagram for nanosilica and micron-rubber modified neat epoxy resin. Nanosilica used was Nanopox F400 and micron-rubber used was Ablipox 1000. Both these products are developed by nanoresins, AG. EP type is

control neat resin; ER type contains 9wt% micron-rubber; ES type contains 10wt% nanosilica; and ESR type contains 9wt% micron-rubber and 10wt% nanosilica. ES type showed 6 and 3 times fatigue life improvement in high-cycle and low-cycle fatigue.

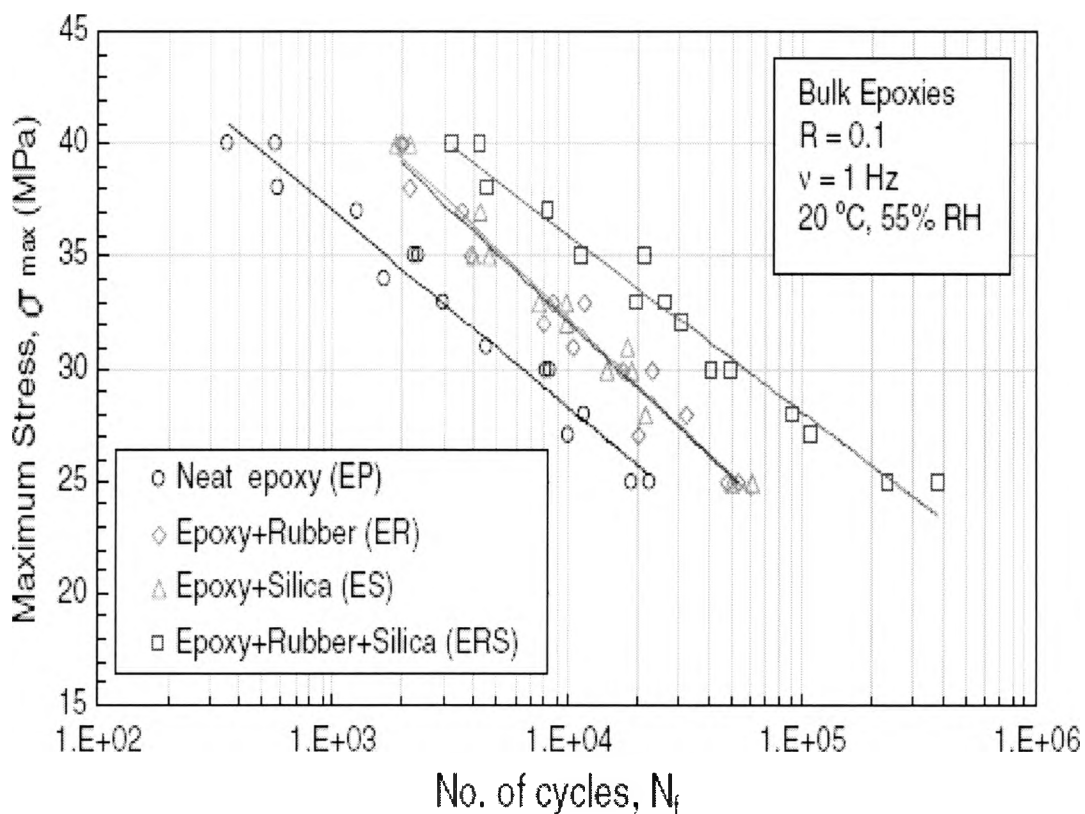


Figure 4.13: S-N Diagram for Nanomodified Neat Epoxy Resin (Manjunatha, Taylor, Kinloch, and Sprenger, 2009)

Figure 4.14 shows the linear trend in S-N diagram for control and 6wt% nanosilica nanocomposites. Nanosilica modification showed 10 and 3 times improvement in fatigue life in high-cycle and low-cycle fatigue, respectively.

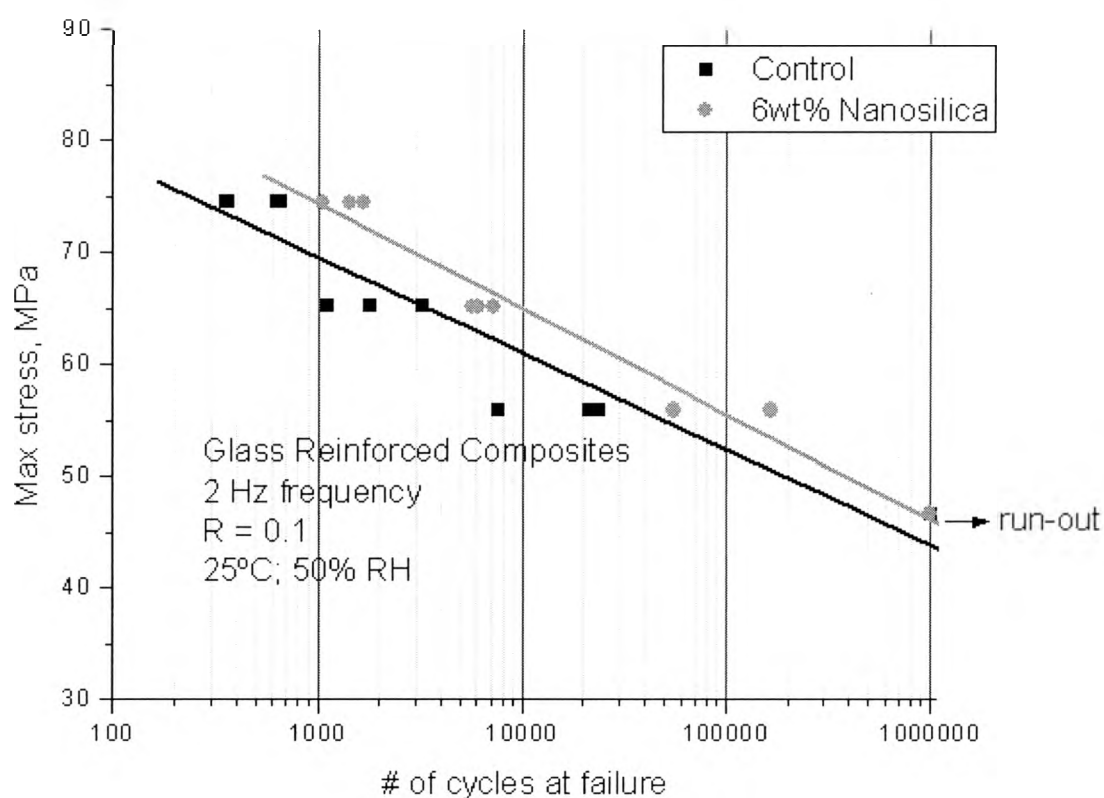


Figure 4.14: S-N Diagram for Glass reinforced composites

4.3 Stiffness Degradation Curves

The fatigue damage mechanism of composites is highly complex. Different damage mechanisms such as matrix cracking and delamination reduce stored energy, which in turn reduces stiffness. There is always a correlation between damage and stiffness reduction. Thus, stiffness reduction is the only parameter that can be monitored to evaluate the useful life of a component. Stiffness degradation was monitored for all fatigue tests. Fatigue secant modulus is defined as maximum stress at particular cycle

divided by corresponding axial strain. For example, $E(1)$ and $E(n)$ represent fatigue secant modulus at 1st and n th cycle, respectively. Figure 4.15 and 4.16 shows stiffness degradation for control and 6wt% nanosilica composites. X-axis represents cycle ratio, n/N and Y-axis represents modulus ratio, $E(n)/E(1)$. These curves exhibit typical three stage pattern as represented by Fujii and Amijima (1993) for woven composites. These curves have following three stages:

Stage I: In this stage modulus decreases rapidly. This stage is about cycle ratio (n/N) of 0.1 that is 10% of fatigue life. It is observed that 35 to 40% of modulus is lost in this stage.

Stage II: This stage constituted about 70% of the total fatigue life for control composites. By the end of this stage total 70% of modulus is lost for control composites. The trend is little different for 6wt% nanosilica composites. This stage contributed about 75% of fatigue life and by the end of this stage total 65% modulus was lost. This is quite bit of improvement in fatigue performance.

Stage III: Final failure occurs with the breakage of fibers. The stiffness decreases rapidly again during the last few cycles before the specimen fails. This stage contributed about 20% of fatigue life for control composites and 15% of 6wt% nanosilica composites.

There is very impressive improvement in fatigue performance especially at high-cycle fatigue for 46.6 MPa maximum stress. Figure 4.14 shows superimposed stiffness degradation curves for 46.6 MPa maximum stresses. It should be noted that both control and 6wt% nanosilica composites survived 1 million cycles at this stress level. The tests

were stopped after 1 million cycles. From stiffness degradation curves it is evident that by the end of 1 million cycles control composites lost about 65% of modulus whereas 6wt% nanosilica composites lost only 45% of modulus. It is clear that if fatigue tests were continued after 1 million cycles until specimen breaks, 6wt% nanosilica composites would survive much more number of cycles than control composites.

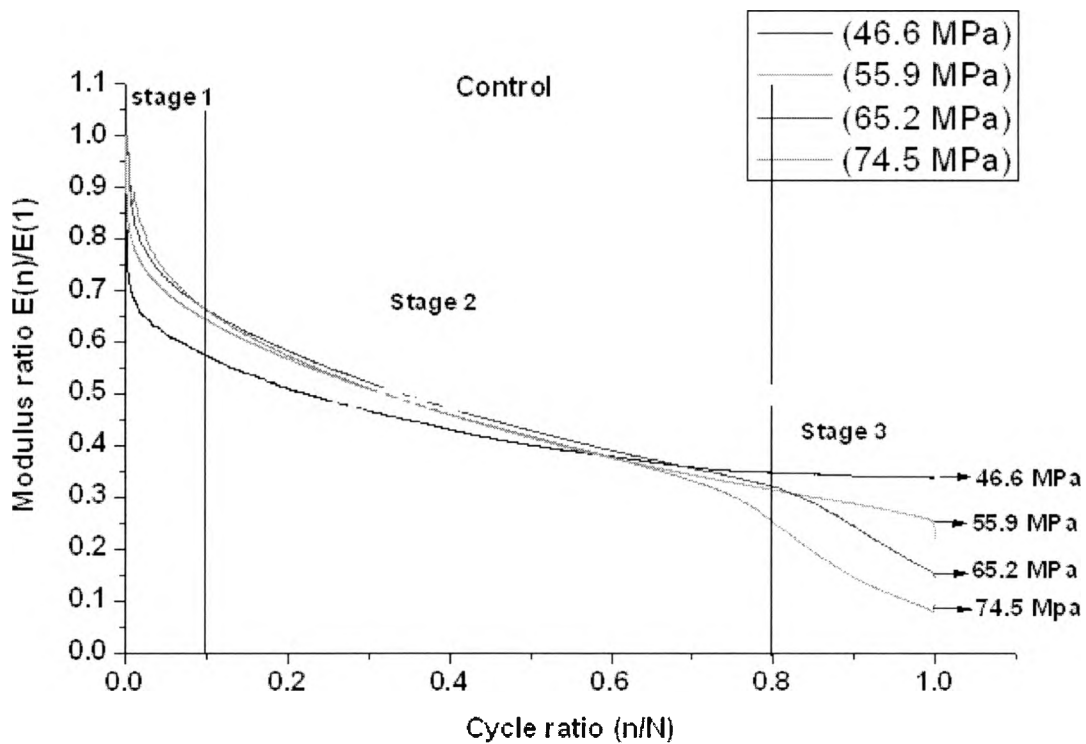


Figure 4.15: Stiffness degradation curve of Control specimens

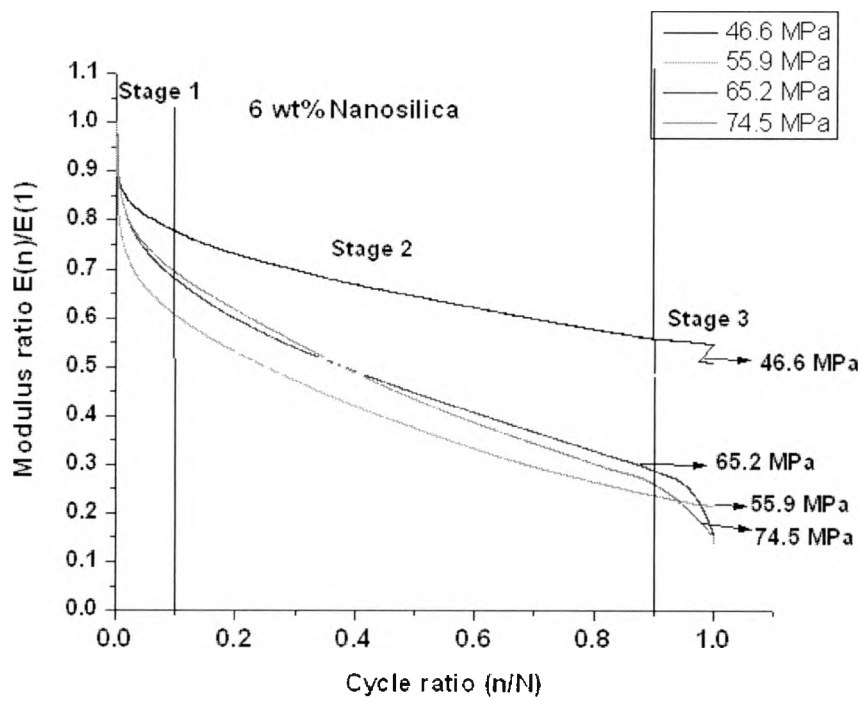


Figure 4.16: Stiffness degradation curve of nanomodified specimens

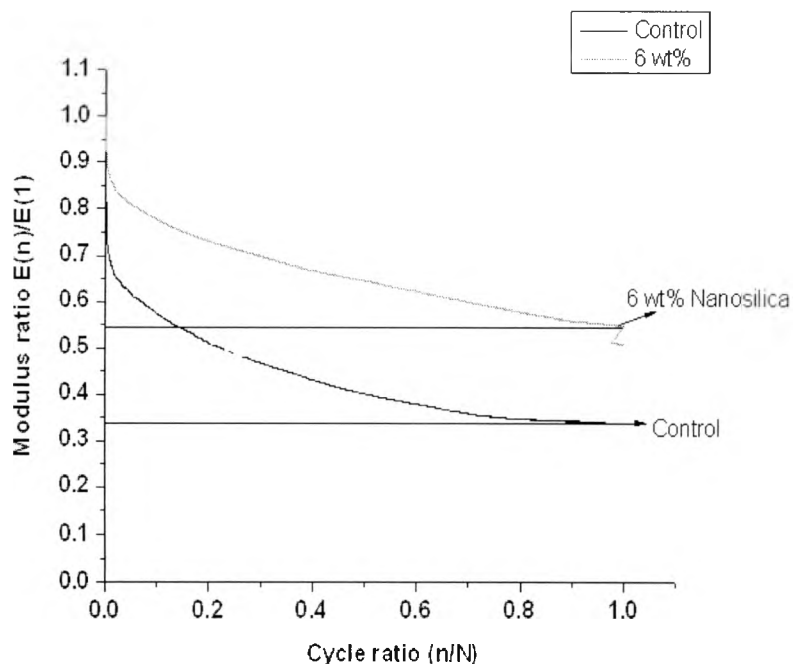


Figure 4.17 Superimposed stiffness degradation curves for 46.6 MPa

4.4 HNT-epoxy Neat Resin Static Tests

As explained in detail in chapter 2, three different dispersion techniques were used to disperse HNT in epoxy matrix. These techniques were centrifugal planetary mixing (THINKY), high-shear mixing (IKA), and low-shear mechanical mixing (Dispermat). Tensile, flexural, and Izod-impact tests were conducted for 2.5wt%, 5wt%, and 10wt% HNT loading. Five tests were conducted in each category. Table 4.9 shows these test results.

Table 4.9: Flexural, Izod-impact, and Tensile test results (High-shear mixing)

HNT loading	0.0	2.5	5.0	10.0
Flexural Strength, MPa	107.839	82.363	90.731	87.35
Stdev	(7.570)	(7.162)	(3.564)	(10.386)
Flexural Modulus, GPa	2.250	2.216	2.193	1.771
Stdev	(0.508)	(0.772)	(0.919)	(0.455)
Izod Impact, J/m	13.113	12.448	8.481	8.176
Stdev	(3.282)	(1.928)	(1.023)	(0.405)
Tensile Strength, MPa	67.370	53.627	58.7	54.237
Stdev	(5.449)	(2.166)	(9.715)	(6.050)
Tensile Modulus, GPa	3.080	2.724	2.628	3.080
Stdev	(0.360)	(0.315)	(0.172)	(0.108)
% elongation (Tension)	4.144	3.050	3.255	2.318
Stdev	(0.490)	(0.775)	(1.193)	(0.495)

With high-shear mixing technique HNT-epoxy neat resin showed lower performance in flexure, Izod-impact, and tensile tests will all three HNT weight percentages. HNT nanoparticles were washed with acetone and acetone was dried using vacuum oven at 75°C. It can be concluded that high-shear is definitely not a good mixing technique for HNT/epoxy system. It may not be dispersing HNT uniformly. High-shear mixing applied 76,906 s⁻¹ shear rate. This very high shear rate might have damaged HNT. It is interesting that the color of mixture after high-shear mixing changed from milky white to reddish yellow to red for 2.5wt%, 5wt%, and 10wt% HNT as shown in Figure 4.15. This color change may be coming due to curing agent.



Figure 4.18: HNT-epoxy mixture after high-shear mixing (2.5wt%, 5wt%, and 10wt% HNT)

Table 4.10: Flexural, Izod-impact, and Tensile Test Results (centrifugal planetary mixing)

HNT loading	0.0	2.5	5.0	10.0
Flexural Strength, MPa	107.839	79.120	88.413	94.372
Stdev	(7.570)	(10.196)	(7.909)	(16.462)
Flexural Modulus, GPa	2.250	2.217	1.785	1.913
Stdev	(0.508)	(0.385)	(0.551)	(0.664)
Izod Impact, J/m	13.113	10.387	10.565	8.589
Stdev	(3.282)	(0.952)	(1.603)	(0.909)
COV	25.030	9.170	15.175	10.584

With planetary centrifugal mixing technique HNT-epoxy neat resin showed lower performance in flexure and Izod-impact for all three HNT weight percentages. It can be concluded that centrifugal mixing does not disperse HNT uniformly within epoxy matrix.

With low-shear mechanical mixing technique HNT-epoxy neat resin showed better performance in flexure and Izod-impact at 2.5wt% HNT loading. Tensile test performance showed little decline with 2.5wt% HNT loading compared to control composites. HNT nanoparticles were mixed thoroughly in acetone for 30 minutes using mechanical mixer at room temperature. Then resin was added in solution of acetone and HNT. Later this mixture was mixed for 2 hours using mechanical mixing at 75°C. This surface treatment with acetone at elevated temperature is definitely helping in uniform dispersion of HNT. Overall this technique is promising for uniformly dispersing HNT in epoxy. More studies with different HNT percentages are required to confirm these improvements. There is also need to conduct detail SEM analysis especially on fractured

surfaces to evaluate interfacial adhesion between epoxy and HNT particles. Table 4.12 consolidates tests results for 2.5 wt% HNT-epoxy resin system using three different mixing techniques.

Table 4.11: Flexural, Izod-impact, and Tensile Test Results (low-shear mechanical mixing)

HNT loading	0.0	2.5
Flexural Strength, MPa	107.839	116.120
Stdev	(7.570)	(8.185)
Flexural Modulus, GPa	2.250	2.827
Stdev	(0.508)	(0.251)
Izod Impact, J/m	13.113	10.439
Stdev	(3.282)	(2.011)
Tensile Strength, Mpa	67.370	64.590
Stdev	(5.449)	(6.898)
Tensile Modulus, Gpa	3.080	2.836
Stdev	(0.360)	(0.214)
% elongation(tension)	4.144	3.520
Stdev	(0.490)	(0.817)

Table 4.12: Flexural, Izod-impact, and Tensile Test Results for 2.5wt% HNT loading with three different mixing techniques

	Control	High-shear mixing	Centrifugal mixing	Low-shear mixing
Flexural Strength, MPa	107.839	82.363	79.120	116.120
Flexural Modulus, GPa	2.250	2.216	2.217	2.827
Izod Impact, J/m	13.113	12.448	10.387	10.439
Tensile Strength, Mpa	67.370	53.627	N/A	64.590
Tensile Modulus, Gpa	3.080	2.724	N/A	2.836
% elongation (tension)	4.144	3.050	N/A	3.520

4.5 Analysis of variance (ANOVA)

ANOVA was performed on tensile strength, flexural strength and interlaminar shear strengths for control and nanocomposites.

4.5.1 One-way ANOVA Tensile Strength versus Nanosilica Percentage

The Homogeneity of variance assumption was confirmed for tensile strength using Levene's statistics which resulted in the value of $P < 0.030$.

Table 4.14 shows the results of the ANOVA for tensile strength at $\alpha = 0.01$. This analysis shows P value of 0.0001 which is less than 0.03 that shows nanoparticle has significant impact on the tensile strength.

The Student-Newman-Keuls procedure was used to perform pair-wise comparisons among the means of the three nanoparticle groups and control (0 wt%) as shown in Table 4.15. All the means of the nanoparticle loadings were significant compared to control (0 wt%), but the level of significance reduces when comparing between nanoparticle loadings.

Table 4.13: Univariate Analysis of Variance for Tensile Strength

	Sum of Squares	df	Mean Square	F	Significance
Nanoparticle	1324.654	3	441.551	13.916	0.0001
Error	507.671	16	31.729		
Total	1832.324	19			

Table 4.14: Student Newman Keuls Test for Tensile Strength

Nanoparticles	N	Subset for Alpha = 0.01		
		1	2	3
Control	5	92.0840		
8 wt%	5		101.4020	
7 wt%	5			109.4920
6 wt%	5			113.2760
Significance		1.000	1.000	0.304

4.5.2 One-way ANOVA: Flexural Strength versus Nanosilica Percentage

The Homogeneity of variance assumption was confirmed for tensile strength using Levene's statistics which resulted in the value of $P < 0.001$.

Table 4.16 shows the results of the ANOVA for tensile strength at $\alpha = 0.01$. It shows that nanoparticle has significant impact on the flexural strength. The Student-Newman-Keuls procedure was used to perform pair-wise comparisons among the means of the three nanoparticle groups and control (0 wt%) as shown in Table 4.17. It is observed that the means of all the nanoparticles group were significant compared to control (0 wt%).

Table 4.15: Univariate Analysis of Variance for Flexure Strength

	Sum of Squares	df	Mean Square	F	Significance
Nanoparticle	4365.467	3	1455.156	34.980	0.0001
Error	665.603	16	41.600		
Total	5031.070	19			

Table 4.16: Student Newman Keuls Test for Flexural Strength

Nanoparticles	N	Subset for Alpha = 0.01	
		1	2
Control	5	145.6552	
8 wt%	5		178.8528
7 wt%	5		179.7820
6 wt%	5		180.5989
Significance		1.000	0.905

4.5.3 One-way ANOVA Interlaminar Shear Strength versus Nanosilica Percentage

The Homogeneity of variance assumption was confirmed for Interlaminar Shear strength using Levene's statistics which resulted in the value of $P < 0.276$.

Table 4.18 shows the results of the ANOVA for Interlaminar Shear strength at $\alpha = 0.01$. It shows that nanoparticle has significant impact on the Interlaminar Shear strength. The Student-Newman-Keuls procedure was used to perform pair-wise comparisons among the means of the three nanoparticle groups and control group (0 wt%). The means of the nanoparticle groups were all significant compared to control groups.

Table 4.17: Univariate Analysis of Variance for Interlaminar Shear Strength

	Sum of Squares	df	Mean Square	F	Significance
Nanoparticle	140.100	3	46.700	77.677	0.0001
Error	9.619	16	0.601		
Total	149.719	19			

Table 4.18: Student Newman Keuls Test for Flexural Strength

Nanoparticles	N	Subset for Alpha = 0.01	
		1	2
Control	5	24.2359	
8 wt%	5		29.5993
7 wt%	5		30.0126
6 wt%	5		31.0207
Significance		1.000	0.021

The conclusions of this research study are presented in Chapter 5.

CHAPTER 5

CONCLUSIONS

Polymer matrix composites, especially E-glass/Epoxy dominate the wind turbine blade market because of their superior fatigue characteristics, high specific stiffness, and ability to make complex geometries. Wind turbine failure is a major issue as failure rates are as high as 20% within three years. The overall pressure field on the blade causes a “bending moment” and torque at the root. A “bending moment” refers to the tendency of wind turbine blades to bend and twist during operation. This constant and variable amplitude cyclic bending and twisting of wind turbine blades is fatigue (Richardson, 2009).

The major causes of blade failure are related to manufacturing errors and design of blades. Besides manufacturing and design, inherent performance of existing material system is also a key factor. Current wind turbine blades are fabricated with 2D woven glass fabric reinforcement stacked layer-by-layer to achieve required thickness. Such 2D components have limited life in fatigue environments due to inherently low matrix dominated interlaminar shear strengths (ILSS). Low ILSS leads to poor bond between two layers, delamination, and splitting of laminates. Addition of nanoparticles in polymer matrix has been discovered as a means to enhance fracture toughness and ILSS that would

improve fatigue performance. Two different nanoparticles, Nanosilica and Halloysite nanotubes (HNT) were used to nanomodify epoxy resin.

The nanosilica modified epoxy was further used to manufacture E-glass reinforced composites using low-cost VARTM process. Three different loadings were used 6wt%, 7wt%, and 8wt%. Extensive mechanical characterization was performed to evaluate tensile strength, tensile modulus, elongation at break, flexural strength flexural modulus, interlaminar shear strength (ILSS).

1. Nanosilica (Nanopox F400) was already uniformly dispersed in epoxy matrix with high concentration of 40wt%. This highly concentrated nanosilica was mixed in required quantity of epoxy. It is observed that simple hand mixing followed by centrifugal mixing provides uniform dispersion. The simple mixing technique is great advantage when manufacturing huge parts such as wind turbine blades.
2. Low-cost VARTM process was used successfully to manufacture high quality composites with average fiber volume fraction of 0.52.
3. All nanosilica nanocomposites (6wt%, 7wt%, and 8wt%) showed considerable improvement in tensile strength, tensile modulus, elongation at break, flexural strength flexural modulus, interlaminar shear strength (ILSS) compared to control composites.
4. It is also observed that nanosilica modification toughens the composites. It is evident from percentage elongation at break and area under stress-strain curves.
5. Analysis of variance (ANOVA) indicates that in flexural test, tensional test and interlaminar shear strength test, nanosilica modified epoxy composites were

significant compared to the control group but in most cases, the nanosilica modified epoxy composites were not significant when compared amongst themselves.

6. 6wt% nanosilica loadings showed highest improvement in tensile strength, percentage elongation at break, and ILSS. Also these nanosilica nanocomposites showed larger area under stress-strain curve compared to 7wt% and 8wt%.

Control and 6wt% nanosilica nanocomposites were further studied extensively under load-controlled axial tension-tension fatigue loadings at 2Hz, 5Hz frequency and R ratio of 0.1. Maximum stresses applied on these composites were 74.5, 65.2, 55.9, and 46.6 MPa. Stiffness degradation was monitored for all fatigue tests.

1. It is observed that frequency has detrimental effect on fatigue life of composites at 5Hz frequency. There was considerable drop in fatigue life especially in high-cycle fatigue. At 46.6 MPa maximum stress, control composites survived 1 million cycles at 2Hz frequency as opposed to only 15820 cycles at 5Hz frequency.
2. The surface temperature on the specimen was monitored during fatigue testing. It is observed that at 5Hz frequency surface temperature rose up to 58°C at 74.5 MPa maximum stress as opposed to 51°C at 2 Hz frequency. At 2Hz frequency 6wt% nanosilica composites showed slightly lower surface temperature.

The temperature gradient developed within specimen might lead to premature failure of the component. Author suggests conducting further fatigue tests at 1 Hz frequency.

3. 6wt% nanosilica modification showed 10 and 3 times improvement in fatigue life in high-cycle and low-cycle fatigue, respectively.
4. Both control and 6wt% nanosilica composites survived 1 million cycles at maximum stress of 46.6 MPa. It should be noted that tests were stopped at 1 million cycles. From stiffness degradation curves it is evident that by the end of 1 million cycles control composites lost about 65% of modulus whereas 6wt% nanosilica composites lost only 45% of modulus.
5. Stiffness degradation curves showed three stage pattern which is very typical for woven composites.

In first stage modulus decreased rapidly. This stage lasted about 10% of fatigue life. It is observed that 35 to 40% of modulus is lost in this stage.

The second stage constituted about 70% of the total fatigue life for control composites. By the end of this stage total 70% of modulus was lost for control composites. The trend was little different for 6wt% nanosilica composites. This stage contributed about 75% of fatigue life and by the end of this stage total 65% modulus was lost. This is quite bit of improvement in fatigue performance.

Final failure occurs with the breakage of fibers. In third stage, the stiffness decreased rapidly during the last few cycles before the specimen broke. This stage

contributed about 20% of fatigue life for control composites and 15% of 6wt% nanosilica composites.

There is very little literature available on mechanical properties improvement using Halloysite nanotubes. There is also quite disparity in optimum weight percentage of HNT that leads to improvement in impact and fracture toughness. The dispersion techniques researchers used were very tedious and time-consuming. Therefore, it was decided to characterize HNT-epoxy neat resin at 2.5, 5, and 10wt% loadings. Three different dispersion techniques were used; planetary centrifugal mixing, high-shear mixing, and mechanical low-shear mixing.

1. Centrifugal mixing is very simple mixing technique. The major drawback is the amount of resin that can be handled at a time. THINKY ARV-310 model had limitation of 310 g resin which is approximately 270 mL epoxy resin. The cost of this model varies from \$15k to \$25K based on whether vacuum capability is available or not. Higher capacity models such as 1000 g are expensive. With this technique all HNT-epoxy neat resin (2.5, 5, and 10wt%) showed lower performance compared to control epoxy neat resin in impact, tensile, and flexural properties.
2. High shear mixing is also batch process but can handle much large quantity at a time. IKA Labor pilot 2000/4 model could handle almost 4000 mL at a time. But

this is very time-consuming process in terms of assembling, disassembling, and cleaning after every batch. This equipment cost about \$15K.

In this research, 40 Hz frequency was used which provided a shear rate of $76,906 \text{ s}^{-1}$. It is observed that high-shear mixing might have damaged HNT nanoparticles. It is interesting that the color of mixture after high-shear mixing changed from milky white to reddish yellow to red for 2.5wt%, 5wt%, and 10wt% HNT, respectively. With this technique all HNT-epoxy neat resin (2.5, 5, and 10wt%) showed lower performance compared to control epoxy neat resin in impact, tensile, and flexural properties.

3. Low shear mechanical mixing is simple technique but it also could handle limited resin at a time. Dispermat CC model was used in this research. This model could handle 1000 g at a time with speed range up to 16000 rpm providing maximum shearing rate of 1067 s^{-1} . This is much low shear-rate compared to high-shear mixer. Obviously one needs to mix nanoparticles for longer duration. This technique was promising compared to centrifugal mixing and high-shear mixing. For 2.5wt% HNT-epoxy neat resin flexural strength and flexural modulus showed 8% and 25% improvement compared to control epoxy neat resin. But other properties Izod-impact strength and tensile properties deteriorated. Lower percentages such as 0.8wt% and 1.6wt% should be evaluated.
4. Due to inconsistent test results in HNT-epoxy neat resin in three different techniques, glass reinforced composites were not manufactured using HNT nanoparticles. More studies with different HNT percentages are required to

confirm improvement using low-shear mechanical mixing. There is also need to conduct detail SEM analysis especially on fractured surfaces to evaluate interfacial adhesion between epoxy and HNT particles.

The objectives of this research were to develop material system that has improved fatigue performance without knocking off flexural and tensile properties. 6wt% is optimum loading of nanosilica to improve fatigue life along with improvement in flexural and tensile properties.

REFERENCES

Amateau, M. (n.d.). *Engineering Composite Materials EMCH 471*. Retrieved March 20, 2010, from www.4esm.psu.edu:
<http://www.4esm.psu/academics/courses/emch471jNotes/chapter18.PDF>

Balakrishnan, S., & Raghavan, D. (2005). Chemically Functionalized Clay-Epoxy Nanocomposites: Vernonia Oil-Based Surfactant. *Reinforced Plastics and Composites*, 785-793.

Battat, B. (2001). *2001 Material Ease 16*. Retrieved March 20, 2010, from ammtiac.alionscience.com: <http://ammtiac.alionscience.com>

Blackman, B., Kinloch, A. J., Sohn Lee, J., Taylor, A. C., Agarwal, R., Schueneman, G., et al. (2007). The Fracture and Fatigue Behaviour of Nano-Modified Epoxy Polymers. *Material Science*, 7049-7051.

Bolick, R. (2005). *A Comparative Study of Unstitched, Stitched and Z-Pinned Plain Woven Composites under Fatigue Loading (Ph.D dissertation)* North Carolina Agricultural and Technical State University.

Callister, W. (2008). *An Introduction, Material Science and Engineering* John Wiley Publications.

Carlos, K. (1994). *Fatigue Behavior of 3-D Triaxially Braided Composites, (THESIS)* North Carolina Agricultural and Technical State University.

Chen, H., Ye, L., & Ye, Y. (2007). High impact strength epoxy nanocomposites with natural nanotubes. *Polymer*, 6426-6433.

Cheng, J. (2006). *Polysynate Ester/Small Diameter Carbon Nanotubes Nanocomposite (Master's Thesis)* Austin: University of Texas.

Deng, S., Ye, L., & Friedrich, K. (2007). Fracture Behaviours of Epoxy Nanocomposites with Nano-silica at Low and Elevated Temperature. *Material Science*, 2766-2774.
(2004). *DESIGN STUDIES FOR TWIST-COUPLED WIND TURBINE Blades*. Sandia National Laboratories.

Fawaz, Z., & Ellyin, F. (1995). A New Methodology for The Prediction of Fatigue Failure in Multidirectional FiberReinforced Laminates. *Composites Science and Technology*, 47-55.

Fiber Reinforcement forms. (2010, February 5). Retrieved February 20, 2010, from Compositesworld: <http://www.compositesworld.com/articles/fiber-reinforcement-forms>

Fujii, T., Amijima, S., & Okubo, K. (1993). Microscopic Fatigue Processes in a Plain Weave Glass-Fiber Composite. *Composites Science and Technology*, 327-333.

Johnsen, B. B., Kinloch, A. J., Mohammed, R., Taylor, A. C., & Sprenger, S. (2007). Toughening Mechanisms of Nanoparticle Modified Epoxy Polymers. *Polymer*, 530-541.

Johnson, S. J., Van Dam, C. P., & Berg, D. E. (2008). *Active Load Control Technique for Wind Turbines*. Livermore: Sandia National Laboratories.

Karapappas, P., Vavouliotis, P., Tsotra, P., & Kostopoulos, V. (2009). Enhanced Fracture Property of Carbon Reinforced Composites by the Addition of Multi-Wall Carbon Nanotubes. *Composite Materials*, 0001-9.

Koo, J. H. (2006). *Polymer Nanocomposites Processing, Characterization, and Applications* McGraw-Hill Professional Publishing.

Lee, L. J., Fu, K. E., & Yang, J. N. (1996). Prediction of Fatigue Damage and Life for Composite Laminates Under Service Loading Spectra. *Composites Science Technology*, 635-648.

Li, C., Liu, J., Qu, X., Guo, B., & Yang, Z. (2008). Polymer-Modified halloysite Composite Nanotubes. *Applied Polymer Science*, 3638-3646.

Locks, J., & Valencia, U. (2004). *Design Studies for Twist-Coupled Wind Turbine Blades* Sandia National Laboratories.

Mallick, P. (1993). *Fiber Reinforced Composites. Materials, Manufacturing, and Design* New York: Marcel Decker, Inc.

Manas-Zloczower, I. (2009). *Mixing and Compounding Polymer: Theory and Practice* Hanser-Gardner Publications.

Mandell, J. F., Samborsky, D. D., & Agastra, P. (2008). Composite Materials Fatigue Issues in Wind Turbine Blade Construction. *Society for the Advancement of Manufacturing and Process Engineering*.

Manjunatha, C. M., Taylor, A. C., Kinloch, A. J., & Sprenger, S. (2009). The Cyclic Fatigue Behaviour of an Epoxy Polymer Modified with Micron-Rubber and Nano-Silica Particles. *Material Science*, 4487-4490.

May, C. A. (1987). *Epoxy Resins: Chemistry and Technology* New York: Marcel Dekker Inc.

Mazumdar, 2. (2002). *Composites Manufacturing Materials, Products, and Process Engineering* New York: CRC Press.

McConnell, V. (2010, February 5). *Composite World*. Retrieved February 21, 2010, from Composite world.com: <http://www.compositesworld.com/articles/resin-systems-update-the-greening-of-thermosets>

MDA Composites (2009, march 4). Retrieved march 23, 2010, from www.mdacomposite.org: <http://www.mdacomposites.org>

Naturalnano. (2009, August 21). Retrieved August 21, 2009, from Naturalnano.com: <http://www.naturalnano.com>

Owen, M. (1974). Fatigue Damage in Glass-fibre Reinforced Plastics. *Composite Materials*, 313-40.

Ratna, D., Divekar, S., Patchaiappan, S., Samui, A. B., & Chakraborty, B. C. (2007). Poly(Ethylene Oxide)/Clay nanocomposites for Solid Polymer Electrolyte Applications. *Polymer International*, 900-904.

Reifsnider, K. (1990). *Damage and Damage Mechanics of Composite Materials*. New York: Elsevier.

Richardson, R. (2009). *Wind Turbine Blade Composites Design* Retrieved November 14, 2009, from Dassault systemes composite white paper: <http://www.plmv5.com>

Seemann, W. (1994). *Patent No. 5,316,462*. U.S.A.

Seemann, W. (1994). *Patent No 5,316,462*. U.S.A.

Strong, B. A. (2008). *Fundamentals of Basic Manufacturing Materials, Methods, and Applications*. Dearborn: Society of Manufacturing Engineers.

Tang, X., & Whitcomb, J. D. (1999). Progressive Failure Behaviours of 2D Woven Composites. *Composite Materials*.

Tate, J. S., Akinola, T. A., Pulin, P., & Massingill, J.(2009). Nanommodified E-glass Composites: Mechanical Properties. *SAMPE* Baltimore.

Tate, J. S., Kabakov, D., Koo, J. H., & Lao, S. (2009). Nanommodified Phenolic/E-Glass Composites. *SAMPE* Baltimore.

Tate, J. S., Kelkar, A. D., & Whitcomb, J. D. (2006). Effect of Braid Angle on Fatigue Performance of Biaxial Braided Composites. *International Journal of Fatigue*, 1239-1247.

Tate, J., Kabakov, D., Koo, J. H., & Lao, S. (2009). Nanoreinforced Phenolic Composites-Flammability and Mechanical Properties. *SAMPE*, (p. B107). Baltimore.

Thomasnet (2008, January 13). Retrieved March 23, 2010, from www.thomasnet.com:
<http://www.thomasnet.com>

Thomsen, O. T. (2009, February 10). *Wind turbine blades: the bigger, the better*. Retrieved November 20, 2009, from environmental research letters:
<http://environmentalresearchweb.org/cws/article/opinion/37719>

Xu, Y., & Hoa, S. V. (2008). Mechanical Properties of Carbon Fiber Reinforced Epoxy/Clay Nanocomposites. *Composite Science and Technology*, 854-861.

Yamashita, S. H., Takei, T., & Sugano, T. (1992). Interlaminar Reinforcement of Laminated Composites by Addition of Oriented Whiskers in the Matrix. *Composite Materials*, 1254-1268.

Zac-Williams, A. (2006). *Fatigue Behavior of 45 Degrees Fiberglass Braided Composites (THESIS)* North Carolina Agricultural and Technical State University.

VITA

Adekunle Temitope Akinola was born in Ado-Ekiti, Nigeria, on March 24, 1980, the son of Esther Akinola and Michael Akinola. After completing his work at Unity Secondary School, Ado-Ekiti, Nigeria, in 1997, he entered University of Uyo, Nigeria in 1999. He received his Bachelor of Science from University of Uyo, Nigeria, in 2006. In August 2008, he entered the Graduate College of Texas State University-San Marcos.

Permanent Address: 5A Kayode Aluko Close off Kayode Taiwo Avenue, Magodo GRA

Lagos, Nigeria

This thesis was typed by Adekunle T. Akinola